Supplement of Geosci. Model Dev., 12, 5055–5075, 2019
https://doi.org/10.5194/gmd-12-5055-2019-supplement

Geoscientific Model Development
Open Access
EGU

Supplement of

SELEN^4 (SELEN version 4.0): a Fortran program for solving the gravitationally and topographically self-consistent sea-level equation in glacial isostatic adjustment modeling

Giorgio Spada and Daniele Melini

Correspondence to: Giorgio Spada (giorgio.spada@gmail.com)

Contents

List of Figures

List of Tables

. . . computemus in tempore, videamusque quid inde sequatur. (Gottfried Wilhelm Leibniz)

Abstract. The aim of this supplement is to give a condensed (but hopefully self-contained) account of the GIA theory, providing a physical background to the numerical implementation of the Sea Level Equation in program *SELEN*^{4}. A number of technical aspects and also discussed, along with some strictly necessary, basic mathematical definitions. The material presented here should be accessible to all students at a *PhD* level in Earth Sciences.

S1 Introduction

This document is organised into several sections, whose content is briefly summarised here.

In **Section S2**, we define the *surface mass distributions* and we introduce basic concepts as *sea level*, *topography*, the *ocean function* and *continent function*; the *mass conservation principle* is also presented. **Section S3** deals with the geometrical and physical properties of the *Earth models* that are employed with *SELEN*^{4} and introduces the *loading and the tidal Love numbers*. The response to surface loads is studied in **Section S4** by introducing the *surface Green's functions* and building *surface response functions* for sea level, for the geoid height and for vertical displacements. In **Section S5** we deal with the essentials of *Earth rotation*, introducing the *Liouville equations* for polar motion and defining the *excitation functions*; furthermore two different *rotation theories* are illustrated for which we study the *Polar Motion Transfer Function*. **Section S6** discusses the responses to Earth's rotational variations by introducing the *rotation Green's functions* and the *rotation response functions* for sea level, for the geoid height and for vertical displacements. In **Section S7** we perform a *spatiotemporal discretisation* of all the terms included in the SLE with the aid of the spherical harmonic functions and of a geodesic grid. Finally, in **Section S8** we present a suite of self-contained, short special topics; some of them are meant to be of support to the development of the above sections, some others are discussing specific geophysical aspects of the GIA process, and some are dealing with technical aspects.

This supplement (hereafter referred to as SSM19) and the main text (SM19) contain a remarkable number definitions involving physical quantities and mathematical symbols. We have made everywhere efforts to use a clear and self-explanatory notation, which admittedly sometimes is not standard in the GIA literature. To facilitate the reader, in Table S7 we provide the acronyms that we have used in the text, a glossary with a list of recurrent symbols and notations is given in Table S8, and numerical values of important constants are listed in Table S9.

S2 Surface mass distributions

In this Section various quantities are defined, useful to describe the distribution of the ice and of the water masses over the surface of the Earth and its time evolution. We first define the *ocean function*, which in a given location is determined by the ice thickness and by the Earth's topography, and its complementary *continent function*. The surface mass distribution is described in terms of the *surface load* function. With the aid of the ocean function, the time-variations of the surface load with respect to a reference state are expressed in terms of changes in the *ice thickness*, variations in *sea level*, and changes in the *oceans geometry*. By the principle of mass conservation, a general form of the Sea Level Equation (SLE) is also established.

S2.1 Ocean Function

The *ocean function* (OF) is

$$O(\gamma,t) \equiv \begin{cases} 1, & \text{if } T + \dfrac{\rho^i}{\rho^w} I < 0 \\ 0, & \text{if } T + \dfrac{\rho^i}{\rho^w} I \geq 0, \end{cases} \tag{S1}$$

where γ stands for (θ,λ), θ and λ are colatitude and longitude, respectively, t is time, ρ^i and ρ^w are the density of ice and water, respectively (throughout this supplement, ρ^i and ρ^w are assumed to be constants). With $I(\gamma,t)$ we denote the *ice*

thickness ($I(\gamma,t) \geq 0$), and $T(\gamma,t)$ is the *topography*, given by

$$T(\gamma,t) = -B, \tag{S2}$$

where $B(\gamma,t)$ is *sea level*. As fas as we know, the OF has been first defined and decomposed in series of spherical harmonics by Prey (1922); the reader is referred to Balmino et al. (1973) and Lambeck (1980) for modern determinations of the OF and of its harmonic spectrum.

The *continent function* $C(\gamma,t)$ (or CF) is defined as the complement to one of the OF, *i.e.,*

$$C(\gamma,t) = 1 - O. \tag{S3}$$

According to the values of T and I, five different mutually exclusive conditions can be met, which are discussed in detail below and illustrated in Table S1 and Figure S1 and in terms of O and C.

Condition 1: ice-free ocean. The topography is $T < 0$ and since $I = 0$, from Eqs. (S1) and (S3) we obtain $O = 1$ and $C = 0$, respectively.

Condition 2: floating ice. Where ice is floating, $T < 0$ and $I > 0$. By the condition of isostatic equilibrium, all the columns have the same mass:

$$\rho^w B(\gamma,t) = \rho^i I + \rho^w y, \tag{S4}$$

where y is the thickness of the water layer beneath the ice column (see Figure S2a). Since $y > 0$, using Eq. (S2), the floating ice condition reads

$$T(\gamma,t) + \frac{\rho^i}{\rho^w} I(\gamma,t) < 0, \tag{S5}$$

stating that the ice is lighter than the water column. Hence, from Eqs. (S1) and (S3) we obtain $O = 1$ and $C = 0$, respectively. Since from Figure (S2a) we have $y = B - (I - x)$, where x is the thickness of the ice above sea level, Eq. (S4) provides $x = \left(1 - \rho^i/\rho^w\right) I$.

Condition 3: ice grounded below sea level. In this condition, illustrated in Figure S2b, the topography is $T < 0$ and the ice thickness is $I > 0$, like in the case of floating ice (Figure S2a). However, the system is not in isostatic equilibrium, and the ice column turns out to be heavier than the water column. *i.e.,* $\rho^i I \geq \rho^w B$, or

$$T(\gamma,t) + \frac{\rho^i}{\rho^w} I(\gamma,t) \geq 0, \tag{S6}$$

Condition	Sea level	Topography	Ice thickness	$T + \frac{\rho^i}{\rho^w} I$	OF	CF
1 - Ice-free ocean	$B > 0$	$T < 0$	$I = 0$	< 0	1	0
2 - Floating ice	$B > 0$	$T < 0$	$I > 0$	< 0	1	0
3 - Ice grounded below sl	$B > 0$	$T < 0$	$I > 0$	≥ 0	0	1
4 - Ice grounded above sl	$B < 0$	$T > 0$	$I > 0$	≥ 0	0	1
5 - Ice-free land	$B < 0$	$T > 0$	$I = 0$	≥ 0	0	1

Table S1. Values of the ocean function OF (Eq. S1) and of its complement CF=1-OF (S3) according to the values of topography T and of ice thickness I, with a description of the five possible conditions described in the text. Here "sl" stands for sea level.

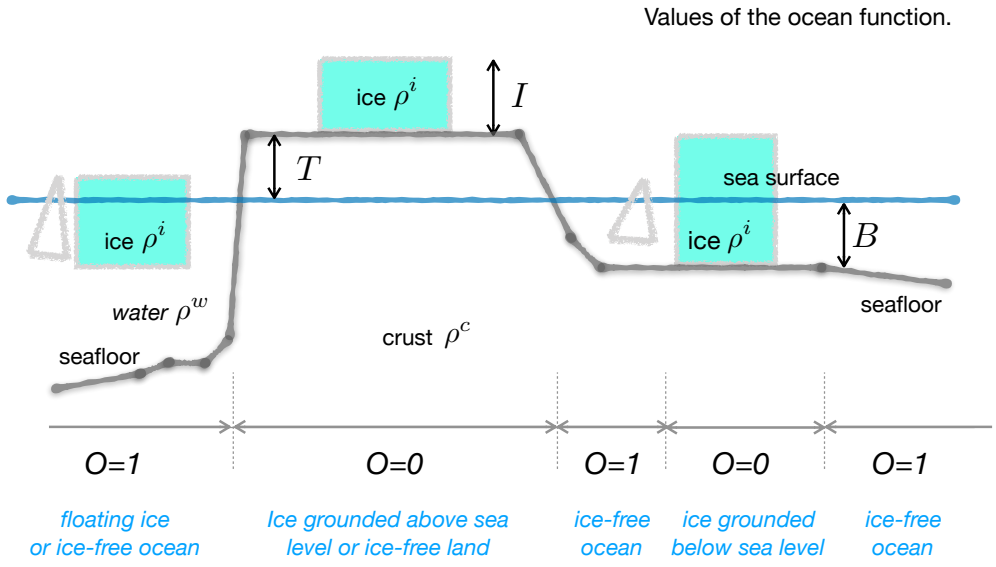

Figure S1. Possible values of the OF, corresponding to the five different conditions listed in Table S1, according to the values of T (topography) and I (ice thickness). With $B = -T$ we denote sea level.

hence according to the definitions given by Eqs. (S1) and (S3), we have $O = 0$ and $C = 1$.

Condition 4: ice grounded above sea level. When ice is grounded above sea level, the topography and the ice thickness are $T > 0$ and $I > 0$, respectively. In this case, from Eqs. (S1) and (S3), we have $O = 0$ and $C = 1$.

Condition 5: ice-free land. Across ice-free lands, where according to Figure S1 we have $T > 0$ and $I = 0$, Eqs. (S1) and (S3) give $O = 0$ and $C = 1$, respectively.

S2.2 Topography and sea level

From the definition of topography given by Eq. (S2), it is possible to draw a few important consequences. We first define *sea-level change* by the difference

$$\mathcal{S}(\gamma, t) = B - B_0, \tag{S7}$$

where $B_0 = B(\gamma, t_0)$ is sea level in a reference equilibrium state attained for $t \leq t_0 \equiv 0$ (the time discretisation adopted in this study is described in §S8.1). Then, taking the difference between Eq. (S2) and the same equation evaluated at present time (*i.e.,*

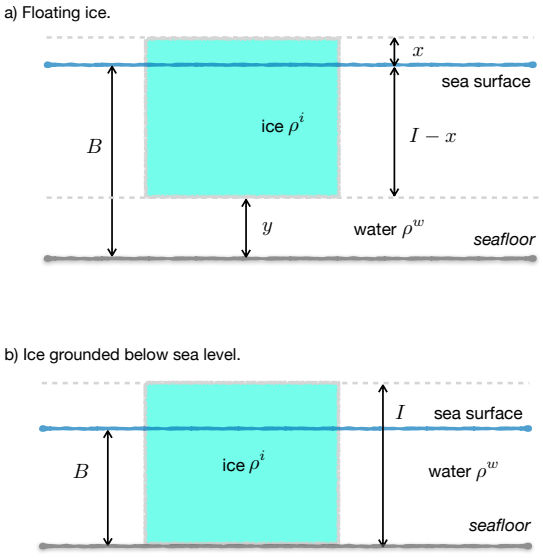

Figure S2. Diagrams showing floating ice (a) and ice grounded below sea level (b), where I and B are the ice thickness and sea level, respectively.

$t = t_N$), we obtain

$$T(\gamma,t) - T(\gamma,t_N) = -(B - B_N) \tag{S8}$$

$$= -((B - B_0) - (B_N - B_0)), \tag{S9}$$

where $B_N = B(\gamma,t_N)$. Hence, using Eq. (S7) and defining $T_N = T(\gamma,t_N)$, we have

$$T(\gamma,t) = T_N - (\mathcal{S} - \mathcal{S}_N). \tag{S10}$$

This last equation, which shall be referred to as "PT equation" in the following, allows for the reconstruction of *paleo-topography* (*i.e.,* the time history of topography $T(\gamma,t)$) once present topography $T(\gamma,t_N)$ is known and the solution of the SLE is has been found (*i.e.,* sea-level change $\mathcal{S}(\gamma,t)$ is determined at all times t and places γ). Using *e.g.,* model ETOPO1 (see Amante and Eakins, 2009; Eakins and Sharman, 2012) as a representation for the modern relief, the PT equation can be used to refine the value of $T(\gamma,t)$ using successive iterations of the SLE.

The method of reconstruction based on Eq. (S10) has been first introduced by Peltier (1994) and since then applied to paleogeographic investigations made in the framework of GIA studies (see *e.g.,* Spada and Galassi, 2017, and references therein). It is worth to note that Peltier (1994) has also defined another quantity, which he has defined *true paleo-topography*, as follows

$$PT(\gamma,t) = T + I, \tag{S11}$$

where T is topography and I is ice thickness. It is clear that $PT(\gamma,t)$ can be easily reconstructed once T has been determined by solving the SLE, since I is given *a priori*.

S2.3 Surface load

This section is devoted to the description of the *surface load* L associated to the ice and water distributions at the Earth's surface. We shall also consider its variation $\mathcal{L}$ with respect to a reference state, since it has a central role in the numerical implementation of the SLE.

Surface load. In SM19, we have defined the *surface load* $L(\gamma, t)$ by means of

$$M(t) = \int_e L dA, \tag{S12}$$

where $M(t)$ is the mass distributed over the whole Earth's surface in the form of ice or water, and

$$dA = a^2 d\gamma \tag{S13}$$

is the area element, being a the average Earth's radius and

$$d\gamma = \sin\theta d\theta d\lambda \tag{S14}$$

is the area of the infinitesimal solid angle. Hence, according to Eq. (S12), the surface load represents the mass acting on the Earth's surface per unit area, *i.e.,*

$$L(\gamma, t) = \frac{dM}{dA}. \tag{S15}$$

Surface mass distribution. At a given time t, the mass $M(t)$ distributed over the Earth's surface can be expressed as

$$M(t) = M^i + M^w, \tag{S16}$$

where M^i and M^w are the mass of the ice and of the water at time t, respectively. We now consider these two terms separately.

The ice mass term stems from two contributions, with

$$M^i(t) = M^{i,gr} + M^{i,fl}, \tag{S17}$$

where superscript gr denotes grounded ice (either above or below sea level), while fl indicates floating ice. By the definition of CF (see Eq. S3), we can equivalently write

$$M^i(t) = \rho^i \int_e IC dA + \rho^i \int_{fl} I dA, \tag{S18}$$

where the first integral over the whole Earth's surface accounts for the contribution of all the grounded ice $M^{i,gr}$, while the second accounts for the floating ice contribution $M^{i,fl}$.

In a similar way, $M^w(t)$ stems from two terms, with

$$M^w(t) = M^{w,if} + M^{w,fl}, \tag{S19}$$

where superscripts if and fl indicate contributions from the ice-free oceans and from ocean regions where there is floating ice, respectively. Using the condition of isostasy given by Eq. (S4), we obtain

$$M^w(t) = \rho^w \int_{if} B dA + \int_{fl} \left(\rho^w B - \rho^i I\right) dA. \tag{S20}$$

Hence, using Eqs. (S18) and (S20) in (S16), the total mass of the (ice+water) system is

$$M(t) = \rho^i \int_e IC dA + \rho^i \int_{fl} I dA + \rho^w \int_{if} B dA + \rho^w \int_{fl} B dA - \rho^i \int_{fl} I dA, \tag{S21}$$

where we note that the integrals of I over region fl cancel out and those involving B can be merged taking advantage of the OF definition (see Eq. S1), so that

$$M(t) = \int_e \left(\rho^i IC + \rho^w BO\right) dA, \tag{S22}$$

which compared to Eq. (S12) provides the following compact (and symmetrical) expression for the surface load

$$L(\gamma,t) = \rho^i IC + \rho^w BO. \tag{S23}$$

Surface load variation. The *surface load variation* is defined as the difference between the actual surface load and its value in a previous reference state:

$$\mathcal{L}(\gamma,t) = L - L_0, \tag{S24}$$

which using Eq. (S23) gives

$$\mathcal{L}(\gamma,t) = \rho^i(IC - I_0C_0) + \rho^w(BO - B_0O_0). \tag{S25}$$

We now define the *ice thickness variation* as

$$\mathcal{I}(\gamma,t) = I - I_0, \tag{S26}$$

and the *ocean function variation*

$$\mathcal{O}(\gamma,t) = O - O_0\,, \tag{S27}$$

where subscript 0 indicates reference values. Also using the definition of topography given by Eq. (S2) and of sea-level change (S7), (S25) can be manipulated as follows

$$\begin{aligned}
\mathcal{L}(\gamma,t) &= \rho^i\left((I_0+\mathcal{I})C - I_0C_0\right) + \rho^w\left((B_0+\mathcal{S})O - B_0O_0\right) \\
&= \rho^i\mathcal{I}C + \rho^i I_0(C - C_0) + \rho^w\mathcal{S}O + \rho^w B_0(O - O_0) \\
&= \rho^i\mathcal{I}C - \rho^i I_0(O - O_0) + \rho^w\mathcal{S}O - \rho^w T_0(O - O_0) \\
&= \rho^i C\mathcal{I} + \rho^w O\mathcal{S} - (\rho^i I_0 + \rho^w T_0)\mathcal{O}.
\end{aligned} \tag{S28}$$

Thus, the load variation can be conveniently decomposed as

$$\mathcal{L}(\gamma,t) = \mathcal{L}^a + \mathcal{L}^b + \mathcal{L}^c, \tag{S29}$$

with

$$\mathcal{L}^a(\gamma,t) \equiv \rho^i\mathcal{W} \tag{S30}$$

$$\mathcal{L}^b(\gamma,t) \equiv \rho^w\mathcal{Z} \tag{S31}$$

$$\mathcal{L}^c(\gamma,t) \equiv \rho^r\mathcal{X}, \tag{S32}$$

where

$$\mathcal{W}(\gamma,t) \equiv C\mathcal{I} \tag{S33}$$

$$\mathcal{Z}(\gamma,t) \equiv O\mathcal{S} \tag{S34}$$

$$\mathcal{X}(\gamma,t) \equiv Q\mathcal{O}, \tag{S35}$$

and we have defined the auxiliary variable

$$Q(\gamma) \equiv -\left(\frac{\rho^i}{\rho^r}\, I_0 + \frac{\rho^w}{\rho^r}\, T_0\right), \tag{S36}$$

being $\rho^r > 0$ an arbitrary reference density. We note that adopting the decomposition (S29) for the load variation $\mathcal{L}$, variables $\mathcal{W}$, $\mathcal{Z}$ and $\mathcal{X}$ are uniquely associated to variations of the ice thickness, of sea level and of the OF, respectively.

Variable $\mathcal{Z}$ defined by Eq. (S34), which can be interpreted as the "projection" of sea-level change $\mathcal{S}$ on the OF, shall play an important role in the development of the pseudo-spectral approach to the SLE detailed in §S7 below. We note that, symmetrically, in Eq. (S33) $\mathcal{W}$ projects the ice thickness variation $\mathcal{I}$ on the CF.

S2.4 Mass conservation

The mass conservation principle states that

$$M(t) = M_0, \tag{S37}$$

where $M(t)$ is the mass of the (ice+water) system at an arbitrary time t and M_0 is the mass at the reference time t_0. Note that we assume that the mass of the solid Earth is unvaried. Defining the *mass variation* as

$$\mathcal{M}(t) = M - M_0, \tag{S38}$$

the mass conservation principle reads

$$\mathcal{M}(t) \equiv \int_e \mathcal{L}\, dA = 0, \tag{S39}$$

where $\mathcal{L}$ is the surface load variation defined by Eq. (S24). An equivalent expression is

$$< \mathcal{L}(\gamma,t) >^e = 0, \tag{S40}$$

where the average over the *whole Earth's surface* of a scalar function $F(\gamma,t)$ is defined as

$$< F(\gamma,t) >^e (t) \equiv \frac{1}{A^e} \int_e F(\gamma,t) dA. \tag{S41}$$

We anticipate that using Eq. (S432), (S40) implies

$$\mathcal{L}_{00}(t) = 0, \tag{S42}$$

where $\mathcal{L}_{00}$ is the coefficient of degree $l = 0$ of the expansion coefficient of $\mathcal{L}(\gamma,t)$ in series of (complex) spherical harmonics. In this work we shall only consider *physically plausible* loads, which obey the principle of mass conservation given by (S39) or by the equivalent forms (S40) or (S42).

Using the expression for the surface load variation given by Eq. (S25), the mass conservation principle can be also stated as

$$\mathcal{M}(t) = \rho^i \int_e (IC - I_0 C_0)\, dA + \rho^w \int_e (BO - B_0 O_0)\, dA = 0 \tag{S43}$$

which can be rearranged as

$$\mu(t) + \rho^w \int_e (BO - B_0 O_0)\, dA = 0, \tag{S44}$$

where

$$\mu(t) = \rho^i \int_e (IC - I_0 C_0)\, dA \tag{S45}$$

represents the time-variation of the grounded ice mass $M^{i,gr}$ (see Eq. S18). We note, in passing, that from the definition of whole Earth surface average (S41), Eq. (S45) can be equivalently written as

$$\mu(t) = \rho^i A^e < IC - I_0 C_0 >^e . \tag{S46}$$

Using simple algebra, from Eq. (S44) we obtain

$$\begin{aligned}
\mu + \rho^w \int_e \big((B - B_0 + B_0)O - B_0 O_0\big)\, dA &= 0 \\
\mu + \rho^w \int_e \big((B - B_0)O + B_0(O - O_0)\big)\, dA &= 0 \\
\mu + \rho^w \int_e \mathcal{S} O dA + \rho^w \int_e B_0 \mathcal{O} dA &= 0 \\
\mu + \rho^w A^o < \mathcal{S} >^o - \rho^w \int_e T_0 \mathcal{O} dA &= 0 \\
\mu + \rho^w A^o \left(< \mathcal{R}^{sur} >^o + c + < \mathcal{R}^{rot} >^o\right) - \rho^w \int_e T_0 \mathcal{O} dA &= 0,
\end{aligned} \tag{S47}$$

where we have used the definition of sea-level change (Eq. S7) and of the OF variation (S27), we have taken advantage of SLE in the form given by Eq. (26) in SM19, $\mathcal{R}^{sur}$ and $\mathcal{R}^{rot}$ are the *surface* and the *rotation* sea-level response functions defined by Eqs. (27) and (28) of SM19, respectively, and the *ocean average* of a scalar function $F(\gamma, t)$ is defined as

$$< F >^o (t) \equiv \frac{1}{A^o} \int_o F(\gamma, t) dA, \tag{S48}$$

where label o stands for *ocean*, and the integration is over the region where $O = 1$ at time t. Hence, in an equivalent manner we can write

$$< F >^o (t) \equiv \frac{1}{A^o} \int_e F(\gamma, t) O(\gamma, t) dA, \tag{S49}$$

where now the integration is over the entire Earth's surface. Furthermore, being

$$A^o(t) = \int_o dA \tag{S50}$$

the area of the oceans, the ocean average of $F(\gamma,t)$ can be also expressed by

$$< F >^o (t) \equiv \frac{\int\limits_o F(\gamma,t) dA}{\int\limits_o dA}. \tag{S51}$$

The mass conservation constraint expressed by Eq. (S47) is now easily solved for the c constant, providing:

$$c(t) = \mathcal{S}^{ave} - < \mathcal{R}^{sur} >^o - < \mathcal{R}^{rot} >^o, \tag{S52}$$

where

$$\mathcal{S}^{ave}(t) = \mathcal{S}^{equ} + \mathcal{S}^{ofu} = < \mathcal{S} >^o \tag{S53}$$

is the average of over the oceans and we have defined two spatially invariant terms

$$\mathcal{S}^{equ}(t) \equiv -\frac{\mu}{\rho^w A^o} \tag{S54}$$

and

$$\mathcal{S}^{ofu}(t) \equiv \frac{1}{A^o} \int\limits_e T_0 \mathcal{O} dA. \tag{S55}$$

As discussed in SM19, terms $\mathcal{S}^{equ}(t)$ (*equivalent sea-level change*) and $\mathcal{S}^{ofu}(t)$ are both dependent upon variations of the OF caused by variations of the geometry of the oceans. We note that if a constant OF is imposed, as in the traditional Farrell and Clark (1976) (FC76) theory, $\mathcal{S}^{ofu}(t)$ vanishes and $\mathcal{S}^{equ}(t)$ is equivalent to $\mathcal{S}^{eus}(t)$, the *eustatic sea-level change* (this term is attributed to Suess, 1906). Substitution of Eq. (S52) into Eq. (26) of SM19 proves Eq. (31) of SM19.

S3 Earth models and Love numbers

In this section, we first describe the geometrical and physical features of the Earth models that can be adopted in the framework of *SELEN*^{4}. Then, we review the definition of loading and tidal Love numbers and we describe their form both in the time and in the Laplace domains. These constitute essential ingredients for the construction of the surface and of the rotational response functions which shall be introduced in later sections.

S3.1 Spherically symmetric models

The Earth models accessible by *SELEN*^{4}, and therefore considered in this theory supplement, are all characterised by the spherically symmetric structure shown in Figure S3. In the literature, these models are often referred to as "1-D GIA models", since the density field, the elastic and the rheological parameters only depend on radius r. However, note that since the surface load is distributed unevenly over the Earth's surface, the response of 1-D GIA models shall be 3-D, in general. The 1-D models had (and are still having) a fundamental role in the development of the Post Glacial Rebound (PGR) and of the GIA theories for a spherical Earth. References to fundamental papers on the subject are given below. The reader is also referred to Whitehouse (2009, 2018) and Spada (2017) for in-depth reviews of GIA and PGR.

In 1-D GIA modelling, it is assumed that: *i)* the Earth is isotropic, self-gravitating, and usually incompressible (*i.e.,* its volume is assumed to be constant), *ii)* the core is fluid, uniform, and inviscid (*i.e.,* with zero viscosity), *iii)* the Earth's mantle

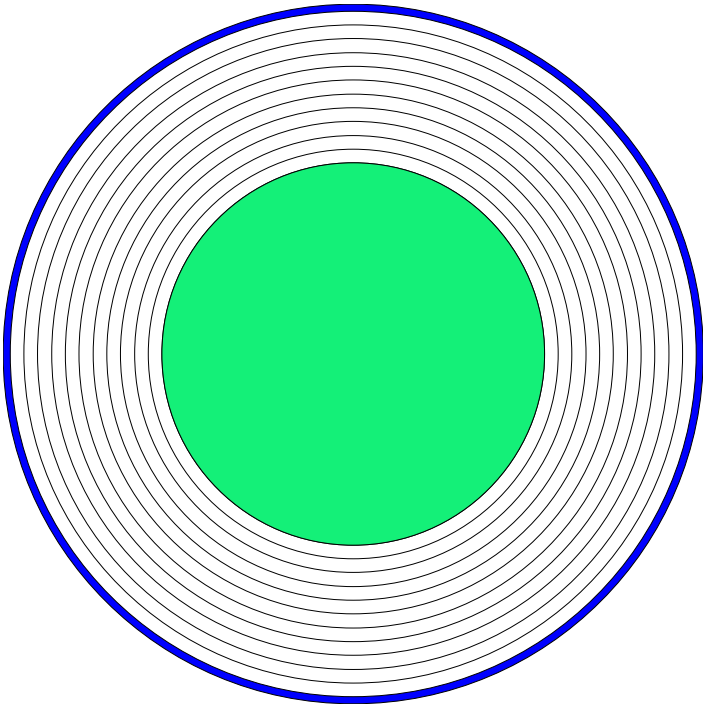

Figure S3. A 1-D (spherically symmetric) GIA model. The elastic lithosphere is in blue. The mantle is composed of N_v Maxwell viscoelastic layers of arbitrary thickness, rheological parameters, rigidity and density. The fluid uniform core is in green.

is spherically layered and characterised by a Maxwell linear viscoelastic rheology, *iv)* the lithosphere is purely elastic and characterised by a uniform thickness. For such 1-D GIA models, the response of the Earth is conveniently described by Love numbers (Love, 1911), for which closed-form solutions are available in some cases (Vermeersen et al., 1996a; Vermeersen and Sabadini, 1997). For the simplest 1-D model, constituted by a homogeneous incompressible sphere (the so-called *Kelvin Earth model*), an elegant analytical expression of the Love numbers is available (see *e.g.,* Munk and MacDonald, 1960). However, the complexity of the analytical solutions increases considerably with the number of layers, even excluding self-gravitation effects (see Wu and Ni, 1996). *SELEN*^{4} is designed to assimilate Love numbers of general multi-layered 1-D models. These are often computed making use of the well established *viscoelastic normal mode theory*, due to Peltier (1974), which indeed can be extended also to more advanced models, like those characterised by compressible (*e.g.,* Vermeersen et al., 1996b) or transient (*e.g.,* Yuen et al., 1986; Caron et al., 2017) rheologies.

Love numbers represent the response of the 1-D GIA models to a unit, localised and impulsive (*i.e.,* δ-like, where δ is Dirac's delta function) surface load or to a change in the external potential. In the first case they are referred to as *loading Love numbers* (LLNs), in the second case to as *tidal Love numbers* (TLNs). Here we only give the essentials on this subject in a quite informal manner; the reader is referred to Love (1911), Longman (1962), Longman (1963) and Farrell (1972) for the fundamental definitions, and to Peltier (1974), Lambeck (1980), Wu and Peltier (1982) and Wu and Peltier (1984) for a detailed discussion on the use of Love numbers in the context of GIA. For the relevance of Love numbers in the rotational dynamics

of the Earth, the reader is referred to Lambeck (1980) while for a condensed review also describing the various analytical and numerical methods available for the computation of the Love numbers, see Spada et al. (2011) and references therein. This same work also provides community-agreed, high-precision numerical values of Love numbers for realistic 1-D GIA models.

We remark that the values of the LLNs and TLNs of harmonic degree $l = 1$ depend on the choice of the origin of the reference frame adopted to describe the deformation and the change in the geopotential (*e.g.,* Spada et al., 2011). In the following, we assume that the Love numbers are expressed in the centre of mass (CM) reference frame of the system (Earth + Load). For a discussion, see *e.g.,* Greff-Lefftz and Legros (1997) and Greff-Lefftz (2000).

S3.2 Loading Love numbers

The '*k*' LLN determines, at harmonic degree l, the change in the gravitational potential of the Earth associated with the deformations induced by a localised surface load. In the framework of the viscoelastic normal modes theory (Peltier, 1974; Vermeersen et al., 1996a; Vermeersen and Sabadini, 1997), it is shown that the '*k*' LLN is a causal function characterised by two distinct parts. The first (*elastic part* of the LLN) is in-phase with the impulsive load and only depends on the elastic constants and density profile of the Earth, the second (*viscous part*) is also sensitive to the rheological profile and is characterised by a delayed multi-exponential form. Hence the '*k*' LLN has the general form

$$k_l^L(t) = k_l^{Le}\,\delta(t) + H(t)\,\sum_{i=1}^{M} k_{li}^L\,\mathrm{e}^{s_{li}t}, \tag{S56}$$

where k_l^{Le} is the elastic LLN, $H(t)$ is the unit step function defined by Eq. (S290), the terms k_{li}^L describe the viscous components of the LLN, each associated to frequency $s_{li} = -1/\tau_{li}$ where τ_{li} are the characteristic relaxation times of the Earth's model, and M is the number of viscoelastic normal modes, determined by the rheological layering. We note that the viscous part of the LLN has the form of a Prony series (*e.g.,* Tschoegl, 2012). In the special case of a rigid (*i.e.,* undeformable) Earth, we have $k_l^{Le} = k_{li}^L = 0$. The non-rigid response is, in general, determined by the (model dependent) values of k_l^{Le}, k_{li}^L, and s_{li}^L. In Eq. (S56) we note that $k_l^L(t)$ has dimensions of $[\mathrm{T}^{-1}]$; the same holds for k_{li}^L, while k_l^{Le} is non-dimensional.

In a similar way, it is possible to define a loading Love number '*h*' that determines, for each harmonic degree l, the vertical displacement of the Earth's surface in response to a localised load. Such LLN, which with '*k*' is an essential component of sea-level Green's function (see Eq. S88 below), has also the multi-exponential form

$$h_l^L(t) = h_l^{Le}\,\delta(t) + H(t)\,\sum_{i=1}^{M} h_{li}^L\,\mathrm{e}^{s_{li}t}, \tag{S57}$$

where h_l^{Le} and h_{li}^L describe the elastic and the viscous parts of $h_l^L(t)$, respectively, and the s_{li} are the same as for the '*k*' LLn (Eq. S56). For a rigid Earth, the surface load does not induce vertical displacements, hence $h_l^{Le} = h_{li}^L = 0$. Although horizontal movements do not enter into the sea-level Green's function, the expression for the LLN 'ℓ' corresponding to horizontal displacement is useful since GIA produces, in addition to gravity changes and vertical movements, significant horizontal movements, now detectable using ground-based geodetic techniques (see *e.g.,* King et al., 2010, and references therein). In analogy with the expressions for '*h*' and '*k*' above, 'ℓ' reads

$$\ell_l^L(t) = \ell_l^{Le}\,\delta(t) + H(t)\,\sum_{i=1}^{M} \ell_{li}^L\,\mathrm{e}^{s_{li}t}, \tag{S58}$$

where ℓ_l^{Le} and ℓ_{li}^L define the elastic and viscous parts of $\ell_l^L(t)$, respectively. The LLNs for horizontal displacements are also sometimes referred to as *Shida Love numbers* (Shida, 1912; Lambeck, 1980).

Since numerical methods for computing the LLNs very often rely upon the Correspondence Principle of linear viscoelasticity (*e.g.,* Tschoegl, 2012), it is useful to consider the Laplace transform (LT) of the LLNs, *i.e.,*

$$k_l^L(s) = k_l^{Le} + \sum_{i=1}^{M} \frac{k_{li}^L}{s - s_{li}} \tag{S59}$$

$$h_l^L(s) = h_l^{Le} + \sum_{i=1}^{M} \frac{h_{li}^L}{s - s_{li}} \tag{S60}$$

$$\ell_l^L(s) = \ell_l^{Le} + \sum_{i=1}^{M} \frac{\ell_{li}^L}{s - s_{li}}, \tag{S61}$$

where s is the complex Laplace variable (for the definition of LT and some basic LTs, the readers are referred to Table S2).

For incompressible and stably stratified Earth models (*i.e.,* models in which density is not varying in consequence of deformation, and the density is increasing with depth, the inverse decay times s_{li} are real-valued and negative (*e.g.,* Vermeersen et al., 1996a; Vermeersen and Sabadini, 1997; Spada et al., 2011). We note that the numerical values s_{li} and the number of modes M only depend on the density and rheological profile of the Earth model and not on the type of forcing, either loading or tidal, so that they are the same for the LLNs and the TLNs. At a given harmonic degree l, the s_{li} are roots of an algebraic equation of degree M in the Laplace domain, often referred to as *secular equation*

$$N_l(s) = 0, \tag{S62}$$

where the *secular polynomial* is

$$N_l(s) = \prod_{k=1}^{M} (s - s_{lk}) = \sum_{k=0}^{M} n_{kl} s^k, \tag{S63}$$

where n_{kl} are the (real-valued) coefficients of the polynomial. With varying harmonic degree, the s_{li}'s define the *spectrum of relaxation* of the Earth model (*e.g.,* Spada et al., 1992b). For the 1-D GIA model considered in this work (see Figure S3), $M = 4N_v$ where N_v is the number of Maxwell viscoelastic layers that compose the mantle (for a review and more details, see *e.g.,* Vermeersen et al., 1996a; Spada et al., 2011). For Earth models characterised by more complex rheologies, also including transient components of deformation (see *e.g.,* Sabadini et al., 1985; Yuen et al., 1986), the secular equation is still an algebraic equation, but M increases with N_v following different laws.

The *fluid* LLNs are defined as the values attained by the LLNs at long times, when a new state of equilibrium is reached after a unit step surface load has been applied (*i.e.,* after the Earth has *creeped*). These can be computed by taking the limit for $t \mapsto \infty$ of Eqs. (S56-S58) after convolving them with the unit step function $H(t)$, or, equivalently, taking the limit for $s \mapsto 0$ of Eqs. (S59-S61), thus obtaining

$$k_l^{Lf} = k_l^{Le} - \sum_{i=1}^{M} \frac{k_{li}^L}{s_{li}} \tag{S64}$$

$$h_l^{Lf} = h_l^{Le} - \sum_{i=1}^{M} \frac{h_{li}^L}{s_{li}} \tag{S65}$$

$$\ell_l^{Lf} = \ell_l^{Le} - \sum_{i=1}^{M} \frac{\ell_{li}^L}{s_{li}}, \tag{S66}$$

for the three LLNs, respectively. We note that the fluid values of the LLNs $\left(k_l^{Lf}, h_l^{Lf}, \ell_l^{Lf}\right)$ are dimensionless and do not depend upon the viscosity profile adopted, but they are sensitive to the density layering of the mantle (see *e.g.,* Spada et al., 2011).

	Time domain: $f(t) = LT^{-1}[f(s)]$	Laplace domain: $f(s) = LT\,[f(t)]$
1)	$f(t)$	$\int_0^{\infty} \mathrm{e}^{-st} f(t) dt$
2)	$\delta(t)$	1
3)	$H(t)$	$\frac{1}{s}$
4)	$H(t-\tau)$	$\frac{\mathrm{e}^{-s\tau}}{s}$
5)	e^{at}	$\frac{1}{s-a}$
6)	$H(t-\tau) \int_0^{t-\tau} f(t')dt'$	$\frac{\mathrm{e}^{-s\tau}}{s} f(s)$
7)	$f(t) * g(t)$	$f(s)g(s)$
8)	$\sum_{k=1}^{\nu} \frac{P(\alpha_k)}{Q'(\alpha_k)} \mathrm{e}^{\alpha_k t}$	$\frac{P(s)}{Q(s)}$

Table S2. Some Laplace transforms used in this supplement. In 1) the definition of Laplace Transform is given, where *LT* is the Laplace operator. In 7), symbol $*$ denotes time convolution, *i.e.,* $f(t) * g(t) = \int_{-\infty}^{+\infty} f(t-t')g(t')dt'$. In 8), polynomials $P(s)$ and $Q(s)$ are such that deg(P) < deg(Q) and constants α_k are the ν (distinct) roots of equation $Q(\alpha_k) = 0$, and $Q'(\alpha_k)$ is the derivative of $Q(s)$ computed at $s = \alpha_k$.

S3.3 Tidal Love numbers

According to the viscoelastic normal modes theory, the tidal Love numbers (TLNs) have the same multi-exponential form of the LLNs, but they correspond to different surface boundary conditions, since in this case the forcing is an external potential that does not load the Earth (Munk and MacDonald, 1960; Peltier, 1974; Wu and Peltier, 1982, 1984). Hence they are, in general, numerically distinct (and independent) from the LLNs (see *e.g.,* Spada et al., 2011). Note, however, that

$$k_l^L(t) = k_l^T - h_l^T \tag{S67}$$

and that more complex relationships exist between loading, tidal, and *shear* Love numbers (*e.g.,* Saito, 1974; Molodensky, 1977; Saito, 1978; Lambeck, 1980). Since changes in the centrifugal potential of the Earth are essentially expressed by harmonic functions of degree $l = 2$ (see Lambeck 1980 and §S8.4 below), TLNs of higher harmonic degrees have no direct role in GIA studies.

In close analogy with the expressions found for the LLNs, for the TLNs we thus write

$$k_l^T(t) = k_l^{Te}\,\delta(t) + H(t)\sum_{i=1}^{M} k_{li}^T\,\mathrm{e}^{s_{li}t} \tag{S68}$$

$$h_l^T(t) = h_l^{Te}\,\delta(t) + H(t)\sum_{i=1}^{M} h_{li}^T\,\mathrm{e}^{s_{li}t} \tag{S69}$$

$$\ell_l^T(t) = \ell_l^{Te}\,\delta(t) + H(t)\sum_{i=1}^{M} \ell_{li}^T\,\mathrm{e}^{s_{li}t}, \tag{S70}$$

with LTs

$$k_l^T(s) = k_l^{Te} + \sum_{i=1}^{M} \frac{k_{li}^T}{s - s_{li}} \tag{S71}$$

$$h_l^T(s) = h_l^{Te} + \sum_{i=1}^{M} \frac{h_{li}^T}{s - s_{li}} \tag{S72}$$

$$\ell_l^T(s) = \ell_l^{Te} + \sum_{i=1}^{M} \frac{\ell_{li}^T}{s - s_{li}}, \tag{S73}$$

and fluid limits

$$k_l^{Tf} = k_l^{Te} - \sum_{i=1}^{M} \frac{k_{li}^T}{s_{li}} \tag{S74}$$

$$h_l^{Tf} = h_l^{Te} - \sum_{i=1}^{M} \frac{h_{li}^T}{s_{li}} \tag{S75}$$

$$\ell_l^{Tf} = \ell_l^{Te} - \sum_{i=1}^{M} \frac{\ell_{li}^T}{s_{li}}. \tag{S76}$$

S4 Response to surface loads

In this section we introduce the *surface response functions* (SRFs), which at a given place and time describe the response of the Earth to surface loads in terms of gravity field variations, vertical displacements and relative sea-level change. As we shall see below in detail, from a mathematical standpoint the SRFs are given by spatio-temporal convolutions involving a particular Green's function (containing a suitable combination of LLNs) and the surface load variation function $\mathcal{L}$.

Here we shall consider three SRFs. The first, associated with height variations of the geoid, shall be denoted by $\mathcal{G}^{sur}$ and referred to as the "geoid SRF". The second, referred to as the "vertical displacement SRF", is associated with vertical displacements at the Earth's surface and denoted by $\mathcal{U}^{sur}$. These two SRFs are effectively independent, since as we shall see they are constructed using independent sets of loading Love numbers. The third SRF, *i.e.,* the "sea-level SRF", is defined by the difference

$$\mathcal{R}^{sur}(\gamma,t) = \mathcal{G}^{sur} - \mathcal{U}^{sur}, \tag{S77}$$

and is of particular importance, since it enters directly into the SLE. Our purpose here is to make the three SRFs explicit, also providing formulas for their expansion in series of complex spherical harmonics (CSH), an essential prerequisite for the numerical solution of the SLE.

We note that additional SRFs for other geophysical quantities can be defined as well, such as those for horizontal displacements, gravity anomalies, tilts, *etc.*. These are constructed using Green's functions which entail specific combinations of the three LLNs, and will be considered in future editions of this supplement.

S4.1 Surface Green's functions

All the SRFs have the form

$$\mathcal{SRF}(\gamma,t) = \mathrm{GF} \otimes \mathcal{L}, \tag{S78}$$

where $\mathrm{GF}(\alpha,t)$ is a general *surface Green's function* describing the response to an impulsive load acting at time $t=0$, $\mathcal{L}(\gamma,t)$ is the surface load variation defined in §S2.3, and symbol $\otimes$ denotes the 3-D spatio-temporal convolution

$$(\mathrm{GF} \otimes \mathcal{L})(\gamma,t) \equiv \int_{-\infty}^{+\infty} dt' \int_{e} \mathrm{GF}(\alpha, t-t')\mathcal{L}(\gamma',t')dA', \tag{S79}$$

which implies a 1-D time convolution and a 2-D spatial convolution over the sphere, where α is the angular distance between $\gamma=(\theta,\lambda)$ (the observer) and $\gamma'=(\theta',\lambda')$ (each of the points where the load is applied), given by the law of cosines in spherical trigonometry

$$\cos\alpha = \cos\theta\cos\theta' + \sin\theta\sin\theta'\cos(\lambda-\lambda') \tag{S80}$$

and

$$dA' = a^2 d\gamma' = a^2 \sin\theta' d\theta' d\lambda', \tag{S81}$$

where a is the average Earth radius.

Surface GF for the geoid. Following Eq. (S78), for the geoid SRF we write

$$\mathcal{G}^{sur}(\gamma,t) = \Gamma^g \otimes \mathcal{L}, \tag{S82}$$

where according to *e.g.,* Wu and Peltier (1982) the surface GF for the geoid is

$$\Gamma^g(\alpha,t) \equiv \frac{a}{m^e}\sum_{l=0}^{\infty}\left(\delta(t)+k_l^L(t)\right)P_l(\cos\alpha), \tag{S83}$$

where m^e is Earth's mass, $P_l(\cos\alpha)$ is the degree l Legendre polynomial (see §S8.5), and $k_l^L(t)$ is the gravity potential LLN defined in §S3.2. The impulsive term $\delta(t)$ accounts for the direct effect of the load on changes of the geoid height, while $k_l^L(t)$ describes the indirect effect induced by elastic and viscous deformation. Thus, Γ^g does not vanish in the case of a rigid Earth (*i.e.,* for $k_l^L=0$).

In this supplement and in the numerical implementation of the theory, we shall only consider *physically plausible* surface loads which obey the principle of mass conservation. According to the results of §S2.4, this means that the spherical harmonics expansion of the surface load variation is identically zero, in agreement with Eq. (S42). Since in Eq. (S82) $\mathcal{G}^{sur}$ depends upon the load linearly (the convolution $\otimes$ indeed is a linear operator), a vanishing $\mathcal{L}_{00}(t)$ would imply a vanishing SRF regardless the actual value of the *degree 0* LLNs. For a discussion on LLNs in the presence of mass conserving surface loads, the reader is also referred to Farrell (1972).

We observe that in the reference frame with origin in the Earth CM (including the solid and fluid portions), which is conventionally adopted here since this seems to us to be the most natural choice, there will be no first-degree terms in the

spherical harmonic expansion of the gravitational potential (Hofmann-Wellenhof and Moritz, 2006), nor of its variation in response to surface loads (Greff-Lefftz and Legros, 1997; Greff-Lefftz, 2000). Hence, there must be no degree $l = 1$ terms in the expansion of Γ^g in Eq. (S83). This means that $\delta(t) + k_1^L(t)$ must vanish. Recalling the expression for $k_l^L(t)$ (Eq. S56), this condition is met if $k_1^{Le} = -1$ and $k_{1i}^{Le} = 0$ $(i = 1, 2, \dots M)$. Our following numerical results are consistent with these conditions. Note that other choices are possible, as discussed in Greff-Lefftz and Legros (1997); for instance, in Farrell (1972), the LLNs are expressed in the reference frame with origin at the centre of the undeformed Earth (often this point is indicated as CE).

Surface GF for vertical displacement. According to Eqs. (S78) and (S82), this SRF has the form

$$\mathcal{U}^{sur}(\gamma, t) = \Gamma^u \otimes \mathcal{L}, \tag{S84}$$

where the surface GF for vertical displacement is defined as

$$\Gamma^u(\alpha, t) \equiv \frac{a}{m^e} \sum_{l=0}^{\infty} h_l^L(t) P_l(\cos\alpha), \tag{S85}$$

where $h_l^L(t)$ is the LLN for vertical displacement (Wu and Peltier, 1982). We observe that *i)* since $h_l^L(t)$ is independent on $k_l^L(t)$, $\mathcal{U}^{sur}$ and $\mathcal{G}^{sur}$ are mutually independent, *ii)* contrary to $\mathcal{G}^{sur}$, there is no "direct effect" accounted for in $\mathcal{U}^{sur}$, hence the vertical displacement SRF vanishes for a rigid Earth, *i.e.,* for $h_l^L(t) = 0$, and that *iii)* differently from $k_1^L(t)$, $h_1^L(t)$ is not *a priori* constrained by the choice of the origin of the reference frame in the CM of the whole Earth; its value is numerically determined by the solution of the equilibrium equations (see Spada et al. 2011).

Surface GF for sea level. According to Eq. (S78), the sea-level SRF[1]

$$\mathcal{R}^{sur}(\gamma, t) = \Gamma^s \otimes \mathcal{L}, \tag{S86}$$

where, consistently with Eqs. (S77), (S82) and (S84), the surface GF for sea level Γ^s is

$$\Gamma^s(\alpha, t) \equiv \Gamma^g - \Gamma^u, \tag{S87}$$

hence

$$\Gamma^s(\alpha, t) \equiv \frac{a}{m^e} \sum_{l=0}^{\infty} \left(\delta(t) + k_l^L(t) - h_l^L(t)\right) P_l(\cos\alpha). \tag{S88}$$

We observe that Γ^s has dimensions of $[\mathrm{T}^{-1}\mathrm{LM}^{-1}]$ and that the same holds for Γ^g and Γ^u (note that both $\delta(t)$ and the LLNs have dimensions of $[\mathrm{T}^{-1}]$). Accordingly, $\mathcal{R}^{sur}$ and the other two SRFs considered above, *i.e.,* $\mathcal{G}^{sur}$ and $\mathcal{U}^{sur}$, have dimensions of [L].

To lighten the computations needed to expand $\mathcal{R}^{sur}$ in series of CSH, which shall be accomplished in the following section, it is convenient to define the particular combination of LLNs

$$\eta_l^L(t) = \delta(t) + k_l^L(t) - h_l^L(t), \tag{S89}$$

so that Eq. (S88) simply reads

$$\Gamma^s(\alpha, t) \equiv \frac{a}{m^e} \sum_{l=0}^{\infty} \eta_l^L(t) P_l(\cos\alpha). \tag{S90}$$

[1]Since $\mathcal{R}^{sur}$ is a response function for *sea level*, a more appropriate definition for it could be $\mathcal{S}^{sur}$, probably. However, this could lead to some confusion with symbol $\mathcal{S}$ (sea-level change) that already appears in the SLE. Indeed, the superscript s in Γ^s recalls that we are dealing with sea level.

It is interesting to note that, by virtue of the relationship between LLNs and TLNs given by Eq. (S67), we have

$$\eta_l^L(t) = \delta(t) + k_l^T(t), \tag{S91}$$

showing that the *surface* GF for sea level $\Gamma^s(\alpha,t)$, and consequently the SRF $\mathcal{S}^{sur}$ can be expressed only in terms of the 'k' tidal Love number.

S4.2 Sea-level surface response function

Using the surface load decomposition given by Eq. (S29) into (S86) leads to

$$\mathcal{R}^{sur}(\gamma,t) = \mathcal{R}^a + \mathcal{R}^b + \mathcal{R}^c, \tag{S92}$$

where each of the three terms on the right hand side has the form

$$R(\gamma,t) \equiv \Gamma^s \otimes \rho\mathcal{F}, \tag{S93}$$

in which according to Eqs. (S30-S32), $\rho\mathcal{F} = \rho^i\mathcal{W}$, $\rho\mathcal{F} = \rho^w\mathcal{Z}$ and $\rho\mathcal{F} = \rho^r\mathcal{O}$ for terms $\mathcal{R}^a$, $\mathcal{R}^b$ and $\mathcal{R}^c$, respectively, and $\mathcal{F}$ is a causal piecewise constant (PC) function, defined in §S8.1 (see, in particular, Eq. S296). From Eq. (S93), using (S90) and (S79), and recalling that $dA = a^2 d\gamma$, for R we obtain

$$\begin{aligned}
R(\gamma,t) &= \int_{-\infty}^{+\infty} dt' \int_e \Gamma^s(\alpha,t-t')\,\rho\mathcal{F}(\gamma',t')dA' \\
&= \frac{a^3\rho}{m^e}\int_{-\infty}^{+\infty} dt' \int_\gamma \left(\sum_{l=0}^{\infty} \eta_l^L(t-t')P_l(\cos\alpha)\right)\mathcal{F}(\gamma',t')d\gamma' \\
&= \frac{a^3\rho}{m^e}\sum_{l=0}^{\infty}\int_{-\infty}^{+\infty} dt'\ \eta_l^L(t-t')\int_\gamma P_l(\cos\alpha)\,\mathcal{F}(\gamma',t')d\gamma'.
\end{aligned}$$

We now transform $P_l(\cos\alpha)$ by the Addition Theorem (Eq. S426), we expand $\mathcal{F}$ in series of CSHs according to (S297), and use the orthogonality property (S423) of the spherical harmonics to obtain

$$\begin{aligned}
R(\gamma,t) &= \frac{a^3\rho}{m^e}\sum_{lm}\frac{1}{2l+1}\int_{-\infty}^{+\infty} dt'\ \eta_l^L(t-t')\int_\gamma \mathcal{Y}^*_{lm}(\gamma')\mathcal{Y}_{lm}(\gamma)\mathcal{F}(\gamma',t')d\gamma' \\
&= \frac{a^3\rho}{m^e}\sum_{lm}\frac{1}{2l+1}\int_{-\infty}^{+\infty} dt'\ \eta_l^L(t-t')\int_\gamma \mathcal{Y}^*_{lm}(\gamma')\mathcal{Y}_{lm}(\gamma)\sum_{l'm'}\mathcal{F}_{l'm'}(t')\mathcal{Y}_{l'm'}(\gamma')d\gamma' \\
&= \frac{a^3\rho}{m^e}\sum_{lm}\frac{1}{2l+1}\int_{-\infty}^{+\infty} dt'\ \eta_l^L(t-t')\sum_{l'm'}\mathcal{F}_{l'm'}(t')\mathcal{Y}_{lm}(\gamma)\int_\gamma \mathcal{Y}^*_{lm}(\gamma')\mathcal{Y}_{l'm'}(\gamma')d\gamma' \\
&= \frac{4\pi a^3\rho}{m^e}\sum_{lm}\frac{1}{2l+1}\int_{-\infty}^{+\infty} dt'\ \eta_l^L(t-t')\sum_{l'm'}\mathcal{F}_{l'm'}(t')\mathcal{Y}_{lm}(\gamma)\delta_{ll'}\delta_{mm'} \\
&= \frac{4\pi a^3\rho}{m^e}\sum_{lm}\frac{1}{2l+1}\left(\int_{-\infty}^{+\infty}\eta_l^L(t-t')\mathcal{F}_{lm}(t')dt'\right)\mathcal{Y}_{lm}(\gamma),
\end{aligned} \tag{S94}$$

which represents an expansion in series of CSHs

$$R(\gamma,t)=\sum_{lm}R_{lm}(t)\mathcal{Y}_{lm}(\gamma), \tag{S95}$$

with coefficients

$$R_{lm}(t)=\frac{3\rho}{\rho^e}\frac{C_{lm}}{2l+1}, \tag{S96}$$

where

$$\rho^e=\frac{3m^e}{4\pi a^3} \tag{S97}$$

is the Earth's average density and C_{lm} is the time convolution in parentheses in Eq. (S94).

With the aid of the normal mode forms of the LLNs (Eqs. S56 and S57), and using definition (S89), the time convolution is easily transformed, obtaining

$$\begin{aligned} C_{lm}(t) &\equiv \int_{-\infty}^{+\infty}\big(\delta(t-t')+k_l^L(t-t')-h_l^L(t-t')\big)\mathcal{F}_{lm}(t')dt' \\ &= (1+k_l^{Le}-h_l^{Le})\int_{-\infty}^{+\infty}\delta(t-t')\mathcal{F}_{lm}(t')dt'+\sum_{i=1}^{M}(k_{li}^L-h_{li}^L)\int_{-\infty}^{+\infty}H(t-t')\,\mathrm{e}^{s_{li}(t-t')}\mathcal{F}_{lm}(t')dt'= \\ &= (1+k_l^{Le}-h_l^{Le})\mathcal{F}_{lm}(t)+\sum_{i=1}^{M}(k_{li}^L-h_{li}^L)\int_{-\infty}^{t}\mathrm{e}^{s_{li}(t-t')}\mathcal{F}_{lm}(t')dt', \end{aligned} \tag{S98}$$

where we have used the sifting property of Dirac's delta[2] and the definition of unit step function (Eq. S290). Hence by substituting into Eq. (S96) we obtain

$$R_{lm}(t)=R_{lm}^e+R_{lm}^v, \tag{S99}$$

where the elastic and viscous components of R_{lm} are

$$R_{lm}^e(t)=\frac{3\rho}{\rho^e}e_l^s\mathcal{F}_{lm}(t) \tag{S100}$$

with

$$e_l^s=\frac{1+k_l^{Le}-h_l^{Le}}{2l+1} \tag{S101}$$

and

$$R_{lm}^v(t)=\frac{3\rho}{\rho^e}\frac{1}{2l+1}\sum_{i=1}^{M}\big(k_{li}^L-h_{li}^L\big)\int_{-\infty}^{t}\mathrm{e}^{s_{li}(t-t')}\mathcal{F}_{lm}(t')dt', \tag{S102}$$

respectively.

[2]The sifting property of Dirac's delta $\delta(t)$ reads $\int_{-\infty}^{+\infty}f(t)\delta(t-t_0)dt=f(t_0)$, see *e.g., http://mathworld.wolfram.com/SiftingProperty.html*.

Since $\mathcal{F}(\gamma,t)$ is stepwise constant

$$\mathcal{F}(\gamma,t)=\sum_{k=0}^{N}\left(\mathcal{F}_{k+1}(\gamma)-\mathcal{F}_{k}(\gamma)\right)H(t-t_k), \tag{S103}$$

according to Eq. (S299) the expansion coefficients $\mathcal{F}_{lm}(t)$ in (S100) and (S102) are stepwise constant as well:

$$\mathcal{F}_{lm}(t)=\sum_{k=0}^{N}\Delta\mathcal{F}_{lm,k}H(t-t_k), \tag{S104}$$

where $\Delta\mathcal{F}_{lm,k}$ is given by Eq. (S301) for $k=0,\dots N$. Thus the elastic component of R_{lm} is

$$R^{e}_{lm}(t)=\frac{3\rho}{\rho^{e}}\,e^{s}_{l}\sum_{k=0}^{N}\Delta\mathcal{F}_{lm,k}H(t-t_k). \tag{S105}$$

Using Eq. (S104), the integral that appears in the expression for the viscous component (S102) becomes

$$\begin{aligned}
\int_{-\infty}^{t}\mathrm{e}^{s_{li}(t-t')}\mathcal{F}_{lm}(t')dt' &= \sum_{k=0}^{N}\Delta\mathcal{F}_{lm,k}\int_{-\infty}^{t}\mathrm{e}^{s_{li}(t-t')}H(t'-t_k)dt' \\
&= \sum_{k=0}^{N}\Delta\mathcal{F}_{lm,k}\,H(t-t_k)\int_{t_k}^{t}\mathrm{e}^{s_{li}(t-t')}dt' \\
&= \sum_{k=0}^{N}\Delta\mathcal{F}_{lm,k}\,H(t-t_k)\,\mathrm{e}^{s_{li}t}\left[-\frac{1}{s_{li}}\mathrm{e}^{-s_{li}t'}\right]_{t_k}^{t} \\
&= \sum_{k=0}^{N}\Delta\mathcal{F}_{lm,k}\,H(t-t_k)\left(-\frac{1}{s_{li}}\right)\,\mathrm{e}^{s_{li}t}\left(\mathrm{e}^{-s_{li}t}-\mathrm{e}^{-s_{li}t_k}\right) \\
&= \sum_{k=0}^{N}\Delta\mathcal{F}_{lm,k}\,H(t-t_k)\left(\frac{\mathrm{e}^{s_{li}(t-t_k)}-1}{s_{li}}\right),
\end{aligned} \tag{S106}$$

hence

$$R^{v}_{lm}(t)=\frac{3\rho}{\rho^{e}}\sum_{k=0}^{N}\Delta\mathcal{F}_{lm,k}\,\beta_l(t-t_k)H(t-t_k), \tag{S107}$$

where we have defined

$$\beta^{s}_{l}(t)\equiv\frac{1}{2l+1}\sum_{i=1}^{M}\frac{k^{L}_{li}-h^{L}_{li}}{s_{li}}\left(\mathrm{e}^{s_{li}t}-1\right). \tag{S108}$$

Substituting Eqs. (S105) and (S107) into (S99), we conclude that the coefficients of the CSHs expansion of the generic SRF are

$$R_{lm}(t)=\frac{3\rho}{\rho^{e}}\sum_{k=0}^{N}\Delta\mathcal{F}_{lm,k}\,\left(e^{s}_{l}+\beta^{s}_{l}(t-t_k)\right)H(t-t_k), \tag{S109}$$

hence, according to Eq. (S92), for the individual harmonic components of $\mathcal{R}^{sur}(\gamma,t)$ we obtain:

$$\mathcal{R}^a_{lm}(t) = \frac{3\rho^i}{\rho^e}\sum_{k=0}^{N}\Delta\mathcal{W}_{lm,k}\left(e^s_l+\beta^s_l(t-t_k)\right)H(t-t_k) \tag{S110}$$

$$\mathcal{R}^b_{lm}(t) = \frac{3\rho^w}{\rho^e}\sum_{k=0}^{N}\Delta\mathcal{Z}_{lm,k}\left(e^s_l+\beta^s_l(t-t_k)\right)H(t-t_k) \tag{S111}$$

$$\mathcal{R}^c_{lm}(t) = \frac{3\rho^r}{\rho^e}\sum_{k=0}^{N}\Delta\mathcal{X}_{lm,k}\left(e^s_l+\beta^s_l(t-t_k)\right)H(t-t_k). \tag{S112}$$

We close this section with a consideration about the harmonic degree $l=0$ component of the SRF $\mathcal{R}^{sur}(\gamma,t)$. From Eqs. (S92) and (S110-S112) we have

$$\begin{aligned}
\mathcal{R}^{sur}_{00}(t) &= \mathcal{R}^a_{00}+\mathcal{R}^b_{00}+\mathcal{R}^c_{00}\\
&= \frac{3}{\rho^e}\sum_{k=0}^{N}\left(\rho^i\Delta\mathcal{W}_{00,k}+\rho^w\Delta\mathcal{Z}_{00,k}+\rho^r\Delta\mathcal{X}_{00,k}\right)\left(e^s_l+\beta^s_l(t-t_k)\right)H(t-t_k)\\
&= \frac{3}{\rho^e}\sum_{k=0}^{N}\Delta\mathcal{L}_{00,k}\left(e^s_l+\beta^s_l(t-t_k)\right)H(t-t_k)\\
&= \frac{3}{\rho^e}\sum_{k=0}^{N}\left(\mathcal{L}_{00,k+1}-\mathcal{L}_{00,k}\right)\left(e^s_l+\beta^s_l(t-t_k)\right)H(t-t_k)\\
&= 0,
\end{aligned} \tag{S113}$$

since we are considering mass conserving surface loads, for which with $\mathcal{L}_{00}(t)=0$ (see §S2.4).

S4.3 Other surface response functions

Following the same procedure outlined in previous section, it is possible to decompose the $\mathcal{G}^{sur}$ and $\mathcal{U}^{sur}$ SRFs in individual contributions associated with the surface load components $\mathcal{L}^a$, $\mathcal{L}^b$ and $\mathcal{L}^b$, respectively.

In particular, in analogy with Eqs. (S110-S112), for the geoid SRF we have

$$\mathcal{G}^{sur}(\gamma,t)=\mathcal{G}^a+\mathcal{G}^b+\mathcal{G}^c, \tag{S114}$$

with

$$\mathcal{G}^{sur}_{lm}(t)=\mathcal{G}^a_{lm}+\mathcal{G}^b_{lm}+\mathcal{G}^c_{lm}, \tag{S115}$$

where

$$\mathcal{G}^a_{lm}(t) = \frac{3\rho^i}{\rho^e}\sum_{k=0}^{N}\Delta\mathcal{W}_{lm,k}\left(e^g_l+\beta^g_l(t-t_k)\right)H(t-t_k) \tag{S116}$$

$$\mathcal{G}^b_{lm}(t) = \frac{3\rho^w}{\rho^e}\sum_{k=0}^{N}\Delta\mathcal{Z}_{lm,k}\left(e^g_l+\beta^g_l(t-t_k)\right)H(t-t_k) \tag{S117}$$

$$\mathcal{G}^c_{lm}(t) = \frac{3\rho^r}{\rho^e}\sum_{k=0}^{N}\Delta\mathcal{X}_{lm,k}\left(e^g_l+\beta^g_l(t-t_k)\right)H(t-t_k), \tag{S118}$$

with

$$e_l^g = \frac{1+k_l^{Le}}{2l+1} \tag{S119}$$

and

$$\beta_l^g(t) \equiv \frac{1}{2l+1}\sum_{i=1}^{M}\frac{k_{li}^L}{s_{li}}\left(\mathrm{e}^{s_{li}t}-1\right). \tag{S120}$$

Similar expressions hold for the vertical displacement SRF, with:

$$\mathcal{U}^{sur}(\gamma,t) = \mathcal{U}^a + \mathcal{U}^b + \mathcal{U}^c, \tag{S121}$$

where the coefficient of the harmonic expansion are

$$\mathcal{U}_{lm}^{sur}(t) = \mathcal{U}_{lm}^a + \mathcal{U}_{lm}^b + \mathcal{U}_{lm}^c, \tag{S122}$$

with

$$\mathcal{U}_{lm}^a(t) = \frac{3\rho^i}{\rho^e}\sum_{k=0}^{N}\Delta\mathcal{W}_{lm,k}\left(e_l^u+\beta_l^u(t-t_k)\right)H(t-t_k) \tag{S123}$$

$$\mathcal{U}_{lm}^b(t) = \frac{3\rho^w}{\rho^e}\sum_{k=0}^{N}\Delta\mathcal{Z}_{lm,k}\left(e_l^u+\beta_l^u(t-t_k)\right)H(t-t_k) \tag{S124}$$

$$\mathcal{U}_{lm}^c(t) = \frac{3\rho^r}{\rho^e}\sum_{k=0}^{N}\Delta\mathcal{X}_{lm,k}\left(e_l^u+\beta_l^u(t-t_k)\right)H(t-t_k), \tag{S125}$$

where we have defined

$$e_l^u = \frac{h_l^{Le}}{2l+1} \tag{S126}$$

and

$$\beta_l^u(t) \equiv \frac{1}{2l+1}\sum_{i=1}^{M}\frac{h_{li}^L}{s_{li}}\left(\mathrm{e}^{s_{li}t}-1\right). \tag{S127}$$

We note, in closing, that by the same argument we have used for $\mathcal{R}_{00}^{sur}(t)$ in Eq. (S113), for the geoid SRF and for the surface displacement SRF we have

$$\mathcal{G}_{00}^{sur}(t) = 0 \tag{S128}$$

$$\mathcal{U}_{00}^{sur}(t) = 0, \tag{S129}$$

respectively, since we are assuming a mass conserving (or *plausible*) surface load. Using Eq. (S432), we can equivalently state that the whole-Earth-surface averages are

$$<\mathcal{G}^{sur}(\gamma,t)>^e = 0 \tag{S130}$$

$$<\mathcal{U}^{sur}(\gamma,t)>^e = 0, \tag{S131}$$

which are useful for the interpretation of the geodetic fingerprints of GIA in §S8.9.

S5 Polar motion

Polar motion (or wobble) is the motion of the rotation axis with respect to the Earth's crust (Lambeck, 1980).

The rotational behavior of the Earth in response to geophysical excitations is governed by the Liouville equations, which have been discussed in various treaties (see *e.g.,* Routh, 1905; Munk and MacDonald, 1960; Lambeck, 1980, and references therein). They are obtained by imposing the conservation of angular momentum for a rotating deformable body. For small displacements of the rotation axis, the Liouville equations can be decoupled into two sets of equations, describing polar motion and the variations of the length-of-day, respectively (Lambeck, 1980). For the purpose of modeling rotational effects on sea-level change, it is not necessary to consider the problem of the length-of-day variations. Hence, we deal with the Liouville equations for polar motion, which constitute a set of two coupled linear ordinary differential equations.

S5.1 Liouville equations

The (linearised) Liouville equations are traditionally written[3] as

$$i\frac{\dot{\mathbf{m}}}{\sigma_r} + \mathbf{m} = \mathbf{\Psi}, \tag{S133}$$

where the dot denotes the time derivative,

$$\mathbf{m}(t) \equiv m_1 + i m_2 = \frac{1}{\Omega}(\omega_1 + i\omega_2) \tag{S134}$$

represents the displacement of the pole of rotation, $i = \sqrt{-1}$ is the imaginary unit, Ω is the mean angular velocity of the Earth, ω_1 and ω_2 are the cartesian x and y components of the Earth's angular velocity vector $\overrightarrow{\omega} = (\omega_1, \omega_2, \omega_3)$ in a rotating (non-inertial) reference frame, respectively. Furthermore

$$\mathbf{\Psi}(t) = \Psi_1 + i\Psi_2 \tag{S135}$$

is the *polar motion excitation function*, and the constant

$$\sigma_r = \left(\frac{C - A}{C}\right)\Omega \approx \frac{1}{306}\ \mathrm{d}^{-1} \tag{S136}$$

is the Euler precession frequency for a rigid Earth, C and A being the observed polar and equatorial moments of inertia (Lambeck, 1980). Hereinafter, we shall only consider small excursions of the pole of rotation; hence Eqs. (S133) are consistent with the assumptions $|\mathbf{m}| \ll 1$ and $m_3 \ll 1$, where m_3 is defined by

$$(1 + m_3) = \frac{\omega_3}{\Omega}. \tag{S137}$$

For a more general non-linear approach, also valid for large displacements of the axis of rotation, the reader is referred to *e.g.,*Spada et al. (1992a) and Ricard et al. (1993).

Following Lambeck (1980), here we consider two sources of polar motion excitation separately. The first one is associated with loads acting at the Earth's surface, like for example the waning and waxing continental ice sheets; the second is associated

[3] As mentioned by Munk and MacDonald (1960), quoting the work of Routh (1905), these equations were first obtained by Liouville in 1858. We note that the linearised Liouville equations can be also expressed in a real, matrix form as

$$\frac{1}{\sigma_r}\begin{pmatrix} \dot{m}_x \\ \dot{m}_y \end{pmatrix} + \begin{pmatrix} 0 & 1 \\ -1 & 0 \end{pmatrix}\begin{pmatrix} m_x \\ m_y \end{pmatrix} = \begin{pmatrix} -\Psi_x \\ \Psi_y \end{pmatrix}. \tag{S132}$$

with the rotationally-induced deformations. Here we do not consider possible contributions arising from external torques and momentum transferred to the solid Earth from its fluid portions, which would constitute another source of excitation.

Accordingly, $\mathbf{\Psi}$ can be split into two parts as follows

$$\mathbf{\Psi}(t) = \mathbf{\Psi}^{sur} + \mathbf{\Psi}^{rot} \tag{S138}$$

where $\mathbf{\Psi}^{sur}$ and $\mathbf{\Psi}^{rot}$ are associated to the surface and to the rotation excitations, respectively. While $\mathbf{\Psi}^{sur}$ shall be made explicit below, for $\mathbf{\Psi}^{rot}$ we have

$$\mathbf{\Psi}^{rot}(t) = \frac{k_2^T(t)}{k^s} * \mathbf{m}, \tag{S139}$$

where $k_2^T(t)$ is the degree 2 'k' TLN (see §S3.3), symbol $*$ denotes the operation of time convolution (for the definition of time convolution, see Table S2) and the *secular 'k' Love number* is

$$k^s = \frac{3(C-A)G}{\Omega^2 R_e^5} \simeq 0.942, \tag{S140}$$

where $G = 6.67 \times 10^{-11}$ N m^2 kg^{-2} is the universal gravitational constant, R_e is the equatorial radius of the Earth, and the observed values of C, A, R_e and Ω have been used (Lambeck, 1980).

Substitution of Eq. (S139) into (S133) through (S138) gives

$$i\frac{\dot{\mathbf{m}}}{\sigma_r} + \left(\delta(t) - \frac{k_2^T(t)}{k^s}\right) * \mathbf{m} = \mathbf{\Psi}^{sur}, \tag{S141}$$

where the first term can be neglected when $\mathbf{m}$ varies on time scales exceeding $2\pi/\sigma_r \approx 10$ months. This is fully appropriate in GIA modelling, since the late-Pleistocene ice sheets are evolving on time scales millennia, thus not causing an excitation the "fast" Chandler wobble (Lambeck, 1980), but simply a drift of the mean pole of rotation. Hence, the form of the Liouville equations suitable for GIA studies is

$$\left(\delta(t) - \frac{k_2^T(t)}{k^s}\right) * \mathbf{m} = \mathbf{\Psi}^{sur}. \tag{S142}$$

Dealing with the Liouville equations, it is often convenient to work in the Laplace domain, since this allows to transform time convolutions into simple products and differential equations into algebraic equations (*e.g.,* Tschoegl, 2012). Thus, taking the fundamental property of the time convolution into account (see Table S2), the LT of Eq. (S142) is

$$\left(1 - \frac{k_2^T(s)}{k^s}\right) \mathbf{m}(s) = \mathbf{\Psi}^{sur}(s), \tag{S143}$$

where $k_2^T(s)$, $\mathbf{m}(s)$ and $\mathbf{\Psi}^{sur}(s)$ are the LTs of $k_2^T(t)$, $\mathbf{m}(t)$, and $\mathbf{\Psi}^{sur}(t)$, respectively.

S5.2 Rotation theories

As first pointed by Mitrovica et al. (2005) and later rediscussed in depth by Mitrovica and Wahr (2011), in GIA modeling it is possible to approach the solution of Eq. (S143) into two distinct ways. This is related with the interpretation of the meaning of the secular 'k' Love number, which in previous section has been evaluated using observed values of the relevant geodetic quantities. A problem arises when the secular 'k' is to be employed for a specific GIA model. Indeed, in GIA modelling it is customary to employ Earth models characterised by a lithosphere of finite strength, something that is considered appropriate in view of the relatively short time scale of GIA, compared to the time scale of mantle convection. However, for Earth models that

include such a feature, the long-term equilibrium rotational shape may well differ from the observed shape, due to the elastic stress "frozen" in the elastic lithosphere, even assuming that the Earth has been spinning for a very long time.

Traditional rotation theory. Many previous studies have been based on the so-called *traditional rotation theory*, briefly illustrated by *e.g.,*Spada et al. (2011). In this framework, is assumed that

$$k^s = \lim_{s \mapsto 0} k_2^T(s) \equiv k_2^{Tf}, \tag{S144}$$

i.e., that the secular Love number coincides with the fluid 'k' TLN k_2^{Tf} characterising the employed Earth model (see Eq. S74), possibly including an elastic lithosphere having a long-term finite strength. In conjunction with a coarse description of the Earth's density profile that is sometimes adopted in GIA modelling (*e.g.,* Spada et al., 1992b, 2011) using Eq. (S144) may lead to significant inaccuracies in the prediction of the present-day rate of polar motion.

New (or revised) rotation theory. The *new (or revised) rotation theory* (Mitrovica et al., 2005; Mitrovica and Wahr, 2011), suggests that the k^s values employed in GIA modelling should not depend upon the Earth's elasticity, and that a density closely matching the seismically determined profile (*e.g.,* the PREM profile, see Dziewonski and Anderson 1981) should be employed in order to accurately describe the Earth's rotational response. Furthermore, the k^s value should also account for the Earth's excess ellipticity. Accordingly, they have proposed to model the secular Love number as

$$k^s \equiv k_2^{Tf}(LT = 0) + k^{ee}, \tag{S145}$$

where $k_2^{Tf}(LT = 0)$ is the fluid 'k' TLN of an effectively fluid Earth, characterised by a viscous lithosphere and a PREM density profile, and k^{ee} is a small correction associated to the excess ellipticity. Following Nakiboglu (1982) and Mitrovica and Wahr (2011), in *SELEN*^{4} we have adopted the numerical value $k^{ee} = 0.0082$.

As discussed in detail in Mitrovica and Wahr (2011), the two rotation theories predict responses that differ qualitatively and quantitatively, with the revised one implying a less significant impact of GIA long-wavelength (harmonic degree $l = 2$) geodetic signatures compared to the traditional theory, and a reduced rate of polar drift. In *SELEN*^{4}, both theories can be employed. We remark that in both cases the fast Chandler wobble is filtered out since the onset, according to Eq. (S142).

S5.3 Polar motion transfer function

Regardless the rotational theory adopted (either traditional or revised), the Liouville equations in the Laplace domain (S143) can be formally solved to obtain

$$\mathbf{m}(s) = \mathcal{A}(s)\mathbf{\Psi}^{sur}(s), \tag{S146}$$

where

$$\mathcal{A}(s) = \left(1 - \frac{k_2^T(s)}{k^s}\right)^{-1} \tag{S147}$$

is the *polar motion transfer function* (PMTF). We note that, in the time domain, Eq. (S146) would correspond to the time convolution

$$\mathbf{m}(t) = \mathcal{A}(t) * \mathbf{\Psi}^{sur}(t). \tag{S148}$$

Relationship (S146) can be used to provide a physical interpretation for the PMTF. Indeed, assuming an excitation function $\mathbf{\Psi}(t) \sim \delta(t)$ where the tilde denotes proportionality, and recalling that the LT of a Dirac delta is 1 (see Table S2), from (S148) we would obtain $\mathcal{A}(t) \sim \mathbf{m}(t)$, showing that the PMTF physically represents the polar motion driven by a impulsive (*i.e.,*

δ-like) surface excitation. We also observe that obtaining $\boldsymbol{\Psi}^{sur}(t)$ assuming the knowledge of $\mathcal{A}(t)$ and some astronomical or geodetic observation of $\mathbf{m}(t)$ constitutes a classical deconvolution problem (Lambeck, 1980).

The PMTF is studied in detail in §S8.2, where it is shown that it can be cast in the general form

$$\mathcal{A}(s) = A^e + \frac{A^s}{s} + \sum_{i=1}^{M'} \frac{A_i}{s - a_i}, \tag{S149}$$

where constants A^e, A^s, A_i and a_i, which depend upon the rheological layering of the Earth, are known in the literature as *elastic rotational residue*, *secular rotational residue*, *rotational residues*, and *rotational roots*, respectively (*e.g.,* Spada et al., 2011). All these constants turn out to be quite complex combinations of degree $l = 2$ LLNs and TLNs. Accordingly, using the LT Table (S2), in the time domain the PMTF reads

$$\mathcal{A}(t) = A^e\,\delta(t) + A^s\,H(t) + H(t)\sum_{i=1}^{M'} A_i \mathrm{e}^{a_i t}. \tag{S150}$$

Furthermore, in §S8.2 it is also shown that when the *traditional rotation theory* is employed, we have

$$M' = M - 1 \quad \text{and} \quad A^s \neq 0, \tag{S151}$$

where M is the number of modes, while adopting the *new (or revised) rotation theory* one obtains

$$M' = M \quad \text{and} \quad A^s = 0, \tag{S152}$$

in agreement with Mitrovica and Wahr (2011). In both cases, A^e, A^s, A_i are numerically found to be real-valued (*i.e.,* their imaginary parts are negligible in front of their real parts), and all the a_i's are real-valued and negative that ensures the asymptotic stability of Eq. (S150). We are not aware, however, of theoretical arguments that can justify and provide a motivation for the numerical evidence.

S5.4 Surface loading excitation function

To solve explicitly the Liouville equations (Eq. S146) we need, in addition to the PMTF (S149), an expression for the excitation function $\boldsymbol{\Psi}^{sur}$ that accounts for variations of the Earth's inertia tensor associated with *surface loading*. We note that $\boldsymbol{\Psi}^{rot}$, *i.e.,* the polar motion excitation function associated with the rotation-induced deformation, given by Eq. (S139), has been already assimilated in the PMTF.

Following *e.g.,* Lambeck (1980), the excitation function for surface loading, also referred to as *matter excitation function*, is defined as

$$\boldsymbol{\Psi}^{sur}(t) = \frac{\mathbf{J}^{sur}}{C - A}, \tag{S153}$$

with

$$\mathbf{J}^{sur}(t) = J_{13} + iJ_{23}, \tag{S154}$$

where J_{13} and J_{23} are *variations* (relative to the reference state defined in §S8.1) of the corresponding inertia tensor components induced by surface loading. According to *e.g.,* Ricard et al. (1992), we have

$$\mathbf{J}^{sur}(t) = \big(\delta(t) + k_2^L(t)\big) * \mathbf{J}^{rig}(t) \tag{S155}$$

where $*$ is time convolution, the 'k' LLN of harmonic degree $l = 2$ accounts for the isostatic compensation of the surface load, and $\mathbf{J}^{rig}$ is the inertia variation for a rigid Earth (*i.e.,* $\mathbf{J}^{sur} = \mathbf{J}^{rig}$ for $k_2^L = 0$). Therefore, from Eq. (S153) we obtain

$$\boldsymbol{\Psi}^{sur}(t) = \big(\delta(t) + k_2^L(t)\big) * \boldsymbol{\Psi}^{rig}(t), \tag{S156}$$

where the surface loading excitation function for a rigid Earth is

$$\mathbf{\Psi}^{rig}(t) = \frac{\mathbf{J}^{rig}}{C-A}. \tag{S157}$$

In the analysis of §S8.3 it is shown that $\mathbf{J}^{rig}$ is only determined by the time-variations of the degree $l = 2$ and order $m = \pm 1$ components of the surface load. In consequence of that

$$\mathbf{\Psi}^{rig}(t) = c_{21}^{\psi} \sum_{k=0}^{N} \Delta\mathcal{L}_{21,k}^{*} H(t - t_k), \tag{S158}$$

where the asterisk denotes complex conjugation,

$$\Delta\mathcal{L}_{21,k} = \mathcal{L}_{21,k+1} - \mathcal{L}_{21,k}\,, \tag{S159}$$

and where c_{21}^{ψ} is a positive constant given explicitly by Eq. (S371). In closing, we note that from Table S2 the LT of $\mathbf{\Psi}^{rig}(t)$ can be expressed as

$$\mathbf{\Psi}^{rig}(s) = c_{21}^{\psi} \sum_{k=0}^{N} \Delta\mathcal{L}_{21,k}^{*} \frac{\mathrm{e}^{-st_k}}{s}. \tag{S160}$$

S5.5 Solution of Liouville equations

We have now all the elements needed to solve explicitly the Liouville equations for GIA. By substitution of Eq. (S156) into (S148), we obtain the polar motion displacement in the form of a double time convolution

$$\mathbf{m}(t) = \mathcal{A}(t) * \left(\delta(t) + k_2^L(t)\right) * \mathbf{\Psi}^{rig}(t), \tag{S161}$$

which in the Laplace domain corresponds to the double product

$$\mathbf{m}(s) = \mathcal{A}(s)\left(1 + k_2^L(s)\right)\mathbf{\Psi}^{rig}(s). \tag{S162}$$

It is now convenient to define a *modified PMTF* as

$$\mathcal{A}'(s) \equiv \mathcal{A}(s)\left(1 + k_2^L(s)\right) \tag{S163}$$

which, according to the analysis performed in §S8.2, has the spectral form

$$\mathcal{A}'(s) = A'^{e} + \frac{A'^{s}}{s} + \sum_{i=1}^{M'} \frac{A'_i}{s - a_i}, \tag{S164}$$

where A'^{e}, A'^{s} and A'_i are appropriate constants obtained from A^e, A^s and A_i.

Hence, substituting Eqs. (S160) and (S163) into (S162) using (S164) gives

$$\mathbf{m}(s) = \sum_{k=0}^{N} \psi_k^{rig} \left(A'^{e} + \frac{A'^{s}}{s} + \sum_{i=1}^{M'} \frac{A'_i}{s - a_i} \right) \frac{\mathrm{e}^{-st_k}}{s}, \tag{S165}$$

where we have set

$$\psi_k^{rig} = c_{21}^{\psi} \Delta\mathcal{L}_{21,k}^{*}. \tag{S166}$$

Using the Laplace transforms Table S2, Eq. (S165) can be easily inverted back into the time domain giving

$$\mathbf{m}(t) = \sum_{k=0}^{N} \psi_k^{rig} \left(A'^e + A'^s (t - t_k) + \sum_{i=1}^{M'} \frac{A'^i}{a_i} \left(\mathrm{e}^{a_i (t - t_k)} - 1 \right) \right) H(t - t_k), \tag{S167}$$

which represents the sought explicit solution of the Liouville equations for polar motion.

We note that, taking the time derivative of Eq. (S167) and ignoring δ-like terms arising from the time derivative of $H(t)$, the *rate of polar motion* can be expressed as

$$\dot{\mathbf{m}}(t) = \sum_{k=0}^{N} \psi_k^{rig} \left(A'^s + \sum_{i=1}^{M'} A'^i \mathrm{e}^{a_i (t - t_k)} \right) H(t - t_k). \tag{S168}$$

S6 Rotational response

Here we study of the Earth's response to variations in the centrifugal potential. There are analogies with the theory framework adopted for the surface response functions (SRFs, see §S4.2), but also some important differences. As we have done for the SRFs, here we introduce three rotation response functions (RRFs), *i.e.,* the "geoid RRF" ($\mathcal{G}^{rot}$), the "vertical displacement RRF" ($\mathcal{U}^{rot}$) and the "sea-level RRF" ($\mathcal{R}^{rot}$). The latter, which enters directly into the SLE (see Eq. 31 in SM19), is defined by the difference

$$\mathcal{R}^{rot}(\gamma, t) = \mathcal{G}^{rot} - \mathcal{U}^{rot}. \tag{S169}$$

As we did previously for the SRFs, our purpose is to determine explicit expressions for the three RRFs, providing in particular the CSH expansions which are necessary for the numerical implementation of the SLE in *SELEN*[4].

S6.1 Rotation Green's functions

The harmonic component of the three RRFs considered here (*i.e.,* $\mathcal{G}^{rot}$, $\mathcal{U}^{rot}$, and $\mathcal{R}^{rot}$) have all the general form

$$\mathcal{RRF}_{lm}(t) = \mathrm{GF}_l * \Lambda_{lm}, \tag{S170}$$

where here $\mathrm{GF}_l(t)$ denotes the corresponding *rotation Green's function*, $\Lambda_{lm}(t)$ is degree l and order m harmonic component of the change of centrifugal potential associated with variations in the Earth's angular velocity (see §S8.4), and $*$ denotes the 1-D temporal convolution, *i.e.,*

$$\left(\mathrm{GF}_l * \Lambda_{lm}\right)(t) \equiv \int_{-\infty}^{+\infty} \mathrm{GF}_l(t - t') \Lambda_{lm}(t') dt', \tag{S171}$$

as opposed to the 3-D spatio-temporal convolution employed in the construction of the SRFs (see Eq. S79). For a further clarification about this important difference, the reader is referred to Milne and Mitrovica (1998).

Rotation GF for the geoid. Following Eq. (S170), for the geoid RRF we write

$$\mathcal{G}_{lm}^{rot}(t) = \Upsilon_l^g * \Lambda_{lm}, \tag{S172}$$

where the rotation GF for the geoid is defined by

$$\Upsilon_l^g(t) \equiv \frac{1}{g} \left(\delta(t) + k_l^T(t) \right), \tag{S173}$$

where $k_l^T(t)$ is the degree l tidal 'k' Love number introduced in §S3.3, and g is the reference surface gravity acceleration. The term $\delta(t)$ represents the direct effect of the change in centrifugal potential upon $\mathcal{G}^{rot}$, while $k_l^T(t)$ describes the indirect effect induced by rotational deformation. Thus, the geoid RRF would not vanish in the case of a rigid Earth (*i.e.,* for $k_l^T = 0$). We note that, contrary to the surface geoid GF for surface loads (Eq. S83), the rotation GF $\Upsilon_l^g(t)$ does not imply a sum over the harmonic degrees; for this reason, the l-dependence remains explicit (Milne and Mitrovica, 1998). Furthermore, $\Upsilon_l^s(t)$ does not depend upon the coordinates of the 'observer' $\gamma = (\theta, \lambda)$.

It is interesting to observe that, by virtue of the relationship between LLNs and TLNs expressed by Eq. (S67), the rotation GF for the geoid could be expressed only in terms of loading Love numbers, with

$$\Upsilon_l^g(t) \equiv \frac{1}{g}\left(\delta(t) + k_l^L(t) - h_l^L(t)\right). \tag{S174}$$

Rotation GF for vertical displacement. According to Eq. (S170), the vertical displacement RRF is

$$\mathcal{U}_{lm}^{rot}(t) = \Upsilon_l^u * \Lambda_{lm}, \tag{S175}$$

with the rotation GF for vertical displacement given by

$$\Upsilon_l^u(t) \equiv \frac{1}{g} h_l^T(t), \tag{S176}$$

where $h_l^T(t)$ is the tidal 'h' Love number at harmonic degree l, introduced in §S3.3 (Milne and Mitrovica, 1998). We observe that since $h_l^T(t)$ and $k_l^T(t)$ are mutually independent, $\mathcal{U}^{rot}$ and $\mathcal{G}^{rot}$ are also mutually independent. We also note that, contrary to $\mathcal{G}^{rot}$, for a rigid Earth $\mathcal{U}^{rot}$ vanishes, since in this case $h_l^T(t) = 0$ by definition.

Rotation GF for sea level. According to Eq. (S170), the sea-level RRF is

$$\mathcal{R}_{lm}^{rot}(t) = \Upsilon_l^s * \Lambda_{lm}, \tag{S177}$$

where consistently with Eqs. (S169), (S172) and (S175), the GF is given by the difference

$$\Upsilon_l^s(t) = \Upsilon_l^g - \Upsilon_l^u, \tag{S178}$$

hence

$$\Upsilon_l^s(t) \equiv \frac{1}{g}\left(\delta(t) + k_l^T(t) - h_l^T(t)\right). \tag{S179}$$

We note that Υ_l^s has dimensions of [TL^{-1}] and that the same holds for Υ_l^g and Υ_l^u. Hence, $\mathcal{R}^{rot}$ in Eq. (S177) has dimensions of [L], like $\mathcal{G}^{rot}$ and $\mathcal{U}^{rot}$.

S6.2 Rotation response functions

To obtain explicit expressions for the RRFs, it is convenient to consider the geoid RRF ($\mathcal{G}^{rot}$) first. The expression for vertical displacement ($\mathcal{U}^{rot}$) has a similar structure, while the sea-level RRF ($\mathcal{R}^{rot}$) is simply given by the difference between $\mathcal{G}^{rot}$ and $\mathcal{U}^{rot}$. The details follow.

Rotation response function for the geoid. According to its definition (S172), the geoid RRF in the Laplace domain reads

$$\mathcal{G}_{lm}^{rot}(s) = \Upsilon_l^g(s)\Lambda_{lm}(s), \tag{S180}$$

where taking Eq. (S408) into account, gives

$$\mathcal{G}_{lm}^{rot}(s) = c_{21}^{\lambda}\Upsilon_l^g(s)\delta_{l2}\delta_{m\pm1}\mathbf{m}^*(s), \tag{S181}$$

showing that the only non-vanishing coefficients are those of degree $l=2$ and order $m=\pm 1$, expressed by

$$\begin{aligned}\mathcal{G}_{21}^{rot}(s) &= c_{21}^{\lambda}\Upsilon_2^g(s)\,\mathbf{m}^*(s)\\ &= \frac{c_{21}^{\psi}c_{21}^{\lambda}}{g}\sum_{k=0}^{N}\Delta\mathcal{L}_{21,k}\left(1+k_2^{Te}+\sum_{i=1}^{M}\frac{k_{2i}^T}{s-s_{2i}}\right)\left(A'^e+\frac{A'^s}{s}+\sum_{i=1}^{M'}\frac{A_i'}{s-a_i}\right)\frac{\mathrm{e}^{-st_k}}{s},\end{aligned} \tag{S182}$$

where we have used the definition of the rotation GF for the geoid (Eq. S173), the LT of the 'k' TLN (Eq. S71), the solution of the Liouville equations (Eq. S165), the expression for the surface excitation function (Eq. S160), and where we have also taken advantage of the fact that A'^e, A'^s, A_i' and a_i are real-valued constants. We now note that the product of the two factors in parentheses above is analogous to the product $\left(1+k_2^L(s)\right)\mathcal{A}(s)$ that defines the modified PMTF in Eq. (S163). Thus, without the need of further computations, we arrive at

$$\mathcal{G}_{21}^{rot}(s)=\frac{c_{21}^{\psi}c_{21}^{\lambda}}{g}\sum_{k=0}^{N}\Delta\mathcal{L}_{21,k}\left(g'^e+\frac{g'^s}{s}+\sum_{i=1}^{M'}\frac{g_i'}{s-a_i}+\sum_{i=1}^{M}\frac{g_i''}{s-s_i}\right)\frac{\mathrm{e}^{-st_k}}{s}, \tag{S183}$$

where, according to Eqs. (S358-S361) and (S355-S356), we have introduced the new constants

$$\begin{aligned}g'^e &= \left(1+k_2^{Te}\right)A'^e,\\ g'^s &= \left(1+k_2^{Tf}\right)A'^s,\\ g_i' &= \left(1+k_2^{Te}+\sum_{i'=1}^{M}\frac{k_{2i'}^T}{a_i-s_{i'}}\right)A_i'\equiv\left(1+k_2^T(a_i)\right)A_i',\quad (i=1,\ldots,M')\\ g_i'' &= \left(A'^e+\frac{A'^s}{s_i}+\sum_{i'=1}^{M'}\frac{A_{i'}'}{s_i-a_{i'}}\right)k_{2i}^T\equiv\mathcal{A}'(s_i)\,k_{2i}^T,\quad (i=1,\ldots,M).\end{aligned}$$

Using Table S2, the inverse LT of Eq. (S183) is now readily found, giving the time-domain degree $l=2$ and order $m=1$ CSH coefficient of the geoid RRF:

$$\mathcal{G}_{21}^{rot}(t)=\frac{c_{21}^{\psi}c_{21}^{\lambda}}{g}\sum_{k=0}^{N}\Delta\mathcal{L}_{21,k}\,\gamma^g(t-t_k)\,H(t-t_k), \tag{S184}$$

where all the other coefficients are identically zero, except $\mathcal{G}_{2-1}^{rot}=-(\mathcal{G}_{21}^{rot})^*$, and where we have defined the function

$$\gamma^g(t)\equiv g'^e+g'^s t+\sum_{i=1}^{M'}\frac{g_i'}{a_i}\left(\mathrm{e}^{a_i t}-1\right)+\sum_{i=1}^{M}\frac{g_i''}{s_i}\left(\mathrm{e}^{s_i t}-1\right). \tag{S185}$$

Rotation response function for vertical displacement. Following its definition (S175), the LT of the vertical displacement RRF is

$$\mathcal{U}_{lm}^{rot}(s)=\Upsilon_l^u(s)\Lambda_{lm}(s), \tag{S186}$$

formally identical to the geoid RRF (Eq. S180), but with the important difference that the GF $\Upsilon_l^u(s)$ contains the 'h' TLN instead of the combination '1+k' (this can be seen comparing Eq. S176 with S173). However, it is clear that we can immediately take advantage of the computations above for $\mathcal{G}_{lm}^{rot}$, by making the appropriate substitutions. In particular, in analogy with Eq. (S183), we write

$$\mathcal{U}_{21}^{rot}(s)=\frac{c_{21}^{\psi}c_{21}^{\lambda}}{g}\sum_{k=0}^{N}\Delta\mathcal{L}_{21,k}\left(u'^e+\frac{u'^s}{s}+\sum_{i=1}^{M'}\frac{u_i'}{s-a_i}+\sum_{i=1}^{M}\frac{u_i''}{s-s_i}\right)\frac{\mathrm{e}^{-st_k}}{s}, \tag{S187}$$

where now the constants u'^e, u'^s, u'_i and u''_i are defined as

$$
\begin{aligned}
u'^e &= h_2^{Te}\, A'^e, \\
u'^s &= h_2^{Tf}\, A'^s, \\
u'_i &= \left(h_2^{Te} + \sum_{i'=1}^{M} \frac{h_{2i'}^T}{a_i - s_{i'}} \right) A'_i \equiv h_2^T(a_i)\, A'_i, \quad (i = 1, \ldots, M') \\
u''_i &= \left(A'^e + \frac{A'^s}{s_i} + \sum_{i'=1}^{M'} \frac{A'_{i'}}{s_i - a_{i'}} \right) h_{2i}^T \equiv \mathcal{A}'(s_i)\, h_{2i}^T, \quad (i = 1, \ldots, M).
\end{aligned}
$$

Hence, by the same arguments used for the geoid RRF, we can conclude that

$$
\mathcal{U}_{21}^{rot}(t) = \frac{c_{21}^{\psi} c_{21}^{\lambda}}{g} \sum_{k=0}^{N} \Delta\mathcal{L}_{21,k}\, \gamma^u(t - t_k)\, H(t - t_k), \tag{S188}
$$

all the other coefficients being identically zero, except $\mathcal{U}_{2-1}^{rot} = -(\mathcal{U}_{21}^{rot})^*$, with

$$
\gamma^u(t) \equiv u'^e + u'^s t + \sum_{i=1}^{M'} \frac{u'_i}{a_i} \left(\mathrm{e}^{a_i t} - 1 \right) + \sum_{i=1}^{M} \frac{u''_i}{s_i} \left(\mathrm{e}^{s_i t} - 1 \right). \tag{S189}
$$

Rotation response function for sea level. Since, by definition, $\mathcal{R}^{rot} = \mathcal{G}^{rot} - \mathcal{U}^{rot}$ (see Eq. S169), we immediately conclude, from Eqs. (S184) and (S188), that

$$
\mathcal{R}_{21}^{rot}(t) = \frac{c_{21}^{\psi} c_{21}^{\lambda}}{g} \sum_{k=0}^{N} \Delta\mathcal{L}_{21,k} \gamma^s(t - t_k) H(t - t_k), \tag{S190}
$$

with

$$
\gamma^s(t) = \gamma^g - \gamma^u, \tag{S191}
$$

where γ^g and γ^u are given by Eqs. (S185) and (S189), respectively.

S7 Numerical discretisation of the SLE

In this section, we aim at providing discrete forms of all the terms which appear in the SLE, in view of the numerical implementation in *SELEN*^{4}. The time discretisation is performed on the 1-D grid introduced in §S8.1 below. The spatial discretisation on the surface of the sphere is carried out by either a direct evaluation of the field variables on a spherical grid or by a spectral approach based on the CSH functions, defined in §S8.5. For the spatial discretisation and for the computation of the required surface integrals, we take advantage of the properties of the equal-area, icosahedron-shaped, spherical pixelization introduced by Tegmark (1996) and described in §S8.6. The material presented in this section extends the analysis first presented by Spada and Stocchi (2006) and Spada and Stocchi (2007). A summary of the discretised variables considered in this Section is given in Table S3.

For the reader's convenience, from SM19 we recall that the SLE, in its ultimate "ocean-projected" form, reads

$$
\mathcal{Z}(\gamma, t) = \mathcal{Z}^{ave} + \mathcal{K}^a + \mathcal{K}^b(\mathcal{Z}) + \mathcal{K}^c + \mathcal{K}^{rot}(\mathcal{Z}), \tag{S192}
$$

where the unknown is

$$\mathcal{Z}(\gamma,t) = O\mathcal{S} \tag{S193}$$

where O is the OF, $\mathcal{S}$ is sea-level change, and

$$\mathcal{Z}^{ave}(t) = O\mathcal{S}^{ave} = O\left(\mathcal{S}^{equ} + \mathcal{S}^{ofu}\right), \tag{S194}$$

with $\mathcal{S}^{equ}$ and $\mathcal{S}^{ofu}$ given by Eqs. (S54) and (S55), and

$$\mathcal{K}^{abc}(\gamma,t) \equiv O\mathcal{R}'^{\,abc} \tag{S195}$$
$$\mathcal{K}^{rot}(\gamma,t) \equiv O\mathcal{R}'^{\,rot}, \tag{S196}$$

where

$$\mathcal{R}'^{\,abc}(\gamma,t) = \mathcal{R}^{abc} - <\mathcal{R}^{abc}>^{o} \tag{S197}$$
$$\mathcal{R}'^{\,rot}(\gamma,t) = \mathcal{R}^{rot} - <\mathcal{R}^{rot}>^{o}, \tag{S198}$$

where $\mathcal{R}^{abc}$ denotes each of the three components of the sea-level SRF, $\mathcal{R}^{rot}$ is the sea-level RRF and $<\cdots>^{o}$ indicates the ocean-average.

Our purpose here is to discretise the variables contained in the SLE (S192), in order to reduce it to a spectral form that easily admits a numerical implementation, which shall read as follows

$$\mathcal{Z}_{j,n} = \mathcal{Z}^{ave}_{j,n} + \mathcal{K}^{a}_{j,n} + \mathcal{K}^{b}_{j,n}(\mathcal{Z}) + \mathcal{K}^{c}_{j,n} + \mathcal{K}^{rot}_{j,n}(\mathcal{Z}), \tag{S199}$$

where j stands for lm and subscript n denotes a given time $t = t_n$. The maximum range of harmonics to be included in the discretisation (*i.e.,* l_{max}) shall depend upon the spatial resolution that is to be achieved and from the available computing power. In SM19, we examine the effects of truncating the CSH series to increasing values of l_{max} in a test run of *SELEN*^{4} having some geophysical significance. The maximum range of index n (*i.e.,* N) shall be suggested from the specific chronology of the ice sheets employed in the simulation.

In the following subsections, all the terms in Eq. (S192) and (S194-S198) shall be considered and analyzed in detail. Of course, our ensuing analysis shall also provide convenient forms for all the terms that appear into the "lower level" SLE

$$\mathcal{S}_{j,n} = \mathcal{S}^{ave}_{j,n} + \mathcal{R}'^{\,a}_{j,n} + \mathcal{R}'^{\,b}_{j,n}(\mathcal{Z}) + \mathcal{R}'^{\,c}_{j,n} + \mathcal{R}'^{\,rot}_{j,n}(\mathcal{Z}), \tag{S200}$$

which represents the discretised counterpart of Eq. (39) in SM19.

Notation and conventions. To deal with discretised fields, henceforth we use the following notation and conventions. With $F_{p,n}$ we indicate the scalar field $F(\gamma,t)$ evaluated on a given pixel of coordinates $\gamma_p = (\theta_p, \lambda_p)$ and at time $t = t_n$, where t_n is a point of the time grid that we have conventionally adopted in this work (see §S8.1). Hence we define

$$F_{p,n} \equiv F(\gamma_p, t_n), \tag{S201}$$

where $p = (1,\dots P)$ and $n = (0,\dots N+1)$. The coefficient of the CSH expansion of $F(\gamma,t)$, evaluated at time $t = t_n$, shall be denoted by

$$F_{j,n} \equiv F_j(t_n), \tag{S202}$$

where $j = lm$ indicates a couple of harmonic degrees and orders. Furthermore, to denote a CSH computed at a given grid point of coordinates γ_p, we shall conventionally write

$$\mathcal{Y}_{j,p} \equiv \mathcal{Y}_j(\gamma_p). \tag{S203}$$

Finally, a spatially invariant quantity like *e.g.,* $\mu(t)$, evaluated at time $t = t_n$, shall be simply denoted as

$$\mu_n \equiv \mu(t_n). \tag{S204}$$

Note that confusion between symbols $F_{j,n}$ (Eq. S202) and $F_{p,n}$ (S201) should be easily avoided, since henceforth letters j (or j') will always denote the couple composed by harmonic degree and order lm (or $l'm'$), subscript n (or k) always represents a point on the time grid, while letters p (or p') conventionally indicate a generic pixel on the sphere. Thus, for instance $\mathcal{X}_{j,k}$ indicates a spectral quantity (as denoted by symbol j) that represents the harmonic coefficient of the CSH expansion of field $\mathcal{X}(\gamma,t)$, evaluated at time $t = t_k$, while $U_{p',n}$ denotes scalar function $U(\gamma,t)$ in the spatial domain, evaluated at a pixel of coordinates $\gamma_{p'}$ and time $t = t_n$. Similarly, $T_{p,0}$ indicates the field $T(\gamma,t)$ (*i.e.,* topography) at pixel γ_p and time $t = t_0$. Furthermore, to indicate the (4π-normalised) CSHs, we shall always employ the calligraphic symbol $\mathcal{Y}$ (see §S8.5). Hence, for example, $\mathcal{Y}_{j',p}$ unequivocally identifies the CSH of degree and order $j' = l'm'$, evaluated on the grid at the pixel placed at coordinates γ_p.

S7.1 Ice thickness, topography and ocean function

In this section, we consider the discretised forms of ice thickness $I(\gamma,t)$, of topography $T(\gamma,t)$, and of the ocean function $O(\gamma,t)$. While for variables I and T a discretisation in space and in time is sufficient for solving the SLE, the OF also needs to be decomposed in the spectral domain, since its harmonic coefficients are explicitly required by the solution algorithm; these shall be determined exploiting the properties of the Tegmark grid.

Ice thickness. The ice thickness distribution is the basic input of *SELEN*[4], along with a description of the Earth's rheology. We assume to know the function $I(\gamma,t)$, *i.e.,* the ice thickness at any location and time, based on *a priori* geological information, *ad hoc* hypotheses, glaciological arguments, or reconstructions published in the literature. These typically constrain the time-evolution of ice thickness distribution by the knowledge of Relative Sea Level (RSL) at specific locations since the Last Glacial Maximum (LGM, $\sim 21{,}000$ years ago), using predictions obtained by solving the SLE. Hence, we assume that the array

$$I_{p,n} \equiv I(\gamma_p, t_n), \tag{S205}$$

where $p = (1,\dots P)$ and $n = (0,\dots N+1)$, is given *a priori*. The choice of the time step $\Delta t = t_{k+1} - t_k$ that characterises the time-discretisation in *SELEN* (see §S8.1) is indeed made according to the natural time step of the ice chronology. Typical values in GIA modelling are $\Delta t = 1000$ or $\Delta t = 500$ years. We also note that ice models currently employed in GIA studies[4] are normally defined on traditional, cartesian latitude-longitude grids. Pixelised versions of these datasets, characterised by different spatial resolutions, are made available with the *SELEN*[4] package.

Topography. Consistent with our conventions on notation, at time $t = t_n$, the discretised topography is

$$T_{p,n} \equiv T(\gamma_p, t_n), \tag{S206}$$

where we use the same grid employed to describe the ice thickness distribution in Eq. (S205), $\gamma_p = (\theta_p, \lambda_p)$ denotes the pixels coordinates with $p = (1,\dots P)$, and time is labelled by n, with $n = (0,\dots N+1)$.

Array $T_{p,n}$ is however not known *a priori*. Indeed, according to Eq. (S2) the past topography (or *paleo-topography*) is determined by the history of the sea-level variations, which is not known in advance, *i.e.,* before the SLE is solved. Indeed, the present-day relief serves as a "final condition" for the Earth topography, in order to constrain its evolution in the past. In this way, paleo-topography can be iteratively reconstructed using the PT equation given by Eq. (S10), which in discretised form reads

$$T_{p,n} = T_{p,N} - (\mathcal{S}_{p,n} - \mathcal{S}_{p,N}), \tag{S207}$$

[4]Some of the more recent models belonging to the ICE-*X* family are available from the home page of Prof. WR Peltier, see *http:// www.atmosp.physics.utoronto.ca/ peltier/data.php* - last accessed Jan. 23, 2019.

where $T_{p,N}$ is topography at present time ($t = t_N$), and $\mathcal{S}_{p,n}$ is sea-level change at a given time $t = t_n$ and at pixel γ_p, as given by the SLE in Eq. (S200). Using the definition of *true paleo-topography* TP (see Eq. S11), we have

$$PT_{p,n} = T_{p,n} + I_{p,n}, \tag{S208}$$

where $I_{p,n}$ is the input array containing the ice thickness, and $T_{p,n}$ is given by Eq. (S207).

In *SELEN*^{4}, the present topography is based on the global relief dataset ETOPO1 (see Amante and Eakins, 2009; Eakins and Sharman, 2012). ETOPO1 is provided [5] on a traditional cartesian longitude-latitude grid with a resolution of 1 arc-minute[6], so it needs to be interpolated on the pixels of the Tegmark grid before the code is run. With *SELEN*^{4}, suitably interpolated datasets are provided, characterised by different spatial resolutions.

Ocean function. From its definition

$$O(\gamma, t) \equiv \begin{cases} 1, & \text{if } T + \dfrac{\rho^i}{\rho^w} I < 0 \\ 0, & \text{if } T + \dfrac{\rho^i}{\rho^w} I \geq 0, \end{cases} \tag{S209}$$

the OF is totally determined by I and T. On the Tegmark grid, the OF is written as

$$O_{p,n} \equiv O(\gamma_p, t_n) \equiv \begin{cases} 1, & \text{if } T_{p,n} + \dfrac{\rho^i}{\rho^w}\, I_{p,n} < 0 \\ 0, & \text{if } T_{p,n} + \dfrac{\rho^i}{\rho^w}\, I_{p,n} \geq 0, \end{cases} \tag{S210}$$

where we have used the discretised forms of the topography (Eq. S206) and of the ice thickness distribution (S205), respectively. Hence, by its own definition, the CF is discretised as

$$C_{p,n} = 1 - O_{p,n}. \tag{S211}$$

According to Eq. (S452), the harmonic coefficients of the CSH expansion of the OF, *i.e.,*

$$O_j(t) = \frac{1}{4\pi} \int_\gamma O(\gamma, t) \mathcal{Y}_j^*(\gamma) d\gamma \tag{S212}$$

are found by quadrature on the grid as

$$O_{j,n} = \frac{1}{P} \sum_p O_{p,n} \mathcal{Y}_{j,p}^*, \tag{S213}$$

where the discrete values $O_{p,n}$ are obtained from Eq. (S210). Using the definition of CF, its harmonic coefficients are

$$C_{j,n} = \delta_{l0}\delta_{m0} - O_{j,n}. \tag{S214}$$

S7.2 Spatially invariant terms

In the SLE, several spatially invariant terms appear (see in particular Eq. S192 and those that follow immediately). Most of them shall be analysed here, in order to provide discretised forms suitable for the numerical solution of the SLE. However, note that some others shall be discussed in later sections devoted to the surface and rotational response of the Earth.

[5] See *https://www.ngdc.noaa.gov/mgg/global/* - last accessed 26 Feb 2019.

[6] One arc-minute is $(1/60)^\circ$ and corresponds to an arc of latitude of ~ 1.85 km.

Ocean averages. The ocean-average of a function $F(\gamma,t)$ is a spatially invariant term that often appears in the treatment of the SLE. It is defined as

$$< F >^o (t) \equiv \frac{\int\limits_o F(\gamma,t) dA}{\int\limits_o dA}, \tag{S215}$$

where the surface integrals are over the region where, at time t, the OF has value $O = 1$. Hence, with the aid of the OF, the ocean average can be equivalently written as

$$< F >^o (t) = \frac{\int\limits_e F(\gamma,t) O dA}{\int\limits_e O dA}, \tag{S216}$$

which is easily discretised on the grid using the quadrature rule given by Eq. (S446), obtaining

$$< F >^o_n \equiv < F >^o (t_n) = \frac{\sum\limits_p F_{p,n} O_{p,n}}{\sum\limits_p O_{p,n}}, \tag{S217}$$

where $F_{p,n} = F(\gamma_p, t_n)$ and $O_{p,n}$ is given by Eq. (S210).

Global averages. The global spatial average of function $F(\gamma,t)$, defined as

$$< F >^e (t) \equiv \frac{\int\limits_e F(\gamma,t) dA}{\int\limits_e dA}, \tag{S218}$$

is discretised on the grid according to

$$< F >^e_n \equiv < F >^e (t_n) = \frac{A^c \sum\limits_p F_{p,n}}{4\pi a^2} = \frac{1}{P} \sum_p F_{p,n}\,, \tag{S219}$$

since the area of all cells (or *pixels*) is given by the ratio

$$A^c = \frac{4\pi a^2}{P}. \tag{S220}$$

Area of the oceans. At a given time t, the area of the oceans is

$$A^o(t) = \int\limits_o dA, \tag{S221}$$

where the integral is over the surface where the OF is $O = 1$ at time t. Equivalently, using the OF definition and the quadrature rule given by Eq. (S446), we have

$$A^o(t) = \int_e O dA = A^c \sum_p O(\gamma_p, t), \tag{S222}$$

where A^c is the area of each of the cells in Tegmark grid and the sum is over all the pixels. Hence, in discretised form, the area of the oceans is

$$A^o_n \equiv A^o(t_n) = A^c \sum_p O_{p,n}. \tag{S223}$$

It is worth to note that $A^o(t)$ is proportional to the harmonic degree $l = 0$ component of the OF. In fact, since $\mathcal{Y}_{00,p} = 1$, for harmonic degree $l = 0$, Eq. (S213) provides

$$O_{00,n} = \frac{1}{P} \sum_p O_{p,n}, \tag{S224}$$

which, by comparison with Eq. (S223) and also recalling (S220), shows that A^o_n can be also expressed as

$$A^o_n = 4\pi a^2 O_{00,n}. \tag{S225}$$

Grounded ice mass. According to Eq. (S45), the mass variation of the grounded ice is

$$\mu(t) = \rho^i \int_e (IC - I_0 C_0)\, dA, \tag{S226}$$

where I is ice thickness, C is the CF, and subscript 0 denotes reference quantities. Thus, according to the integration rule given by Eq. (S446), we have

$$\mu(t) = \rho^i A^c \sum_p \big(I(\gamma_p, t) C(\gamma_p, t) - I_0(\gamma_p, t_0) C_0(\gamma_p, t_0)\big), \tag{S227}$$

which at time $t = t_n$ gives

$$\mu_n \equiv \mu(t_n) = \rho^i A^c \sum_p \left(I_{p,n} C_{p,n} - I_{p,0} C_{p,0}\right), \tag{S228}$$

where $I_{p,n}$ and $C_{p,n}$ are given by Eqs. (S205) and (S211), respectively.

Term $\mathcal{S}^{equ}$. This term of the SLE, defined as

$$\mathcal{S}^{equ}(t) \equiv -\frac{\mu(t)}{\rho^w A^o(t)}, \tag{S229}$$

and referred to as *equivalent sea-level change* in the body of the paper, describes the effects of time-variations of the mass of the grounded ice $\mu(t)$, also taking the consequent changes in the area of the oceans $A^o(t)$ into account. Taking advantage of expressions (S223) and (S227) for $A^o(t)$ and $\mu(t)$, respectively, the discretisation of $\mathcal{S}^{equ}(t)$ is straightforward, with:

$$\mathcal{S}^{equ}_n \equiv \mathcal{S}^{equ}(t_n) = -\frac{\mu_n}{\rho^w A^o_n} = -\frac{\rho^i}{\rho^w} \frac{\sum_p \left(I_{p,n} C_{p,n} - I_{p,0} C_{p,0}\right)}{\sum_p O_{p,n}}. \tag{S230}$$

Since $\mathcal{S}^{equ}$ is spatially invariant, in its CSH expansion all the coefficients vanish except those of harmonic degree $l=0$ and order $m=0$, *i.e.,*

$$S^{equ}_{j,n} = S^{equ}_{n}\delta_{l0}\delta_{m0}. \tag{S231}$$

Term $\mathcal{S}^{ofu}$. This second spatially invariant term of the SLE, introduced in §S2.4, and defined as

$$\mathcal{S}^{ofu}(t) \equiv \frac{1}{A^o}\int\limits_e T_0 \mathcal{O} dA, \tag{S232}$$

accounts for time-variations of the ocean function (hence the superscript *ofu*) either associated to the horizontal migration of the shorelines or to transitions between grounded and floating ice (or *viceversa*). Contrary to $\mathcal{S}^{equ}(t)$, this term is not explicitly dependent upon variations of the grounded ice mass.

Using Eq. (S27) and applying the integration rule (S446), we have

$$\mathcal{S}^{ofu}(t) = \frac{A^c}{A^o(t)}\sum_p T(\gamma_p,t_0)\big(O(\gamma_p,t) - O(\gamma_p,t_0)\big), \tag{S233}$$

so that

$$\mathcal{S}^{ofu}_n \equiv \mathcal{S}^{ofu}(t_n) = \frac{\displaystyle\sum_p T_{p,0}\left(O_{p,n} - O_{p,0}\right)}{\displaystyle\sum_p O_{p,n}}, \tag{S234}$$

where we have also used Eq. (S223). Since $\mathcal{S}^{ofu}(t)$ is spatially invariant, the coefficients of its CSH expansion are

$$S^{ofu}_{j,n} = S^{ofu}_{n}\delta_{l0}\delta_{m0}. \tag{S235}$$

Term $\mathcal{S}^{ave}$. According to Eq. (S53), this spatially invariant term is simply given by

$$S^{ave}(t) = S^{equ} + S^{ofu} \tag{S236}$$

and represents the ocean-average of $\mathcal{S}(\gamma,t)$. Thus we have

$$\mathcal{S}^{ave}_n \equiv \mathcal{S}^{ave}(t_n) = \mathcal{S}^{equ}_n + \mathcal{S}^{ofu}_n \tag{S237}$$

where $\mathcal{S}^{equ}_n$ and $\mathcal{S}^{equ}_n$ are given by Eqs. (S230) and (S234), respectively. Furthermore, its CSH coefficients are given by

$$\mathcal{S}^{ave}_{j,n} = \left(S^{equ}_n + S^{ofu}_n\right)\delta_{l0}\delta_{m0}. \tag{S238}$$

Term $\mathcal{Z}^{ave}$. We note that the ocean-projected $\mathcal{S}^{ave}$, *i.e.,* the term $\mathcal{Z}^{ave} = O\mathcal{S}^{ave}$ given by Eq. (S194), is certainly *not* spatially invariant, since O is variable in space and time (*i.e.,* $O = O(\gamma,t)$). However, since $\mathcal{S}^{ave}$ *is* invariant, its CSH expansion is straightforward, with

$$\mathcal{Z}^{ave}_{j,n} = O_{j,n}S^{ave}_n, \tag{S239}$$

where S^{ave}_n is given by Eq. (S237).

The c constant. The so-called "c constant", first introduced by Farrell and Clark (1976), arises from the imposition of mass conservation. According to Eq. (S52), it is given by the following combination of spatially invariant quantities

$$c(t) = \mathcal{S}^{ave} - < \mathcal{R}^{sur} >^o - < \mathcal{R}^{rot} >^o, \tag{S240}$$

which using Eq. (S92), can be immediately discretised as follows

$$c_n \equiv c(t_n) = \mathcal{S}_n^{ave} - < \mathcal{R}^a >_n^o - < \mathcal{R}^b >_n^o - < \mathcal{R}^c >_n^o - < \mathcal{R}^{rot} >_n^o, \tag{S241}$$

where terms $< \mathcal{R}^{abc} >_n^o$ and $< \mathcal{R}^{rot} >_n^o$, are made explicit by Eqs. (S271) and (S286), respectively.

S7.3 Surface response

The three sea-level SRFs $\mathcal{R}^a$, $\mathcal{R}^b$ and $\mathcal{R}^c$ which appear in the SLE (see Eq. S192 and in those that immediately follow) share common structures. Below, we first discretise the surface load variation $\mathcal{L}$, then we make the CSH coefficients of the sea-level SRFs explicit; we evaluate the ocean-averages of the SRFs, and lastly we construct the "primed SRFs" defined by Eq. (S197).

Surface load. Based on Eqs. (S29-S32), the surface load variation is easily expanded in series of CSHs, with

$$\mathcal{L}_{j,n} = \mathcal{L}^a_{j,n} + \mathcal{L}^b_{j,n} + \mathcal{L}^c_{j,n} \tag{S242}$$

with

$$\mathcal{L}^a_{j,n} \equiv \rho^i \mathcal{W}_{j,n} \tag{S243}$$
$$\mathcal{L}^b_{j,n} \equiv \rho^w \mathcal{Z}_{j,n} \tag{S244}$$
$$\mathcal{L}^c_{j,n} \equiv \rho^r \mathcal{X}_{j,n}. \tag{S245}$$

According to Eq. (S33), variable $\mathcal{W}$ is defined as $\mathcal{W} = \mathcal{I}C$, where $\mathcal{I} = I - I_0$ is the ice thickness variation and $C = 1 - O$ is the CF. The CSH coefficients $\mathcal{W}_{j,n}$ in Eq. (S243) above are obtained by direct integration of $\mathcal{W}$ on the Tegmark grid using Eq. (S452), with

$$\mathcal{W}_{j,n} = \frac{1}{P} \sum_p \mathcal{I}_{p,n} C_{p,n} \mathcal{Y}^*_{j,p} = \frac{1}{P} \sum_p \left(I_{p,n} - I_{p,0}\right) \left(1 - O_{p,n}\right) \mathcal{Y}^*_{j,p}. \tag{S246}$$

In Eq. (S244) $\mathcal{Z}_{j,n}$ represents the spectral discrete form of the basic unknown of the final form of the SLE (see Eq. S192 and those that immediately follow), namely the ocean-projected sea-level change $\mathcal{Z} = O\mathcal{S}$. Within the iteration scheme of the SLE described in §S8.7, progressively updated values of $\mathcal{Z}_{j,n}$ are used in Eq. (S244) in order to determine $\mathcal{L}^b_{j,n}$.

Based upon Eq. (S35), we recall that variable $\mathcal{X}$ is defined as $\mathcal{X} = Q\mathcal{O}$, where variable Q is given by Eq. (S36) and $\mathcal{O}$ is the OF variation. Again, integration on the spatial grid using Eq. (S452) provides the CSH coefficients required in Eq. (S245), namely

$$\mathcal{X}_{j,n} = \frac{1}{P} \sum_p Q_p \mathcal{O}_{p,n} \mathcal{Y}^*_{j,p} = \frac{1}{P} \sum_p Q_p \left(O_{p,n} - O_{p,0}\right) \mathcal{Y}^*_{j,p}, \tag{S247}$$

where, using Eq. (S36), we have defined

$$Q_p = -\left(\frac{\rho^i}{\rho^r}\, I_{p,0} + \frac{\rho^w}{\rho^r}\, T_{p,0}\right). \tag{S248}$$

Response functions $\mathcal{R}^{abc}$, $\mathcal{U}^{abc}$, and $\mathcal{G}^{abc}$. Eqs. (S110-S112) of §S4.2 give the CSH coefficients of the three SRFs $\mathcal{R}^a$, $\mathcal{R}^b$ and $\mathcal{R}^c$, respectively, for an arbitrary time. Setting $t = t_n$, where t_n is one of the time grid points, exploiting the property of the

Heaviside step function, and following our conventions for notation, the SRFs harmonic coefficients are discretised as follows

$$\mathcal{R}^a_{j,n} = \frac{3\rho^i}{\rho^e}\left(e^s_l \mathcal{W}_{j,n} + \sum_{k=0}^{n-1} \Delta\mathcal{W}_{j,k}\beta^s_{l,n-k}\right) \tag{S249}$$

$$\mathcal{R}^b_{j,n} = \frac{3\rho^w}{\rho^e}\left(e^s_l\ \mathcal{Z}_{j,n} + \sum_{k=0}^{n-1} \Delta\mathcal{Z}_{j,k}\ \beta^s_{l,n-k}\right) \tag{S250}$$

$$\mathcal{R}^c_{j,n} = \frac{3\rho^r}{\rho^e}\left(e^s_l\ \mathcal{X}_{j,n} + \sum_{k=0}^{n-1} \Delta\mathcal{X}_{j,k}\ \beta^s_{l,n-k}\right), \tag{S251}$$

where we have defined

$$\Delta\mathcal{W}_{j,k} = \mathcal{W}_{j,k+1} - \mathcal{W}_{j,k} \tag{S252}$$

$$\Delta\mathcal{Z}_{j,k} = \mathcal{Z}_{j,k+1} - \mathcal{Z}_{j,k} \tag{S253}$$

$$\Delta\mathcal{X}_{j,k} = \mathcal{X}_{j,k+1} - \mathcal{X}_{j,k}\,, \tag{S254}$$

and

$$\beta^s_{l,k} \equiv \beta^s_l(k\Delta t), \tag{S255}$$

$(k = 0, \ldots N)$, with $\beta^s_l(t)$ given by Eq. (S108). We finally remark that since $\mathcal{W}_{j,0} = \mathcal{Z}_{j,0} = \mathcal{X}_{j,0} = 0$ and since the sums give no contributions for $n = 0$, we have $\mathcal{R}^{abc}_{j,0} = 0$.

We note that following the scheme above, discretised forms for the SRFs $\mathcal{U}^{sur}$ (vertical displacement) and $\mathcal{G}^{sur}$ (geoid height variation) are easily obtained. Indeed, from Eqs. (S123-S125) and (S116-S118), we have

$$\mathcal{U}^{sur}_{j,n} = \mathcal{U}^a_{j,n} + \mathcal{U}^b_{j,n} + \mathcal{U}^c_{j,n} \tag{S256}$$

where

$$\mathcal{U}^a_{j,n} = \frac{3\rho^i}{\rho^e}\left(e^u_l \mathcal{W}_{j,n} + \sum_{k=0}^{n-1} \Delta\mathcal{W}_{j,k}\beta^u_{l,n-k}\right) \tag{S257}$$

$$\mathcal{U}^b_{j,n} = \frac{3\rho^w}{\rho^e}\left(e^u_l\ \mathcal{Z}_{j,n} + \sum_{k=0}^{n-1} \Delta\mathcal{Z}_{j,k}\ \beta^u_{l,n-k}\right) \tag{S258}$$

$$\mathcal{U}^c_{j,n} = \frac{3\rho^r}{\rho^e}\left(e^u_l\ \mathcal{X}_{j,n} + \sum_{k=0}^{n-1} \Delta\mathcal{X}_{j,k}\ \beta^u_{l,n-k}\right), \tag{S259}$$

where, for any value of index k,

$$\beta^u_{l,k} \equiv \beta^u_l(k\Delta t), \tag{S260}$$

with $\beta^u_l(t)$ given by Eq. (S127), and

$$\mathcal{G}^{sur}_{j,n} = \mathcal{G}^a_{j,n} + \mathcal{G}^b_{j,n} + \mathcal{G}^c_{j,n} \tag{S261}$$

with

$$\mathcal{G}^a_{j,n} = \frac{3\rho^i}{\rho^e}\left(e^g_l \mathcal{W}_{j,n} + \sum_{k=0}^{n-1} \Delta\mathcal{W}_{j,k}\beta^g_{l,n-k}\right) \tag{S262}$$

$$\mathcal{G}^b_{j,n} = \frac{3\rho^w}{\rho^e}\left(e^g_l\ \mathcal{Z}_{j,n} + \sum_{k=0}^{n-1} \Delta\mathcal{Z}_{j,k}\ \beta^g_{l,n-k}\right) \tag{S263}$$

$$\mathcal{G}^c_{j,n} = \frac{3\rho^r}{\rho^e}\left(e^g_l\ \mathcal{X}_{j,n} + \sum_{k=0}^{n-1} \Delta\mathcal{X}_{j,k}\ \beta^g_{l,n-k}\right), \tag{S264}$$

where

$$\beta^g_{l,n} \equiv \beta^g_l(k\Delta t), \tag{S265}$$

for any k, with $\beta^g_l(t)$ given by Eq. (S120).

Ocean averages of $\mathcal{R}^{abc}$. The (spatially invariant) ocean-averages of the three SRFs $\mathcal{R}^a$, $\mathcal{R}^b$, and $\mathcal{R}^c$ are evaluated by a straightforward application of the definition of ocean-average. Hence, according to Eq. (S48), we have

$$< \mathcal{R}^{abc} >^o (t) = \frac{1}{A^o(t)} \int\limits_o \mathcal{R}^{abc}(\gamma,t) dA; \tag{S266}$$

then, taking advantage of the spectral decompositions given above for the SRF (Eqs. S110-S112) and for the OF (S212), and since the OF is a real-valued function (*i.e.,* $O = O^*$), we have

$$\begin{aligned}
< \mathcal{R}^{abc} >^o (t) &= \frac{a^2}{A^o(t)} \int\limits_\gamma \mathcal{R}^{abc}(\gamma,t) O^*(\gamma,t) d\gamma && \text{(S267)}\\
&= \frac{a^2}{A^o(t)} \int\limits_\gamma \left(\sum_j \mathcal{R}^{abc}_j(t) \mathcal{Y}_j(\gamma) \right) \left(\sum_{j'} O^*_{j'}(t) \mathcal{Y}^*_{j'}(\gamma) \right) d\gamma && \text{(S268)}\\
&= \frac{a^2}{A^o(t)} \sum_j \sum_{j'} \mathcal{R}^{abc}_j(t) O^*_{j'}(t) \int\limits_\gamma \mathcal{Y}_j(\gamma) \mathcal{Y}^*_{j'}(\gamma) d\gamma && \text{(S269)}\\
&= \frac{4\pi a^2}{A^o(t)} \sum_j \mathcal{R}^{abc}_j(t)\, O^*_j(t), && \text{(S270)}
\end{aligned}$$

where we have exploited the orthonormality of the CSHs. Hence, at a given time $t = t_n$, the ocean-averaged SRFs are

$$< \mathcal{R}^{abc} >^o_n \equiv < \mathcal{R}^{abc} >^o (t_n) = \frac{\sum\limits_j \mathcal{R}^{abc}_{j,n}\, O^*_{j,n}}{O_{00,n}}, \tag{S271}$$

where we have used Eq. (S225).

Primed SRFs $\mathcal{R}'^{\,abc}$. According to Eq. (S197), the primed SRFs are obtained by the unprimed SRFs simply by subtracting their ocean-averages. Hence, their discretisation is straightforward, with

$$\mathcal{R}'^{\,abc}_{j,n} = \mathcal{R}^{abc}_{j,n} - < \mathcal{R}^{abc} >^o_n \delta_{l0}\delta_{m0}, \tag{S272}$$

where $< \mathcal{R}^{abc} >^o_n$ is given by Eq. (S271).

The terms $\mathcal{K}^{abc}$. According to Eq. (S195), the three terms $\mathcal{K}^{abc}$ result from projecting the primed SRFs over the OF, *i.e.,*

$$\mathcal{K}^{abc}(\gamma,t) \equiv O\mathcal{R}'^{\,abc}. \tag{S273}$$

For these terms, we assume a CSH expansion

$$\mathcal{K}^{abc}(\gamma,t) = \sum_j \mathcal{K}^{abc}_j(t) \mathcal{Y}_j(\gamma), \tag{S274}$$

where, according to Eqs. (S430) and (S451), coefficients $\mathcal{K}_j^{abc}(t)$ are evaluated by a numerical quadrature on the grid:

$$\mathcal{K}_j^{abc}(t) = \frac{1}{4\pi}\int_\gamma O(\gamma,t)\,\mathcal{R}'^{\,abc}(\gamma,t)\mathcal{Y}_j^*(\gamma)d\gamma \tag{S275}$$

$$\approx \frac{1}{P}\sum_p O(\gamma_p,t)\,\mathcal{R}'^{\,abc}(\gamma_p,t)\mathcal{Y}_j^*(\gamma_p) \tag{S276}$$

$$= \frac{1}{P}\sum_p O(\gamma_p,t)\left(\sum_{j'}\mathcal{R}'^{\,abc}_{j'}(t)\mathcal{Y}_{j'}(\gamma_p)\right)\mathcal{Y}_j^*(\gamma_p) \tag{S277}$$

$$= \frac{1}{P}\sum_{\substack{p \text{ such that}\\ O(\gamma_p,t)=1}}\left(\sum_{j'}\mathcal{R}'^{\,abc}_{j'}(t)\mathcal{Y}_{j'}(\gamma_p)\right)\mathcal{Y}_j^*(\gamma_p)\,; \tag{S278}$$

hence, at time $t=t_n$, we have

$$\mathcal{K}_{j,n}^{abc} \equiv \mathcal{K}_j^{abc}(t_n) = \sum_{p:\ O_{p,n}=1}\chi_{p,n}^{abc}\,\mathcal{Y}_{j,p}^*\,, \tag{S279}$$

where we have defined the three arrays

$$\chi_{p,n}^{abc} \equiv \frac{1}{P}\sum_j \mathcal{R}'^{\,abc}_{j,n}\mathcal{Y}_{j,p}. \tag{S280}$$

S7.4 Rotational response

For the RRF $\mathcal{R}^{rot}$, the discretisation scheme largely follows the one adopted for the three SRFs terms $\mathcal{R}^{abc}$. Again, we consider separately the various terms depending on $\mathcal{R}^{rot}$, which appear in the SLE.

CSH expansion of $\mathcal{R}^{rot}$. The RRF for sea level which appears in the SLE is given by Eq. (S190). Since it is a pure harmonic function of degree $l=2$ and order $m=\pm1$, its discretisation is straightforward:

$$\mathcal{R}_{j,n}^{rot} = \delta_{l2}\delta_{m\pm1}\frac{c_{21}^{\psi}c_{21}^{\lambda}}{g}\sum_{k=0}^{n-1}\Delta\mathcal{L}_{j,k}\gamma_{n-k}^s \tag{S281}$$

where

$$\Delta\mathcal{L}_{j,k} = \mathcal{L}_{j,k+1} - \mathcal{L}_{j,k}\,, \tag{S282}$$

with $\mathcal{L}_{j,k}$ given by Eq. (S242), and where for any index k, we have

$$\gamma_k^s = \gamma_k^g - \gamma_k^u, \tag{S283}$$

with

$$\gamma_k^g = \gamma^g(k\Delta t) \tag{S284}$$

$$\gamma_k^u = \gamma^u(k\Delta t), \tag{S285}$$

where $\gamma^g(t)$ and $\gamma^u(t)$ are given by Eqs. (S185) and (S189), respectively.

Ocean-average of $\mathcal{R}^{rot}$. The ocean-average of the RRF $\mathcal{R}^{rot}$ is evaluated following the same principles which have led to the evaluation of the ocean-averaged SRF. Indeed, using Eq. (S271), we have immediately

$$< \mathcal{R}^{rot} >_n^o \equiv < \mathcal{R}^{rot} >^o (t_n) = \frac{\sum_j \mathcal{R}_{j,n}^{rot}\, O_{j,n}^*}{O_{00,n}}, \tag{S286}$$

where $\mathcal{R}_{j,n}^{rot}$ is given by (S281).

Primed RRF $\mathcal{R}'^{\,rot}$. According to Eq. (S198), the primed RRF is obtained by the corresponding RRFs by subtracting the ocean-averages; hence, the discretisation is

$$\mathcal{R}'^{\,rot}_{j,n} = \mathcal{R}^{rot}_{j,n} - < \mathcal{R}^{rot} >_n \delta_{l0}\delta_{m0}, \tag{S287}$$

where $< \mathcal{R}^{rot} >_n$ is given by Eq. (S286).

The term $\mathcal{K}^{rot}$. This term of the SLE is stemming from the projection of the primed RRF $\mathcal{R}'^{\,rot}$ over the OF. In analogy with what we have done for the terms $\mathcal{K}^{abc}$ associated to surface loading, we thus write

$$\mathcal{K}_{j,n}^{rot} \equiv \mathcal{K}_j^{rot}(t_n) = \sum_{p:\, O_{p,n}=1} \chi_{p,n}^{rot}\, \mathcal{Y}_{j,p}^*, \tag{S288}$$

where we have defined the array

$$\chi_{p,n}^{rot} \equiv \frac{1}{P} \sum_j \mathcal{R}'^{\,rot}_{j,n} \mathcal{Y}_{j,p}, \tag{S289}$$

with $\mathcal{R}'^{\,rot}_{j,n}$ given by Eq. (S287).

S8 Miscellaneous topics

S8.1 Piecewise constant functions

Here we first define the *unit step function* (also often referred to as Heaviside step function); then, we describe how we are dealing with the time-evolution of scalar functions. The CSH expansion of piecewise-constant functions is discussed at the end of the section.

Unit step function. We define the *unit step function* as

$$H(t) \equiv \begin{cases} 0 & \text{if } t \leq 0 \\ 1 & \text{if } t > 0, \end{cases} \tag{S290}$$

where we note that $H(t)$ is "left-continuous", *i.e.,* $H(0) = 0$. The unit step function is shown in Figure S4a.

Time discretisation. We denote by $F = F(\gamma, t)$ a function that, at a given point $\gamma = (\theta, \lambda)$, varies with time in discrete steps according to the diagram of Figure S4b. This type of "piecewise constant" (PC) time history is particularly convenient for the numerical discretisation adopted in *SELEN*^{4}.

With $F_0(\gamma)$ we denote the value attained by $F(\gamma, t)$ for $-\infty < t \leq t_0 \equiv 0$, and with $F_k(\gamma)$ the value in the time interval $t_{k-1} < t \leq t_k$ $(k = 1, \ldots, N)$. For $t > t_N$, the value of $F(\gamma, t)$ is $F_{N+1}(\gamma)$.

Thus:

$$F(\gamma,t) \equiv \begin{cases} F_0(\gamma), & -\infty < t \leq t_0 \equiv 0 \\ F_1(\gamma), & t_0 < t \leq t_1 \\ F_2(\gamma), & t_1 < t \leq t_2 \\ \ldots & \ldots \\ F_k(\gamma), & t_{k-1} < t \leq t_k \\ \ldots & \ldots \\ F_N(\gamma), & t_{N-1} < t \leq t_N \\ F_{N+1}(\gamma), & t > t_N, \end{cases} \tag{S291}$$

where N is the number of time steps in the interval $0 \leq t \leq t_N$, each time step having the constant length

$$\Delta t \equiv t_k - t_{k-1} \equiv \frac{t_N}{N}, \tag{S292}$$

and where it is useful to remark that, according to Eq. (S291), at the time grid points we have

$$F(\gamma, t_k) = F_k(\gamma), \tag{S293}$$

which is a consequence of the left-continuity of $H(t)$ in Eq. (S290).

Using the definition of unit step function we have

$$
\begin{aligned}
F(\gamma,t) &= F_0(\gamma)\left(1-H(t-t_0)\right)+\sum_{k=1}^{N}F_k(\gamma)\left(H(t-t_{k-1})-H(t-t_k)\right)+F_{N+1}(\gamma)H(t-t_N)\\
&= F_0(\gamma)-F_0(\gamma)H(t-t_0)+\sum_{k=1}^{N}F_k(\gamma)H(t-t_{k-1})-\sum_{k=1}^{N}F_k(\gamma)H(t-t_k)+F_{N+1}(\gamma)H(t-t_N)\\
&= F_0(\gamma)-F_0(\gamma)H(t-t_0)+\sum_{k'=0}^{N-1}F_{k'+1}(\gamma)H(t-t_{k'})-\sum_{k'=1}^{N}F_{k'}(\gamma)H(t-t_{k'})+F_{N+1}(\gamma)H(t-t_N)\\
&= F_0(\gamma)-F_0(\gamma)H(t-t_0)+F_1(\gamma)H(t-t_0)+\sum_{k'=1}^{N-1}F_{k'+1}(\gamma)H(t-t_{k'})+\\
&\quad -\sum_{k'=1}^{N-1}F_{k'}(\gamma)H(t-t_{k'})-F(\gamma)_NH(t-t_N)+F(\gamma)_{N+1}H(t-t_N)\\
&= F_0(\gamma)+\left(F_1(\gamma)-F_0(\gamma)\right)H(t-t_0)+\sum_{k'=1}^{N-1}\left(F_{k'+1}(\gamma)-F_{k'}(\gamma)\right)H(t-t_{k'})+\left(F_{N+1}(\gamma)-F_N(\gamma)\right)H(t-t_N),
\end{aligned}
$$

hence, merging all the contributions, we obtain the compact form

$$F(\gamma,t)=F_0(\gamma)+\sum_{k=0}^{N}\left(F_{k+1}(\gamma)-F_k(\gamma)\right)H(t-t_k). \tag{S294}$$

Accordingly, the *time-variation* of $F(\gamma,t)$, defined as

$$\mathcal{F}(\gamma,t)\equiv F(\gamma,t)-F_0(\gamma), \tag{S295}$$

admits a PC time history as well, with:

$$
\begin{aligned}
\mathcal{F}(\gamma,t) &= \sum_{k=0}^{N}\left(F_{k+1}(\gamma)-F_k(\gamma)\right)H(t-t_k),\\
&= \sum_{k=0}^{N}\left(\,\left(F_{k+1}(\gamma)-F_0(\gamma)\right)-\left(F_k(\gamma)-F_0(\gamma)\right)\,\right)H(t-t_k),\\
&= \sum_{k=0}^{N}\left(\mathcal{F}_{k+1}(\gamma)-\mathcal{F}_k(\gamma)\right)H(t-t_k).
\end{aligned} \tag{S296}
$$

CSH expansion of a PC function. Dealing with the numerical implementation of the SLE, it is often necessary to expand a PC function $\mathcal{F}(\gamma,t)$ in series of CSHs. According to the general expression given by Eq. (S428), the expansion reads

$$\mathcal{F}(\gamma,t)=\sum_{lm}\mathcal{F}_{lm}(t)\mathcal{Y}_{lm}(\gamma), \tag{S297}$$

where using Eq. (S430) the (time-dependent) coefficients turn out to be

$$\mathcal{F}_{lm}(t)=\frac{1}{4\pi}\int_{\gamma}\mathcal{F}(\gamma,t)\mathcal{Y}^*_{lm}(\gamma)d\gamma. \tag{S298}$$

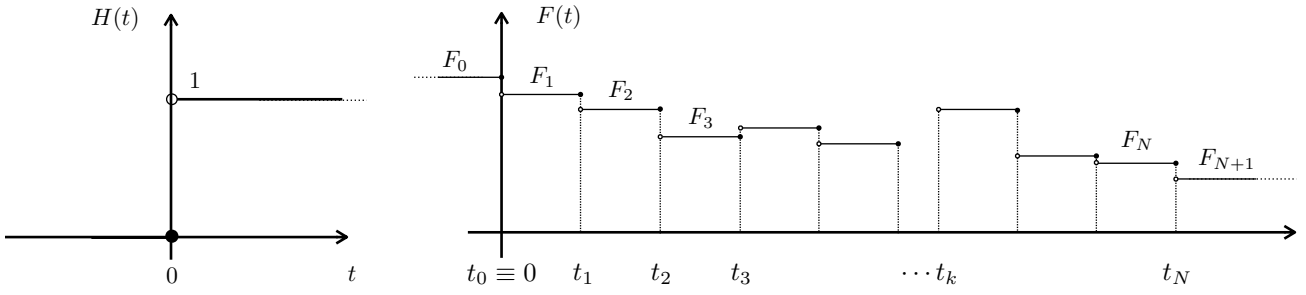

Figure S4. Unit step function (a) and general PC function (b), where $F_k = F_k(\omega)$ is the value of $F(\omega,t)$ in the k-th time interval ($k = 1,\dots N$), $F_0 = F_0(\omega)$ is the value of $F(\omega,t)$ in the reference state before the inception of melting, and $F_{N+1} = F_{N+1}(\omega)$ is the future value.

By substituting Eq. (S296) into (S298) we obtain

$$\mathcal{F}_{lm}(t) = \sum_{k=0}^{N} (\mathcal{F}_{lm,k+1} - \mathcal{F}_{lm,k})\, H(t-t_k), \tag{S299}$$

or, equivalently

$$\mathcal{F}_{lm}(t) = \sum_{k=0}^{N} \Delta\mathcal{F}_{lm,k} H(t-t_k), \tag{S300}$$

where

$$\Delta\mathcal{F}_{lm,k} \equiv \mathcal{F}_{lm,k+1} - \mathcal{F}_{lm,k}, \quad (k = 0,\dots N) \tag{S301}$$

and

$$\mathcal{F}_{lm,k} \equiv \mathcal{F}_{lm}(t_k) = \frac{1}{4\pi} \int_{\gamma} \mathcal{F}_k(\gamma) \mathcal{Y}^*_{lm}(\gamma) d\gamma. \tag{S302}$$

S8.2 Polar motion transfer function

This section is devoted to the study of the Polar Motion Transfer Function (PMTF). We shall obtain the PMTF for both the traditional and the revised rotation theory, described in §S5.2. Then, we shall provide an expression for the modified form of the PMTF, necessary to solve the Liouville equations.

Traditional rotation theory. Our purpose here is to show that when the *traditional rotation theory* is adopted, the PMTF defined by Eq. (S147) takes the form:

$$\mathcal{A}(s) = A^e + \frac{A^s}{s} + \sum_{i=1}^{M'} \frac{A_i}{s - a_i}, \tag{S303}$$

where $M' = M - 1$ and the secular residue A^s is, in general, a non-vanishing constant.

First of all, we recall that the Laplace-transformed Liouville equations (S143) read

$$\left(1 - \frac{k^T(s)}{k^s}\right)\mathbf{m}(s) = \mathbf{\Psi}^{sur}(s), \tag{S304}$$

where $\mathbf{m}$ is the displacement of the pole of rotation, k^s is the secular Love number, $\mathbf{\Psi}^{sur}(s)$ is the surface loading polar motion excitation function and

$$k^T(s) = k^{Te} + \sum_{i=1}^{M} \frac{k_i^T}{s - s_i} \tag{S305}$$

is the Laplace-transformed 'k' TLN of degree $l = 2$. To simplify notation, here we have dropped subscript '2', *i.e.,* we have defined $k^{Te} \equiv k_2^{Te}$, $k_i^T \equiv k_{2i}^T$, and $s_i \equiv s_{2i}$. Now, following *e.g.,* Spada et al. (2011) we approximate the secular Love number with the degree 2 fluid TLN 'k', *i.e.,*

$$k^s = k^{Tf}, \tag{S306}$$

where $k^{Tf} \equiv k_2^{Tf}$ and according to Eqs. (S74) and (S305), we have

$$k^{Tf} \equiv \lim_{s \mapsto 0} k^T(s) \equiv k^{Te} - \sum_{i=1}^{M} \frac{k_i^T}{s_i}. \tag{S307}$$

Taking advantage of Eqs. (S306) and (S307) and using simple algebra, the factor multiplying $\mathbf{m}$ in Eq. (S304) can be rearranged as

$$1 - \frac{k^T(s)}{k^s} = s \sum_{i=1}^{M} \frac{\gamma_i}{s - s_i}, \tag{S308}$$

with constants

$$\gamma_i \equiv -\frac{1}{k^{Tf}} \left(\frac{k_i^T}{s_i}\right), \quad (i = 1, \ldots, M) \tag{S309}$$

so that the Liouville equations take the form

$$\left(\sum_{i=1}^{M} \frac{\gamma_i}{s - s_i}\right)\mathbf{m}(s) = \frac{\mathbf{\Psi}^{sur}(s)}{s}. \tag{S310}$$

By a comparison with Eq. (S146), we note that the PMTF can be expressed as

$$\mathcal{A}(s) = \frac{1}{s \sum_{i=1}^{M} \frac{\gamma_i}{s - s_i}} \tag{S311}$$

showing that, in the hypothesis that all the s_i's are distinct, $\mathcal{A}(s)$ has M simple zeros in $s = s_i$, *i.e.,*

$$\mathcal{A}(s_i) = 0 \quad (i = 0, 1, \ldots M). \tag{S312}$$

Multiplying both the denominator and the numerator of Eq. (S311) by the *secular polynomial* with roots $s = s_i$, defined by Eq. (S63), we obtain

$$\mathcal{A}(s) = \frac{N(s)}{s\sum_{i=1}^{M}\gamma_i \, \frac{N(s)}{s-s_i}}. \tag{S313}$$

We now observe that the ratio

$$B_i(s) \equiv \frac{N(s)}{s-s_i} \tag{S314}$$

is a degree $M-1$ polynomial

$$B_i(s) = \sum_{k=0}^{M-1} b_{k,i} s^k, \tag{S315}$$

with coefficients

$$\begin{aligned} b_{M-1,i} &= n_M \\ b_{k-1,i} &= n_k + b_{k,i} s_i \quad (k = M-1, M-2, \ldots, 1); \end{aligned}$$

thus from Eq. (S313) we have

$$\begin{aligned} \mathcal{A}(s) &= \frac{N(s)}{s\left(\sum_{i=1}^{M}\gamma_i \sum_{k=0}^{M-1} b_{k,i} s^k\right)} \\ &= \frac{N(s)}{s\left(\sum_{k=0}^{M-1}\left(\sum_{i=1}^{M}\gamma_i b_{k,i}\right) s^k\right)} \\ &= \frac{N(s)}{s\sum_{k=0}^{M-1} c_k s^k}. \end{aligned} \tag{S316}$$

Hence, defining the new polynomial

$$C(s) = \sum_{k=0}^{M-1} c_k s^k \tag{S317}$$

with coefficients

$$c_k = \sum_{i=1}^{M} \gamma_i b_{k,i} \quad (k = 0, 1, \ldots M-1), \tag{S318}$$

from Eq. (S316) we see that the PMTF can expressed, in the Laplace domain, by a rational function of s involving two degree M polynomials:

$$\mathcal{A}(s) = \frac{N(s)}{sC(s)}. \tag{S319}$$

The structure of the PMTF suggests the decomposition

$$\mathcal{A}(s) = A^e + \frac{A^s}{s} + \frac{P(s)}{C(s)}, \tag{S320}$$

where $P(s)$ is a degree $M-2$ polynomial with coefficients

$$p_k = n_{k+1} - A^e c_k - A^s c_{k+1} \quad (k = 0, \dots M-2) \tag{S321}$$

and

$$A^s = \lim_{s \mapsto 0} s\mathcal{A}(s) = \frac{n_0}{c_0} \neq 0 \tag{S322}$$

is the *secular rotational residue* while

$$A^e = \lim_{s \mapsto \infty} \mathcal{A}(s) = \frac{n_M}{c_{M-1}} \tag{S323}$$

is the *elastic rotational residue*. Furthermore, *assuming* that $C(s)$ has $M-1$ distinct zeros at $s = a_i$ (*i.e.,* $C(a_i) = 0$) we can follow the usual method for the Laplace inversion of a rational function (*e.g.,* Longman and Sharir, 1971). Hence, defining the *rotational residues* as

$$A_i = \frac{P(a_i)}{C'(a_i)} \quad (i = 1, \dots M-1), \tag{S324}$$

where here the prime denotes the derivative with respect to s, from Eq. (S320) we obtain

$$\mathcal{A}(s) = A^e + \frac{A^s}{s} + \sum_{i=1}^{M'} \frac{A_i}{s - a_i}, \tag{S325}$$

with

$$M' = M - 1, \tag{S326}$$

which confirm Eqs. (S303) and (S151).

New (or revised) rotation theory. Here we show that according to the revised rotation theory, the PMTF defined by Eq. (S147) takes the form:

$$\mathcal{A}(s) = A^e + \frac{A^s}{s} + \sum_{i=1}^{M'} \frac{A_i}{s - a_i}, \tag{S327}$$

where $M' = M$ and the secular rotational residue is, in this case, $A^s = 0$.

The computations below follow quite closely those for the traditional rotation theory, but some important details differ. From Eq. (S143), we first recall that the Laplace-transformed Liouville equations read

$$\left(1 - \frac{k^T(s)}{k^s}\right) \mathbf{m}(s) = \mathbf{\Psi}^{sur}(s), \tag{S328}$$

where $\mathbf{m}(s)$ is polar motion, k^s is the secular Love number, $\mathbf{\Psi}^{sur}(s)$ is the polar motion excitation function for surface loading and

$$k^T(s) = k^{Te} + \sum_{i=1}^{M} \frac{k_i^T}{s - s_i} \tag{S329}$$

is the Laplace-transformed 'k' TLN of degree $l = 2$ where, to simplify notation, we have again dropped subscript '2', *i.e.,* we have set $k^{Te} \equiv k_2^{Te}$, $k_i^T \equiv k_{2i}^T$ and $s_i \equiv s_{2i}$.

Now, following Mitrovica et al. (2005) and Mitrovica and Wahr (2011) we *do not* make the *assumption* $k^s = k^{Tf}$ that is at the basis of the traditional rotation theory. Rather, we assume, for the moment, an arbitrary value of k^s. By substitution of Eq. (S329) into (S328) also using the definition of fluid TLN (S74) and simple algebra, the factor in front of $\mathbf{m}(s)$ in the Liouville equations can be cast in the form

$$1 - \frac{k^T(s)}{k^s} = \varepsilon + s\sum_{i=1}^{M} \frac{\delta_i}{s - s_i}, \tag{S330}$$

where

$$\varepsilon \equiv 1 - \frac{k^{Tf}}{k^s} \tag{S331}$$

where $k^{Tf} = k_2^{Tf}$ and

$$\delta_i \equiv -\frac{1}{k^s}\left(\frac{k_i^T}{s_i}\right), \quad (i = 1, \ldots, M), \tag{S332}$$

where we note that, for $k^s = k^{Tf}$, $\varepsilon = 0$ and according to Eq. (S309) $\delta_i = \gamma_i$, so that the traditional rotation theory is recovered.

Using Eq. (S330), the Liouville equations (S328) become

$$\left(\varepsilon + s\sum_{i=1}^{M} \frac{\delta_i}{s - s_i}\right)\mathbf{m}(s) = \mathbf{\Psi}^{sur}(s), \tag{S333}$$

which compared with (S146) gives the PMTF:

$$\mathcal{A}(s) = \frac{1}{\varepsilon + s\sum_{i=1}^{M} \frac{\delta_i}{s - s_i}} \tag{S334}$$

showing that, in the hypothesis that all the s_i's are distinct, also in this case $\mathcal{A}(s)$ has M simple zeros in $s = s_i$, *i.e.,*

$$\mathcal{A}(s_i) = 0 \quad (i = 0, 1, \ldots M). \tag{S335}$$

Multiplying both the denominator and the numerator of Eq. (S334) by $N(s)$, we obtain

$$\begin{aligned} \mathcal{A}(s) &= \frac{N(s)}{\varepsilon N(s) + s\sum_{i=1}^{M} \delta_i \frac{N(s)}{s - s_i}} \\ &= \frac{N(s)}{\varepsilon N(s) + s\sum_{i=1}^{M} \delta_i B_i(s)} \\ &= \frac{N(s)}{\varepsilon N(s) + s\sum_{k=0}^{M-1}\left(\sum_{i=1}^{M} \delta_i b_{k,i}\right)s^k}, \end{aligned} \tag{S336}$$

where we have used Eqs. (S63), (S314), and (S315). Hence, defining the new degree $M-1$ polynomial

$$D(s) = \sum_{k=0}^{M-1} d_k s^k, \tag{S337}$$

with coefficients

$$d_k = \sum_{i=1}^{M} \delta_i b_{k,i} \quad (k = 0, 1, \ldots M-1), \tag{S338}$$

from Eq. (S336) we see that the PMTF is expressed, as for the traditional rotation theory, as the ratio of two degree M polynomials

$$\mathcal{A}(s) = \frac{N(s)}{E(s)}, \tag{S339}$$

where

$$E(s) \equiv \varepsilon N(s) + sD(s), \tag{S340}$$

with coefficients

$$\begin{aligned} e_0 &= \varepsilon n_0 \\ e_k &= \varepsilon n_k + d_{k-1} \quad (k = 1, \ldots M). \end{aligned}$$

The *secular residue* of $\mathcal{A}$ is

$$A^s = \lim_{s \mapsto 0} s\mathcal{A}(s) = 0, \tag{S341}$$

while the *elastic residue* is

$$A^e = \lim_{s \mapsto \infty} \mathcal{A}(s) = \frac{n_M}{e_M}. \tag{S342}$$

Following the usual method of inverting the rational function (*e.g.,* Longman and Sharir, 1971), the *rotational residues* are

$$A_i = \frac{N(a_i)}{E'(a_i)}, \quad (i = 0, 1, \ldots M), \tag{S343}$$

where the prime denotes the derivative with respect to s, and a_i are the (simple) roots of equation $E(s) = 0$. Hence from (S325) we obtain

$$\mathcal{A}(s) = A^e + \frac{A^s}{s} + \sum_{i=1}^{M'} \frac{A_i}{s - a_i}, \tag{S344}$$

with

$$M' = M, \tag{S345}$$

which confirm Eqs. (S149) and (S152).

Modified form of the PMTF. Here we show that the *modified PMTF* in the Laplace domain, defined in §S5.5 as

$$\mathcal{A}'(s) \equiv \mathcal{A}(s)\left(1 + k_2^L(s)\right) \tag{S346}$$

can be cast in the form

$$\mathcal{A}'(s) = A'^e + \frac{A'^s}{s} + \sum_{i=1}^{M'} \frac{A'_i}{s-a_i} + \sum_{i=1}^{M} \frac{A''_i}{s-s_i}, \tag{S347}$$

where A'^e, A'^s, A'_i and A''_i are appropriate constants, and where in particular $A''_i \equiv 0$.

We start recalling, from Eq. (S149), the general form of the PMTF

$$\mathcal{A}(s) = A^e + \frac{A^s}{s} + \sum_{i=1}^{M'} \frac{A_i}{s-a_i}, \tag{S348}$$

where for the traditional rotation theory $M' = M-1$ and $A^s \neq 0$, while for the new theory $M' = M$ and $A^s = 0$. Furthermore, according to (S59), the degree 2 LLN is

$$k^L(s) = k^{Le} + \sum_{i=1}^{M} \frac{k_i^L}{s-s_i}, \tag{S349}$$

where we have dropped subscript '2' to simplify notation, *i.e.,* we have set $k^{Le} \equiv k_2^{Le}$, $k_i^L \equiv k_{2i}^L$, and $s_i \equiv s_{2i}$.

Direct substitution of Eqs. (S349) and (S348) into (S346) gives

$$\begin{aligned}
\mathcal{A}'(s) &= \left(A^e + \frac{A^s}{s} + \sum_{i=1}^{M'} \frac{A_i}{s-a_i}\right)\left(1 + k^{Le} + \sum_{i=1}^{M} \frac{k_i^L}{s-s_i}\right) \\
&= A^e\left(1+k^{Le}\right) + \sum_{i=1}^{M} \frac{A^e k_i^L}{s-s_i} + \frac{A^s(1+k^{Le})}{s} + \sum_{i=1}^{M'} \frac{(1+k^{Le})A_i}{s-a_i} + \\
&\quad + \sum_{i=1}^{M} \frac{A^s k_i^L}{s(s-s_i)} + \sum_{i'=1}^{M'}\sum_{i=1}^{M} \frac{A_{i'} k_i^L}{(s-a_{i'})(s-s_i)},
\end{aligned} \tag{S350}$$

where we note that since

$$\frac{1}{s(s-s_i)} = \frac{1/s_i}{s-s_i} - \frac{1/s_i}{s}, \tag{S351}$$

the fifth term is

$$\sum_{i=1}^{M} \frac{A^s k_i^L}{s(s-s_i)} = \sum_{i=1}^{M} \frac{A^s k_i^L/s_i}{s-s_i} - \frac{1}{s}\sum_{i=1}^{M} A^s \frac{k_i^L}{s_i}; \tag{S352}$$

furthermore, since

$$\frac{1}{(s-a_{i'})(s-s_i)} = \frac{1/(a_{i'}-s_i)}{s-a_{i'}} - \frac{1/(a_{i'}-s_i)}{s-s_i}, \tag{S353}$$

the sixth term is

$$\begin{aligned}
\sum_{i'=1}^{M'}\sum_{i=1}^{M} \frac{A_{i'} k_i^L}{(s-a_{i'})(s-s_i)} &= \sum_{i'=1}^{M'}\sum_{i=1}^{M} \frac{A_{i'} k_i^L/(a_{i'}-s_i)}{s-a_{i'}} - \sum_{i'=1}^{M'}\sum_{i=1}^{M} \frac{A_{i'} k_i^L/(a_{i'}-s_i)}{s-s_i} \\
&= \sum_{i'=1}^{M'} \frac{1}{s-a_{i'}} \sum_{i=1}^{M} \frac{A_{i'} k_i^L}{a_{i'}-s_i} - \sum_{i=1}^{M} \frac{1}{s-s_i} \sum_{i'=1}^{M'} \frac{A_{i'} k_i^L}{a_{i'}-s_i} \\
&= \sum_{i'=1}^{M'} \frac{F_{i'}}{s-a_{i'}} - \sum_{i=1}^{M} \frac{G_i}{s-s_i},
\end{aligned} \tag{S354}$$

where we have defined

$$F_{i'} \equiv \sum_{i=1}^{M} \frac{A_{i'} k_i^L}{a_{i'} - s_i} \quad (i' = 1, \ldots, M') \tag{S355}$$

$$G_i \equiv \sum_{i'=1}^{M'} \frac{A_{i'} k_i^L}{a_{i'} - s_i} \quad (i = 1, \ldots, M). \tag{S356}$$

Hence, substituting Eqs. (S354) and (S352) into (S350) using (S355) and (S356), we obtain

$$\begin{aligned} \mathcal{A}'(s) &= A^e \left(1 + k^{Le}\right) + \sum_{i=1}^{M} \frac{A^e k_i^L}{s - s_i} + \frac{A^s (1 + k^{Le})}{s} + \sum_{i=1}^{M'} \frac{(1 + k^{Le}) A_i}{s - a_i} + \sum_{i=1}^{M} \frac{A^s k_i^L / s_i}{s - s_i} - \frac{1}{s} \sum_{i=1}^{M} A^s \frac{k_i^L}{s_i} + \\ &\quad + \sum_{i=1}^{M'} \frac{F_i}{s - a_i} - \sum_{i=1}^{M} \frac{G_i}{s - s_i} \\ &= A^e \left(1 + k^{Le}\right) + \frac{A^s}{s} \left(1 + k^{Lf}\right) + \sum_{i=1}^{M} \frac{k_i^L (A^e + A^s / s_i) - G_i}{s - s_i} + \sum_{i=1}^{M'} \frac{(1 + k^{Le}) A_i + F_i}{s - a_i}, \end{aligned} \tag{S357}$$

where we have used the expression for the fluid 'k' LLN given by Eq. (S64). Thus, defining

$$A'^e = \left(1 + k^{Le}\right) A^e, \tag{S358}$$

$$A'^s = \left(1 + k^{Lf}\right) A^s, \tag{S359}$$

$$A'_i = (1 + k^{Le}) A_i + F_i, \quad (i = 1, \ldots, M') \tag{S360}$$

$$A''_i = k_i^L \left(A^e + \frac{A^s}{s_i}\right) - G_i, \quad (i = 1, \ldots, M) \tag{S361}$$

we find that the modified PMTF can be written as

$$\mathcal{A}'(s) = A'^e + \frac{A'^s}{s} + \sum_{i=1}^{M'} \frac{A'_i}{s - a_i} + \sum_{i=1}^{M} \frac{A''_i}{s - s_i}, \tag{S362}$$

which confirms Eq. (S347).

In conclusion, we observe that a remarkable identity exists, already noted[7] in Spada et al. (2011). In fact, from Eqs. (S361) and (S356), we obtain

$$\begin{aligned} A''_i &= k_i^L \left(A^e + \frac{A^s}{s_i}\right) - G_i \\ &= k_i^L \left(A^e + \frac{A^s}{s_i}\right) - \sum_{i'=1}^{M'} \frac{A_{i'} k_i^L}{a_{i'} - s_i} \\ &= k_i^L \left(A^e + \frac{A^s}{s_i} + \sum_{k=1}^{M'} \frac{A_k}{s_i - a_k}\right) \\ &= k_i^L \mathcal{A}(s_i) \quad (i = 1, \ldots, M), \end{aligned} \tag{S363}$$

where we have used the definition of PMFT given by Eq. (S149). But from Eqs. (S312) and (S335), valid for the traditional and the revised rotation theories, respectively, we have

$$\mathcal{A}(s_i) = 0, \tag{S364}$$

[7] V. R. Barletta (2011), personal communication.

so that Eq. (S363) simply gives

$$A_i'' = 0, \quad (i = 1, \ldots, M). \tag{S365}$$

Therefore, $\mathcal{A}'(s)$ has the same structure of $\mathcal{A}(s)$.

S8.3 Inertia variation for a rigid Earth

In this section, devoted to the evaluation of the inertia change for a rigid Earth, we will show that

$$\mathbf{J}^{rig}(t) = \frac{4\pi a^4}{3}\sqrt{\frac{6}{5}}\mathcal{L}_{21}^*(t), \tag{S366}$$

where $\mathcal{L}_{21}$ is the harmonic degree $l = 2$ and order $m = 1$ coefficient of the CSH expansion of the load variation $\mathcal{L}$. We shall also find a convenient expression for the excitation function $\mathbf{\Psi}^{rig}$, both in the time and in the Laplace domains.

Since here we are assuming a rigid Earth, $\mathbf{J}^{rig}$ can only depend upon the surface mass redistribution, so that it must be expressed as a surface integral. Also using the definition of inertia tensor[8], we have

$$\mathbf{J}^{rig}(t) = -\int_e (x_1 x_3 + i\, x_2 x_3) d\mathcal{M}, \tag{S367}$$

where $d\mathcal{M}$ is the change in the unit surface mass. But recalling from Eq. (S24) that the load variation represents the change of mass per unit area, *i.e.,* $\mathcal{L} = d\mathcal{M}/dA$, we obtain:

$$\begin{aligned}
\mathbf{J}^{rig}(t) &= -a^2 \int_\gamma (x_1 x_3 + i x_2 x_3)\mathcal{L}(\gamma, t) d\gamma \\
&= -a^4 \int_\gamma \sin\theta\cos\theta\ \mathrm{e}^{i\lambda}\mathcal{L}(\gamma, t) d\gamma \\
&= \frac{a^4}{3}\sqrt{\frac{6}{5}}\int_\gamma \mathcal{L}(\gamma, t)\mathcal{Y}_{21}(\gamma) d\gamma,
\end{aligned} \tag{S368}$$

where by the definition polar spherical coordinates we have made the substitutions $x_1 = a\sin\theta\cos\lambda$, $x_2 = a\sin\theta\sin\lambda$, $x_3 = a\cos\theta$, and we have used the expression of $\mathcal{Y}_{21}$ given in Table S4. We now expand the (real-valued) scalar field $\mathcal{L}$ in series of CSHs, also using the orthogonality condition, to obtain

$$\begin{aligned}
\mathbf{J}^{rig}(t) &= \frac{a^4}{3}\sqrt{\frac{6}{5}}\int_\gamma \left(\sum_{lm}\mathcal{L}_{lm}^*(t)\mathcal{Y}_{lm}^*(\gamma)\right)\mathcal{Y}_{21}(\gamma) d\gamma \\
&= \frac{a^4}{3}\sqrt{\frac{6}{5}}\sum_{lm}\mathcal{L}_{lm}^*(t)\int_\gamma \mathcal{Y}_{lm}^*(\gamma)\mathcal{Y}_{21}(\gamma) d\gamma \\
&= \frac{4\pi a^4}{3}\sqrt{\frac{6}{5}}\sum_{lm}\mathcal{L}_{lm}^*(t)\delta_{l2}\delta_{m1} \\
&= \frac{4\pi a^4}{3}\sqrt{\frac{6}{5}}\,\mathcal{L}_{21}^*(t),
\end{aligned} \tag{S369}$$

[8]The inertia tensor is $\int_V (x_l x_l \delta_{ik} - x_i x_k) dm$, where the integration is over the volume of the body and dm is the mass element (*e.g.,* Landau et al., 1986).

hence, based upon definition of surface loading excitation function given by Eq. (S157), we have

$$\mathbf{\Psi}^{rig}(t) = c_{21}^{\psi}\mathcal{L}_{21}^{*}(t) \tag{S370}$$

with

$$c_{21}^{\psi} \equiv \frac{4\pi}{3}\sqrt{\frac{6}{5}}\,\frac{a^4}{C-A}. \tag{S371}$$

Assuming, for the harmonic coefficients of the load variation, a PC evolution

$$\mathcal{L}_{21}(t) = \sum_{k=0}^{N} \Delta\mathcal{L}_{21,k}\; H(t-t_k)\,, \tag{S372}$$

from Eq. (S370) we obtain, for $\mathbf{\Psi}^{rig}$, the following expression

$$\mathbf{\Psi}^{rig}(t) = c_{21}^{\psi} \sum_{k=0}^{N} \Delta\mathcal{L}_{21,k}^{*}\; H(t-t_k). \tag{S373}$$

S8.4 Centrifugal potential variations

This section is devoted to the study of the variations of the centrifugal potential $\Lambda(\gamma,t)$ caused by movements of the Earth's rotation axis. In particular, we show that $\Lambda(\gamma,t)$ can be expressed by harmonic functions of degrees $l=2$ and $l=0$, with

$$\Lambda(\gamma,t) = \Lambda_{00}\mathcal{Y}_{00} + \sum_{m=-2}^{2} \Lambda_{2m}\mathcal{Y}_{2m}, \tag{S374}$$

where coefficients Λ_{00} and Λ_{2m} ($|m|\leq 2$) depend upon the components the (time variable) angular velocity vector.

Rotational states. To obtain a suitable expression for the coefficients $\Lambda_{lm}(t)$ in Eq. (S374), in the following we consider the centrifugal potential in two distinct rotation states. In particular, following the scheme outlined in §S8.1, we assume a reference state in which the Earth has been rotating in equilibrium until time $t_0=0$, with its angular velocity vector constantly aligned with the z axis, *i.e.,*

$$\omega_i^0 = \Omega\delta_{i3}, \tag{S375}$$

where Ω is a constant. Subsequently, for $t>t_0=0$, a new dynamical state is attained in response to the forcing imposed by *e.g.,* GIA. In this state, the rotation axis is slightly displaced with respect to the equilibrium axis, so that

$$\omega_i(t) = \Omega(m_i+\delta_{i3}), \tag{S376}$$

where the m_i's ($i=1,2,3$) are small dimensionless quantities ($m_i \ll 1$) introduced in §S5.1. We note that, in the new state, the squared modulus of the angular velocity vector is

$$\begin{aligned}
\omega^2(t) &\equiv \omega_1^2+\omega_2^2+\omega_3^2 && \text{(S377)}\\
&= \Omega^2\left(m_1^2+m_2^2+m_3^2+2m_3+1\right) && \text{(S378)}\\
&= \Omega^2\left(1+2m_3+m^2\right), && \text{(S379)}
\end{aligned}$$

where

$$m^2(t) = m_1^2+m_2^2+m_3^2. \tag{S380}$$

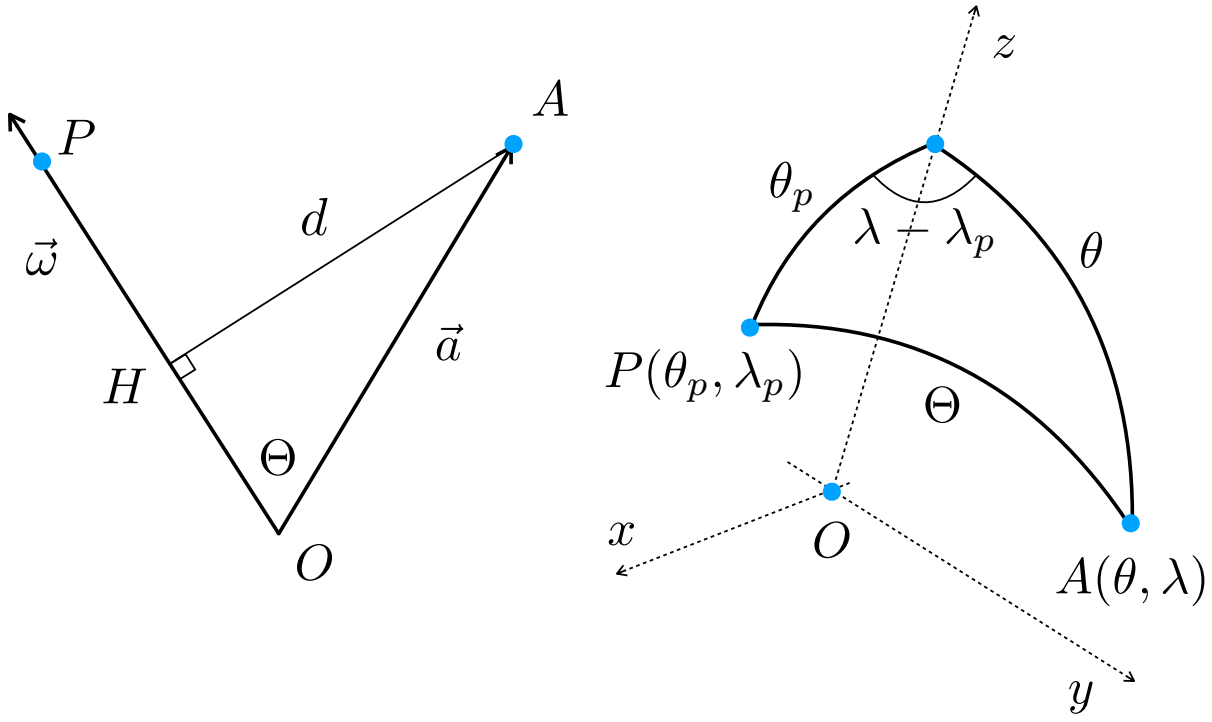

Figure S5. Geometry for the study of variations of the centrifugal potential $\Lambda(\gamma, t)$. A is an Earth-fixed observer at (a, θ, λ), $P = (a, \theta_p, \lambda_p)$ is the instantaneous position of the pole of rotation, and $\vec{\omega}$ is the angular velocity vector. With Θ we denote the the co-latitude of A with respect to P.

Furthermore, denoting by θ_p and λ_p the co-latitude and longitude of the instantaneous pole of rotation, *i.e.,* the point where the rotation axis pierces the Earth's surface (see Figure S5), we have

$$\omega_1(t) \equiv \omega \sin\theta_p \cos\lambda_p = \Omega m_1 \tag{S381}$$

$$\omega_2(t) = \omega \sin\theta_p \sin\lambda_p = \Omega m_2 \tag{S382}$$

$$\omega_3(t) = \omega \cos\theta_p = \Omega(1 + m_3), \tag{S383}$$

where from Eq. (S377) the modulus of the angular rotation vector is $\omega = \omega(t) = \sqrt{\omega_1^2 + \omega_2^2 + \omega_3^2}$.

Centrifugal potential. In the general rotation state, the centrifugal potential experienced by an observer A located at the Earth's surface (hence rotating with the Earth) is

$$U^c(A) = \frac{1}{2}\omega^2 d^2, \tag{S384}$$

where d is the distance between point A and the instantaneous rotation axis $\overrightarrow{\omega}$ (see Figure S5). Since $d = a\sin\Theta$, where Θ is the co-latitude of A with respect to the direction of $\overrightarrow{\omega}$, we have

$$U^c(A) = \frac{1}{2}\omega^2 a^2 \left(1 - \cos^2\Theta\right), \tag{S385}$$

showing that the potential vanishes when the observer is located at the instantaneous pole of rotation (*i.e.,* $\Theta = 0$) or at the antipodes ($\Theta = \pi$) and it is maximum along the equator ($\Theta = \pi/2$).

On one hand, using Table S4, in the general rotation state the centrifugal potential $U^c(A)$ can be easily expressed in terms of degree $l = 0$ and $l = 2$ Legendre polynomials:

$$U^c(A) = \frac{\omega^2 a^2}{3}\left(P_0(\cos\Theta) - P_2(\cos\Theta)\right); \tag{S386}$$

on the other hand, in the reference rotation state, at the same point the centrifugal potential is

$$U^{c0}(A) = \frac{\Omega^2 a^2}{3}\left(P_0(\cos\theta) - P_2(\cos\theta)\right), \tag{S387}$$

where θ is the co-latitude of A in the geographical reference frame. Hence, the centrifugal potential variation experienced at point A is

$$\Lambda(\gamma, t) \equiv U^c - U^{c0}, \tag{S388}$$

which according to Eqs. (S386) and (S387) can be cast in the form

$$\Lambda(\gamma, t) = \Lambda'(t) + \Lambda''(\gamma, t), \tag{S389}$$

where we have defined

$$\Lambda'(t) = \frac{a^2}{3}\left(\omega^2 - \Omega^2\right) \tag{S390}$$

and

$$\Lambda''(\gamma, t) = -\frac{a^2}{3}\left(\omega^2 P_2(\cos\Theta) - \Omega^2 P_2(\cos\theta)\right), \tag{S391}$$

and where $\gamma = (\theta, \lambda)$ are the geographical coordinates of A.

Harmonic degree $l = 0$. Since Λ' in Eq. (S390) is constant over the Earth's surface (*i.e.,* it does not depend on γ), its CSH expansion is straightforward. Indeed, using Eq. (S379), we have

$$\begin{aligned}
\Lambda'(\gamma, t) &= \frac{a^2}{3}\left(\omega^2 - \Omega^2\right) \\
&= \frac{a^2}{3}\left(\Omega^2\left(1 + 2m_3 + m^2\right) - \Omega^2\right) \\
&= \frac{a^2\Omega^2}{3}\left(m^2 + 2m_3\right),
\end{aligned} \tag{S392}$$

hence $\Lambda'(t)$ is a harmonic function of degree $l = 0$, *i.e.,*

$$\Lambda'(t) = \Lambda_{00}\mathcal{Y}_{00} \tag{S393}$$

where $\mathcal{Y}_{00} = 1$ and

$$\Lambda_{00}(t) = \frac{a^2\Omega^2}{3}\left(m^2 + 2m_3\right). \tag{S394}$$

Harmonic degree l = 2. The expansion of $\Lambda''(\gamma,t)$, defined by Eq. (S391), requires some more work. First of all, with the aid of Table S5, we obtain the $l=2$ CSHs at γ_p:

$$\mathcal{Y}_{20}(\gamma_p) \equiv \sqrt{5}P_{20}(\cos\theta_p) = \frac{\sqrt{5}}{2}\left(3\cos^2\theta_p - 1\right), \tag{S395}$$

$$\mathcal{Y}_{21}(\gamma_p) \equiv \sqrt{\frac{5}{6}}P_{21}(\cos\theta_p)\,\mathrm{e}^{i\lambda_p} = -3\sqrt{\frac{5}{6}}\sin\theta_p\cos\theta_p\,\mathrm{e}^{i\lambda_p}, \tag{S396}$$

$$\mathcal{Y}_{22}(\gamma_p) \equiv \sqrt{\frac{5}{24}}P_{22}(\cos\theta_p)\,\mathrm{e}^{2i\lambda_p} = 3\sqrt{\frac{5}{24}}\sin^2\theta_p\,\mathrm{e}^{2i\lambda_p}. \tag{S397}$$

Then, applying the Addition Theorem expressed by Eq. (S426) to the spherical triangle with sides Θ, θ and θ_p, we have

$$P_2(\cos\Theta) = \frac{1}{5}\sum_{m=-2}^{2}\mathcal{Y}^*_{2m}(\gamma_p)\mathcal{Y}_{2m}(\gamma), \tag{S398}$$

which makes it possible to express the centrifugal potential variation only in terms of γ and γ_p, *i.e.,* of the geographical coordinates of points A and P, respectively (see Figure S5). In fact, substitution of Eq. (S398) into (S391), also taking (S395) into account, provides

$$\Lambda''(\gamma,t) = -\frac{a^2}{3}\left(\frac{\omega^2}{5}\sum_{m=-2}^{2}\mathcal{Y}^*_{2m}(\gamma_p)\mathcal{Y}_{2m}(\gamma) - \frac{\Omega^2}{\sqrt{5}}\mathcal{Y}_{20}(\gamma)\right) = \tag{S399}$$

$$\begin{aligned} &= -\frac{a^2}{3}\left(\frac{\omega^2}{5}\mathcal{Y}_{20}(\gamma_p) - \frac{\Omega^2}{\sqrt{5}}\right)\mathcal{Y}_{20}(\gamma) + \\ &\quad -\frac{a^2\omega^2}{15}\mathcal{Y}^*_{21}(\gamma_p)\mathcal{Y}_{21}(\gamma) - \frac{a^2\omega^2}{15}\mathcal{Y}^*_{22}(\gamma_p)\mathcal{Y}_{22}(\gamma) + \\ &\quad -\frac{a^2\omega^2}{15}\mathcal{Y}^*_{2-1}(\gamma_p)\mathcal{Y}_{2-1}(\gamma) - \frac{a^2\omega^2}{15}\mathcal{Y}^*_{2-2}(\gamma_p)\mathcal{Y}_{2-2}(\gamma), \end{aligned} \tag{S400}$$

which has the form of a CSH expansion at degree $l=2$, *i.e.,*

$$\Lambda''(\gamma,t) = \sum_{m=-2}^{2}\Lambda_{2m}\mathcal{Y}_{2m}, \tag{S401}$$

where the coefficients Λ_{2m}, considered separately below, can be expressed entirely in terms of the polar motion vector components m_i. Note that since $\Lambda''(\gamma,t)$ is real-valued, we just need to compute the three terms Λ_{20}, Λ_{21} and Λ_{22}, being $\Lambda_{2-m} = (-1)^m\,\Lambda^*_{2m}$ from Eq. (S431).

Degree l=2 and order m=0. This zonal coefficient Λ_{20} appears in front of $\mathcal{Y}_{20}(\gamma)$ in Eq. (S400). Using Eqs. (S395), (S383) and (S379) and some algebra gives

$$\begin{aligned} \Lambda_{20}(t) &= -\frac{a^2}{3}\left(\frac{\omega^2}{5}\mathcal{Y}_{20}(\gamma_p) - \frac{\Omega^2}{\sqrt{5}}\right) \\ &= -\frac{a^2}{6\sqrt{5}}\left(3\omega^2\cos^2\theta_p - \omega^2 - 2\Omega^2\right) \\ &= \frac{a^2\Omega^2}{6\sqrt{5}}(m_1^2 + m_2^2 - 2m_3^2 - 4m_3). \end{aligned} \tag{S402}$$

Degree l=2 and order m=1. The tesseral coefficient Λ_{21} multiplies $\mathcal{Y}_{21}(\gamma)$ in Eq. (S400). Thus, using (S396), we have

$$\begin{aligned}\Lambda_{21}(t) &= -\frac{a^2\omega^2}{15}\mathcal{Y}^*_{21}(\gamma_p)\\ &= -\frac{a^2\omega^2}{15}\left(-3\sqrt{\frac{5}{6}}\right)\sin\theta_p\cos\theta_p\left(\cos\lambda_p - i\sin\lambda_p\right)\\ &= \frac{a^2\Omega^2}{\sqrt{30}}\left(m_1(1+m_3) - im_2(1+m_3)\right),\end{aligned} \tag{S403}$$

where from Eqs. (S381) and (S382) we have employed the identities $\omega_1\omega_3 = \Omega^2 m_1(1+m_3) = \omega^2\sin\theta_p\cos\theta_p\cos\lambda_p$ and $\omega_2\omega_3 = \Omega^2 m_2(1+m_3) = \omega^2\sin\theta_p\cos\theta_p\sin\lambda_p$.

Degree l=2 and order m=2. The sectorial coefficient Λ_{22} is the term in front of $\mathcal{Y}_{22}(\gamma)$ in Eq. (S400). Thus, using (S397) we obtain

$$\Lambda_{22}(t) = -\frac{a^2\omega^2}{15}\mathcal{Y}^*_{22}(\gamma_p) \tag{S404}$$

$$= -\frac{a^2\omega^2}{\sqrt{120}}\sin^2\theta_p\left(\cos 2\lambda_p - i\sin 2\lambda_p\right) \tag{S405}$$

$$= \frac{a^2\omega^2}{2\sqrt{30}}\left(m_2^2 - m_1^2 + 2im_1m_2\right), \tag{S406}$$

where based upon Eqs. (S381) and (S382), we have used $\omega_1^2 - \omega_2^2 = \omega^2\sin^2\theta_p\cos 2\lambda_p = \Omega^2(m_1^2 - m_2^2)$ and $\omega_1\omega_2 = \frac{\omega^2}{2}\sin^2\theta_p\sin 2\lambda_p = \Omega^2 m_1 m_2$.

CSH expansion of Λ. Recalling Eqs. (S389), (S393), and (S401), we conclude that in the geographical reference frame, the CSH expansion of the centrifugal potential variation only contains terms of degree $l = 0$ and $l = 2$:

$$\Lambda(\gamma,t) = \Lambda_{00}\mathcal{Y}_{00} + \sum_{m=-2}^{2}\Lambda_{2m}\mathcal{Y}_{2m}, \tag{S407}$$

in agreement with Eq. (S374). The coefficients of the expansion are:

$$\begin{aligned}\Lambda_{00}(t) &= \frac{a^2\Omega^2}{3}\left(m^2 + 2m_3\right),\\ \Lambda_{20}(t) &= \frac{a^2\Omega^2}{6\sqrt{5}}\left(m_1^2 + m^2 - 2m_3^2 - 4m_3\right),\\ \Lambda_{21}(t) &= \frac{a^2\Omega^2}{\sqrt{30}}\left(m_1(1+m_3) - im_2(1+m_3)\right),\\ \Lambda_{22}(t) &= \frac{a^2\Omega^2}{2\sqrt{30}}\left(m_2^2 - m_1^2 - 2im_1m_2\right),\end{aligned}$$

where neglecting quadratic terms in $m_i \ll 1$, as it is appropriate for small excursions of the rotation axis and consistently with the linearised polar motion theory of §S5.1, gives:

$$\begin{aligned}
\Lambda_{00}(t) &\simeq +\frac{2a^2\Omega^2}{3} m_3 \\
\Lambda_{20}(t) &\simeq -\frac{2a^2\Omega^2}{3\sqrt{5}} m_3, \\
\Lambda_{21}(t) &\simeq +\frac{a^2\Omega^2}{\sqrt{30}} (m_1 - i m_2), \\
\Lambda_{22}(t) &\simeq 0.
\end{aligned}$$

However, as pointed by Han and Wahr (1989) and Milne and Mitrovica (1998), rotational perturbations due to GIA induce m_3 variations which are several orders of magnitude smaller than either m_1 or m_2. Thus, we conclude that the variation in the centrifugal potential is, to a good approximation, a pure degree $l = 2$ and order $m = \pm 1$ harmonic function, whose CSH expansion simply contains the coefficients $\Lambda_{2\pm1}$, where

$$\Lambda_{21}(t) = c_{21}^{\lambda} \mathbf{m}^*, \tag{S408}$$

with

$$c_{21}^{\lambda} = \frac{a^2\Omega^2}{\sqrt{30}}. \tag{S409}$$

We note, in closing, that using Eqs. (S407) and (S408), it is possible to obtain a simple expression for the centrifugal potential variation, as a function of the observer coordinates, namely:

$$\begin{aligned}
\Lambda(\gamma, t) &= \Lambda_{21} \mathcal{Y}_{21} + \Lambda_{2-1} \mathcal{Y}_{2-1} \\
&= \Lambda_{21} \mathcal{Y}_{21} + \Lambda_{21}^* \mathcal{Y}_{21}^* \\
&= 2\,\mathrm{Re}\left(\Lambda_{21} \mathcal{Y}_{21}\right) \\
&= -\frac{1}{2} a^2 \Omega^2 \left(m_1 \cos\lambda + m_2 \sin\lambda\right) \sin 2\theta.
\end{aligned} \tag{S410}$$

S8.5 Spherical harmonic functions

The spherical harmonic functions play an important role in the context of the development of the SLE, since the equation is solved by a (pseudo)spectral method in which all the fields are decomposed in series of spherical harmonics. In this section of the supplement, we introduce the Legendre polynomials, the associated Legendre polynomials, and the complex spherical harmonics. The expansion of a scalar function in series of harmonic functions is accomplished using both complex and real-valued harmonics. Here we only provide the basic definitions and properties; for a more in-depth presentation the reader is referred to the classical textbooks (*e.g.,* Ferrers, 1877; Sternberg et al., 1946; MacRobert, 1947) and to more recent contributions (*e.g.,* Atkinson and Han, 2012; Wieczorek and Meschede, 2018) or web resources[9].

Legendre polynomials. The Legendre polynomials (LPs) $P_l(x)$ are[10] functions of variable x, defined in the interval $-1 \leq x \leq +1$. The LPs are solutions of the Legendre differential equation

$$\frac{d}{dx}\left(\left(1-x^2\right)\frac{dP_l(x)}{dx}\right) + l(l+1)P_l(x) = 0, \tag{S411}$$

[9] See: *https://en.wikipedia.org/wiki/Spherical_harmonics* and *http://mathworld.wolfram.com/SphericalHarmonic.html* - last accessed 24 Jan 2019.

[10] See also *http://mathworld.wolfram.com/LegendrePolynomial.html* - last visited May 16, 2019.

where l ($l = 0, 1, \ldots$) is the *degree* of the LP. A compact expression for the LPs is given by Rodriguez formula

$$P_l(x) = \frac{1}{2^l l!} \frac{d^l}{dx^l}(x^2 - 1)^l. \tag{S412}$$

We note that $P_l(x)$ is a degree l polynomial in x. The low-degree ($l = 0, 1, 2$) LPs are listed in Table S4; in particular, we note that

$$P_0(x) = 1. \tag{S413}$$

Associated Legendre polynomials. The associated Legendre polynomials[11] $P_{lm}(\cos\theta)$ (ALPs) are defined as the canonical solution to the general Legendre differential equation

$$(1 - x^2)\frac{d^2 P_{lm}(x)}{dx^2} - 2x\frac{dP_{lm}(x)}{dx} + \left(l(l+1) - \frac{m^2}{1 - x^2}\right) P_{lm}(x) = 0, \tag{S414}$$

where integers l ($l = 0, 1, \ldots$) and m ($m = 0, 1, \ldots l$) are the *degree* and the *order* of the ALP, respectively. Solutions of Eq. (S414) corresponding to arbitrary real or complex values of l and m are referred to as *associated Legendre functions*. The ALPs can be obtained in terms of m order derivatives of the Legendre polynomials, as follows

$$P_{lm}(x) = (-1)^m (1 - x^2)^{m/2} \frac{d^m}{dx^m} P_l(x), \tag{S415}$$

where in this definition of $P_{lm}(x)$ we have included the so-called "Condon-Shortley phase factor" $(-1)^m$. We also note that the ALPs of order $m = 0$ coincide with the corresponding LP, *i.e.,*

$$P_{l0}(x) = P_l(x). \tag{S416}$$

The P_{lm}'s defined by Eq. (S415) are also referred to as *un-normalised* ALPs. For them, the following orthogonality condition holds

$$\int_{-1}^{+1} P_{lm}(x) P_{l'm}(x) dx = \frac{2(l+m)!}{(2l+1)(l-m)!} \delta_{ll'}, \tag{S417}$$

where δ_{ij} is the Kronecker delta (see Table 1 of Wieczorek and Meschede, 2018).

Fully normalised associated Legendre polynomials. Along with the un-normalised P_{lm}'s, various *normalised* forms of the ALPs exist, which have been recently categorized by Wieczorek and Meschede (2018). One of these forms is of interest here, since it is usually employed in the field of geodesy and spectral analysis, and referred to as the *fully normalised* form of the ALP (or FNALP). We note that in Wieczorek and Meschede 2018) the term *fully normalised* is not adopted and this form is rather referred to as a 4π-normalised (real) form.

The FNALPs of degree l and order m are defined by

$$\overline{P}_{lm}(x) = \sqrt{(2 - \delta_{0m})(2l+1)\frac{(l-m)!}{(l+m)!}}\, P_{lm}(x), \tag{S418}$$

where $P_{lm}(x)$ is the usual un-normalised form given by Eq. (S415). Note that by virtue of definition (S415), the FNALPs include the Condon-Shortley phase factor. Using (S418) and (S417) it is easily verified that for the FNALPs the following orthogonality condition holds true

$$\int_{-1}^{+1} \overline{P}_{lm}(x) \overline{P}_{l'm}(x) dx = 2(2 - \delta_{0m})\, \delta_{ll'}, \tag{S419}$$

[11] A nice introduction is found at the page *https://en.wikipedia.org/wiki/Associated_Legendre_polynomials* - last accessed 16 May, 2019.

in agreement with Wieczorek and Meschede (2018).

Complex Spherical Harmonics. The complex spherical harmonics (CSHs) are complex-valued functions of colatitude θ and longitude λ, defined on the unit sphere *i.e.,* for $0 \leq \theta \leq \pi$ and $0 \leq \lambda \leq 2\pi$. In this work, for the development of the SLE theory and for the numerical implementation, we use conventionally the so-called 4π-normalised form of the CSHs. Other choices, characterised by different normalisations are however possible, as explained in Wieczorek and Meschede (2018). Indeed, in a previous treatment of the SLE (Spada and Stocchi, 2006), "quantum mechanics" (or "1-normalised") complex spherical harmonics have been used.

For *non-negative orders*, the 4π-normalised CSHs are defined as

$$\mathcal{Y}_{lm}(\gamma) = \sqrt{(2l+1)\frac{(l-m)!}{(l+m)!}}\, P_{lm}(\cos\theta)\mathrm{e}^{im\lambda}, \quad m \geq 0, \tag{S420}$$

where γ = (θ,λ), $P_{lm}(\cos\theta)$ is the un-normalised ALP given by Eq. (S415), and integers l ($l = 0, 1, \ldots$) and m ($|m| \leq l$) are harmonic *degree* and *order* of the CSH, respectively.

For *negative orders,* the CSHs are obtained as

$$\mathcal{Y}_{l-m}(\gamma) = (-1)^m \mathcal{Y}^*_{lm}(\gamma) \tag{S421}$$

where the asterisk denotes complex conjugation.

We observe that, using Eq. (S418), the CSHs can be also written in terms of FNALPs, with

$$\mathcal{Y}_{lm}(\gamma) = \frac{1}{\sqrt{2-\delta_{0m}}}\, \overline{P}_{lm}(\cos\theta)\mathrm{e}^{im\lambda}. \tag{S422}$$

A few properties of the Complex Spherical Harmonics. We only give a few essential properties, needed for the development of the SLE theory.

1. Orthonormality. The CSH are orthonormal. In particular, due to the particular choice of the normalization factor in Eq. (S420), the following *orthogonality condition* holds

$$\int_\gamma \mathcal{Y}_{lm}(\gamma)\mathcal{Y}^*_{l'm'}(\gamma)\, d\gamma = 4\pi\, \delta_{ll'}\delta_{mm'}, \tag{S423}$$

which motivates the attribute "4π-normalised" of the CSH.

2. Degree 0 CSH. By definition of CSHs (see Eq. S420), since $P_{00} = 1$ (see S416 and S413), it turns out that

$$\mathcal{Y}_{00}(\gamma) = 1. \tag{S424}$$

Other low-degree CSHs are listed in Table S4.

3. Addition Theorem. We consider two points on the unit sphere, with coordinates $\gamma = (\theta, \lambda)$ and $\gamma' = (\theta', \lambda')$, and we denote with Θ the angular distance between γ and γ' along the great circle connecting the two points. By the law of cosines (or "cosine rule for sides") in spherical trigonometry, we have

$$\cos\Theta = \cos\theta\cos\theta' + \sin\theta\sin\theta'\cos(\lambda - \lambda'), \tag{S425}$$

and the Addition Theorem for CSHs states that

$$P_l(\cos\Theta) = \frac{1}{2l+1}\sum_{m=-l}^{l} \mathcal{Y}^*_{lm}(\gamma')\mathcal{Y}_{lm}(\gamma), \tag{S426}$$

where $P_l(x)$ is the degree l LP given by Eq. (S412).

4. Average of the CSHs. All the CSHs have a vanishing average over the sphere, except $\mathcal{Y}_{00}(\gamma)$. This can be seen immediately using the definition of average (see Eq. S218), the orthogonality condition (S423) and using (S424):

$$\begin{aligned} < \mathcal{Y}_{lm}(\gamma) >^e &\equiv \frac{1}{4\pi a^2} \int\limits_e \mathcal{Y}_{lm}(\gamma) dA \\ &= \frac{1}{4\pi a^2} \int\limits_e \mathcal{Y}_{lm}(\gamma) a^2 d\gamma \\ &= \frac{1}{4\pi} \int\limits_\gamma \mathcal{Y}_{lm}(\gamma) \mathcal{Y}^*_{00}(\gamma) d\gamma \\ &= \delta_{l0}\delta_{m0}. \end{aligned} \tag{S427}$$

Expansion in series of CSHs. It is often useful to expand a scalar, square-integrable, real-valued, time-dependent function as an infinite series of CSHs, with

$$F(\gamma,t) = \sum_{lm} F_{lm}(t) \mathcal{Y}_{lm}(\gamma), \tag{S428}$$

where $F_{lm}(t)$ are the (complex) *coefficients of the CSH expansion* and we use the notation

$$\sum_{lm} \equiv \sum_{l=0}^{\infty} \sum_{m=-l}^{l}. \tag{S429}$$

Multiplying both sides of Eq. (S428) by $\mathcal{Y}^*_{l'm'}(\gamma)$, where l' and m' are an arbitrary degree and order, integrating over the unit sphere and using the orthogonality condition (S423), the coefficients of the CSH expansion are easily obtained:

$$\begin{aligned} F(\gamma,t)\mathcal{Y}^*_{l'm'}(\gamma) &= \sum_{lm} F_{lm}(t) \mathcal{Y}_{lm}(\gamma) \mathcal{Y}^*_{l'm'}(\gamma) \\ \int\limits_\gamma F(\gamma,t)\mathcal{Y}^*_{l'm'}(\gamma) d\gamma &= \sum_{lm} F_{lm}(t) \int\limits_\gamma \mathcal{Y}_{lm}(\gamma) \mathcal{Y}^*_{l'm'}(\gamma) d\gamma, \\ \int\limits_\gamma F(\gamma,t)\mathcal{Y}^*_{l'm'}(\gamma) d\gamma &= 4\pi \sum_{lm} F_{lm}(t) \delta_{ll'}\delta_{mm'} \\ \int\limits_\gamma F(\gamma,t)\mathcal{Y}^*_{l'm'}(\gamma) d\gamma &= 4\pi F_{l'm'}(t), \end{aligned}$$

hence, for an arbitrary degree l and order m, we have

$$F_{lm}(t) = \frac{1}{4\pi} \int\limits_\gamma F(\gamma,t) \mathcal{Y}^*_{lm}(\gamma) d\gamma, \tag{S430}$$

where, taking Eq. (S421) into account, we have the symmetry condition on the coefficients

$$F_{l-m}(t) = (-1)^m F^*_{lm}(t). \tag{S431}$$

It can be easily verified that the degree $l = 0$ coefficient in the CSH expansion (S428) simply represents the average of $F(\gamma, t)$ over the sphere. In fact, using $l = m = 0$ and Eq. (S424) into (S430) we see that

$$\begin{aligned} F_{00}(t) &= \frac{1}{4\pi}\int_{\gamma} F(\gamma,t)d\gamma \\ &= \frac{1}{4\pi a^2}\int_{e} F(\gamma,t)dA \\ &\equiv < F(\gamma,t) >^{e}, \end{aligned} \tag{S432}$$

where according to (S218) $< F(\gamma,t) >^{e}$ is the *spatial average* of $F(\gamma,t)$ over the sphere of radius a.

Expansion in series of FNALPs. In the field of geodesy and spectral analysis, real harmonic functions are generally preferred to complex harmonics (see *e.g.,* Heiskanen and Moritz, 1967). Here we show that a CSH expansion like

$$F(\gamma) = \sum_{lm} F_{lm}\mathcal{Y}_{lm}(\gamma), \tag{S433}$$

where we have omitted the time-dependence of F for the sake of simplicity, is equivalent to a (real) FNALP expansion restricted to positive orders, with

$$F(\gamma) = \sum_{\substack{lm \\ m\geq 0}} (\overline{u}_{lm}\cos m\lambda + \overline{v}_{lm}\sin m\lambda)\,\overline{P}_{lm}(\cos\theta), \tag{S434}$$

where the cosine and sine real-valued coefficients $\overline{u}_{lm}$ and $\overline{v}_{lm}$ are univocally determined by F_{lm}. The demonstration is straightforward, and is based on condition (S431), on Eq. (S422), and some algebra. The details follow:

$$\begin{aligned} F(\gamma) &= \sum_{lm} F_{lm}\mathcal{Y}_{lm}(\gamma) \\ &= \sum_{l}\left(\sum_{m<0} F_{lm}\mathcal{Y}_{lm} + F_{l0}\mathcal{Y}_{l0} + \sum_{m>0} F_{lm}\mathcal{Y}_{lm}\right) \\ &= \sum_{l}\left(\sum_{m'>0} F_{l-m'}\mathcal{Y}_{l-m'} + F_{l0}\mathcal{Y}_{l0} + \sum_{m>0} F_{lm}\mathcal{Y}_{lm}\right) \\ &= \sum_{l}\left(\sum_{m'>0} (-1)^{m'}F^{*}_{lm'}(-1)^{m'}\mathcal{Y}^{*}_{lm'} + F_{l0}\mathcal{Y}_{l0} + \sum_{m>0} F_{lm}\mathcal{Y}_{lm}\right) \\ &= \sum_{l}\left(\sum_{m>0} F^{*}_{lm}\mathcal{Y}^{*}_{lm} + F_{l0}\mathcal{Y}_{l0} + \sum_{m>0} F_{lm}\mathcal{Y}_{lm}\right) \\ &= \sum_{\substack{lm \\ m\geq 0}} (2-\delta_{0m})\,\mathrm{Re}\,(F_{lm}\mathcal{Y}_{lm}) \\ &= \sum_{\substack{lm \\ m\geq 0}} (2-\delta_{0m})\,(\mathrm{Re}(F_{lm})\mathrm{Re}(\mathcal{Y}_{lm}) - \mathrm{Im}(F_{lm})\mathrm{Im}(\mathcal{Y}_{lm})) \\ &= \sum_{\substack{lm \\ m\geq 0}} (2-\delta_{0m})\,\frac{1}{\sqrt{2-\delta_{0m}}}\,(\mathrm{Re}(F_{lm})\cos m\lambda - \mathrm{Im}(F_{lm})\sin m\lambda)\,\overline{P}_{lm}(\cos\theta) \\ &= \sum_{\substack{lm \\ m\geq 0}} (\overline{u}_{lm}\cos m\lambda + \overline{v}_{lm}\sin m\lambda)\,\overline{P}_{lm}(\cos\theta), \end{aligned} \tag{S435}$$

hence, for a general time-dependent scalar function $F(\gamma,t)$, the relationship between the coefficients of the CSH expansion (S433) and those of the real expansion (S434) over the FNALPs is:

$$\overline{u}_{lm}(t) = +\sqrt{2-\delta_{0m}}\,\mathrm{Re}\,(F_{lm}(t)) \tag{S436}$$

$$\overline{v}_{lm}(t) = -\sqrt{2-\delta_{0m}}\,\mathrm{Im}\,(F_{lm}(t))\,; \tag{S437}$$

we note that this relationship can be equivalently stated as

$$\overline{u}_{lm}(t) + i\,\overline{v}_{lm}(t) = \sqrt{2-\delta_{0m}}\,F^{*}_{lm}(t), \tag{S438}$$

where $F^{*}_{lm}(t)$ is the complex conjugate of $F_{lm}(t)$.

S8.6 The Tegmark grid

In all the versions of program *SELEN* published so far (Spada and Stocchi, 2006, 2007; Spada et al., 2012; Spada and Melini, 2015), the spatial discretisation of the SLE has been accomplished with the aid of the equal-area, icosahedron-shaped, spherical pixelization introduced by Tegmark (1996), and employed in astrophysics to study the Cosmic Microwave Background (*e.g.,* Tegmark et al., 2003). The Tegmark grid is also employed in *SELEN*^{4}. The grid is particularly convenient for the manipulation of harmonic functions, for the computation of power spectra, and for the numerical evaluation of surface integrals (quadrature) on the sphere.

Properties of the Tegmark grid. The Tegmark grid is characterised by a "resolution parameter" R that determines the density of the pixels on the surface of the unit sphere, and consequently the size of the grid cells. For a given value of R, the number of pixels on the grid is

$$P = 40R(R-1)+12, \tag{S439}$$

where each pixel is the center of slightly distorted, hexagonal equal-area grid cells. As an example, Figure S6 shows four Tegmark pixelizations characterised by resolutions $R = 18$, 28, 44, and 60.

For a given pixelization, the cell area is

$$A^c = \frac{4\pi a^2}{P}, \tag{S440}$$

where $a = 6371$ km is Earth's radius. Thus, the angular half-amplitude of a disk on the sphere having an area A^c, is

$$\delta = \left(\frac{180^\circ}{\pi}\right)\cos^{-1}\left(1-\frac{2}{P}\right), \tag{S441}$$

where δ is expressed in degrees. For a sufficiently large number of pixels, the cell can be assimilated to a disk on a plane. An *approssimate value* for the radius of the disk is

$$r_{cell} \approx \frac{2a}{\sqrt{P}}, \tag{S442}$$

an expression which is useful to obtain a quick estimate of the grid spacing.

Tegmark (1996) has shown that a sufficiently accurate numerical integration of harmonic functions up to degree l_{max} demands a commensurately large number of pixels, with

$$P \geq \frac{l^2_{max}}{3}. \tag{S443}$$

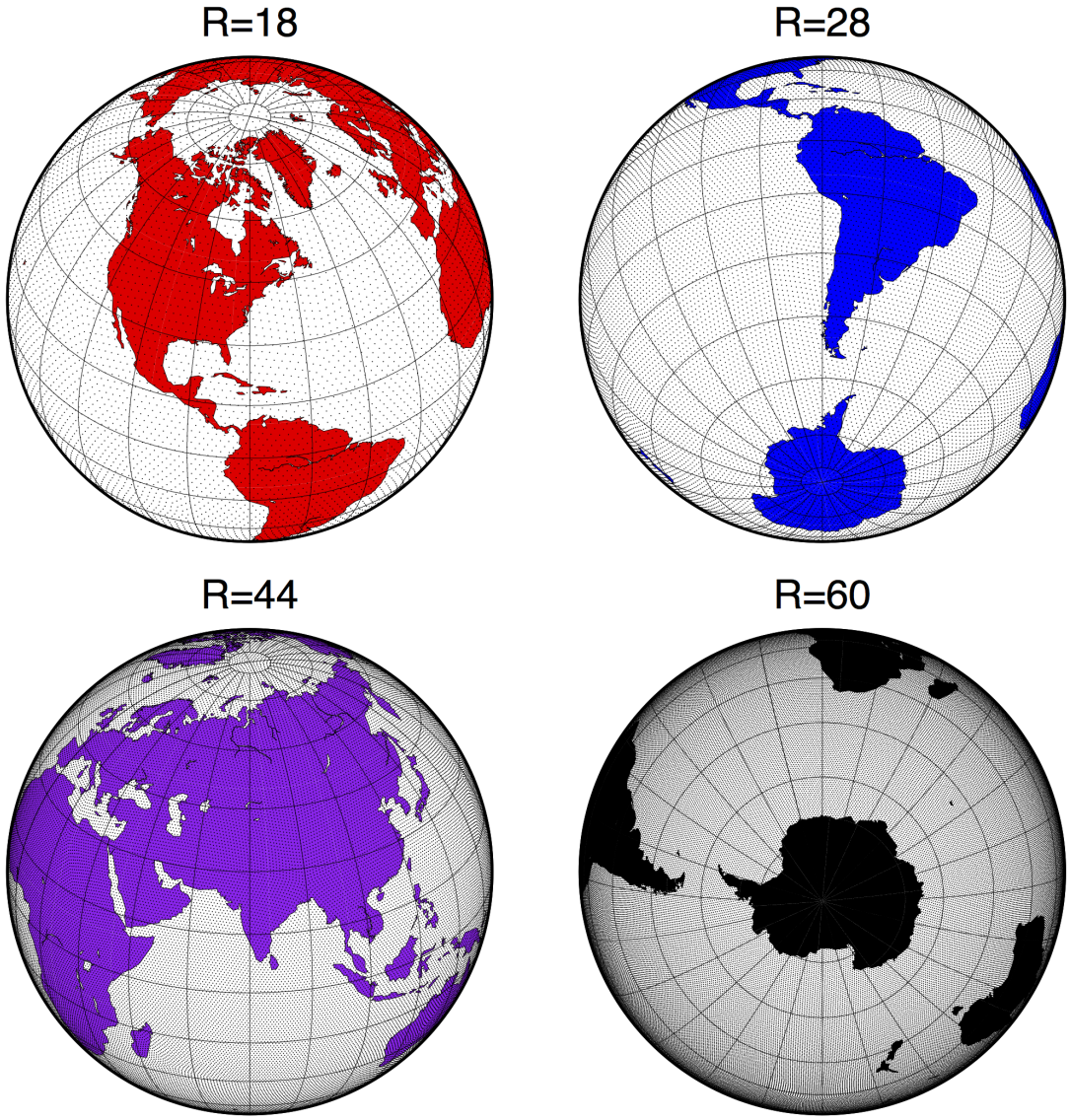

Figure S6. Four pixelizations of the sphere according to the icosahedron-based algorithm by Tegmark (1996), with increasing spatial resolutions $R = 18, 28, 44$ and 60 (for the geometrical properties of these and other pixelizations, see Table S6).

This implies that, for a given value of P, there is an upper limit to the l_{max} value that can be safely employed in the numerical solution of the SLE, namely $l_{max} \leq L_M$. Values of l_{max} exceeding L_M would not guarantee that some fundamental properties of the CSHs (such as their orthonormality) can be numerically reproduced on the grid with a sufficient precision. According to Eq. (S443), we have

$$L_M = \sqrt{3P}. \tag{S444}$$

We also note that the constraint given by Eq. (S443) can be employed to provide a very rough *rule of thumb* that gives the minimum spatial resolution R that is to be employed for a fixed l_{max}. In fact, since from (S439), $P \sim 40R^2$, (S443) gives $40R^2 \geq l_{max}^2/3$, hence

$$R \geq \frac{l_{max}}{10}. \tag{S445}$$

The statistics of the Tegmark grid are summarised in Table S6 for some values of the resolution parameter R.

Quadrature rule. In the numerical implementation of the SLE, the Tegmark grid is intensively exploited, especially for computing coefficients of the CSH expansions of relevant scalar fields (Spada and Stocchi, 2006, 2007; Spada et al., 2012; Spada and Melini, 2015). Of course, other integration methods are possible, such as the traditional Gauss-Legendre quadrature (*e.g.,* Press 2007). However, the almost regular grid of points implied by the icosahedron method of Tegmark (1996) makes it very attractive for problems in spherical geometry, where a maximally regular pixelization is needed to optimise the algorithm.

The Tegmark grid provides a set of equal-weight integration points which allow for a straightforward, nearly optimal quadrature on the sphere, *i.e.,*

$$\int_e F(\gamma)\, dA \approx A^c \sum_p F(\gamma_p), \tag{S446}$$

where

$$\sum_p \equiv \sum_{p=1}^{P} \tag{S447}$$

denotes the sum over all the pixels, we have taken advantage of the equal-area property of the grid, $F(\gamma_p)$ is the value of $F(\gamma)$ at the pixel (the center of the cell) and $\gamma_p = (\theta_p, \lambda_p)$ denotes the spherical coordinates (colatitide and longitude) of the pixels. Eq. (S446) constitutes the basic principle adopted in our numerical implementation of the SLE.

The quadrature rule given by Eq. (S446) can be applied to the computation of the coefficients of the CSH expansion of a general scalar field, a problem that is often encountered in this supplement. As discussed in §S8.5 above, the CSH expansion of a scalar function $F(\gamma, t)$ reads

$$F(\gamma, t) = \sum_{lm} F_{lm}(t) \mathcal{Y}_{lm}(\gamma), \tag{S448}$$

where, using the orthonormality property of the CSHs given by Eq. (S423), the computation of the coefficients $F_{lm}(t)$ demands the evaluation of the following surface integral over the unit sphere:

$$F_{lm}(t) = \frac{1}{4\pi} \int_\gamma F(\gamma, t) \mathcal{Y}^*_{lm}(\gamma) d\gamma, \tag{S449}$$

where $\mathcal{Y}^*_{lm}(\gamma)$ is the complex conjugate of $\mathcal{Y}_{lm}(\gamma)$. Recalling that $d\gamma$ is such that $dA = a^2 d\gamma$ and applying Eq. (S446) provides the CSH coefficients

$$F_j(t) = \frac{1}{P} \sum_p F(\gamma_p, t) \mathcal{Y}^*_j(\gamma_p), \tag{S450}$$

where conventionally letter j stands for the couple lm. Setting $t = t_n$, where t_n is a specific point of the time grid adopted in this work (see §S8.1) gives

$$F_j(t_n) = \frac{1}{P}\sum_p F(\gamma_p, t_n)\mathcal{Y}_j^*(\gamma_p), \tag{S451}$$

which, according to the conventions described in §S7, can be written in compact form as

$$F_{j,n} = \frac{1}{P}\sum_p F_{p,n}\mathcal{Y}_{j,p}^*. \tag{S452}$$

S8.7 Numerical solution of the SLE

In *SELEN*^{4}, the SLE is solved iteratively in the spectral domain. Since some of the computations are performed directly on a grid, the term *pseudo*spectral is often invoked, with reference to this approach. The equation is decomposed in series of CSHs and the harmonic components constitute the unknowns in the iteration. By an harmonic synthesis, the coefficients are subsequently employed to retrieve the solution in the space domain by summation over the CSHs. An iterative approach is natural in the context of integral Fredholm equations (*e.g.,* Jerri, 1999), and it has been utilized systematically in the literature since the integral nature of the SLE has been recognized first (Farrell and Clark, 1976; Spada, 2017).

A very detailed treatment of the iterative approach to the SLE is given by Kendall et al. (2005), who however is based on a formalism that differs from the one employed here. The iterative solution scheme of the SLE also takes advantage of the so-called pseudo-spectral method (Mitrovica and Peltier, 1991; Mitrovica and Milne, 2003), in which the original unknown field $\mathcal{S}$ (*i.e.,* sea-level change) is substituted by the ocean-projected unknown field $\mathcal{Z} = O\mathcal{S}$ (see Eq. S192), thus making the cumbersome evaluation of Wigner coupling coefficients (Plag and Jüettner, 2001) unnecessary.

Execution phases. The execution of *SELEN*^{4} sees six distinct phases.

- Phase 1. Some basic data are input from external files. These include the spherical coordinates (longitude and colatitude) of the Tegmark pixels (γ_p), a set of pre-computed CSHs ($\mathcal{Y}_{j,p}$) to a given maximum degree l_{max}, a pixelization of the modern Earth's relief ($T_{p,N}$), and the full history of the ice thickness ($I_{p,n}$). Furthermore, the program reads the combinations of Love numbers that build the Green's functions (*i.e.,* arrays $\beta_{l,n}^{ug}$ and γ_n^{ug}), which are employed to compute the isostatic and rotational response functions. These quantities must be pre-computed and supplied by the User. However, our release of *SELEN*^{4} comes with a small set of these input fields, corresponding to different spatial resolutions.

- Phase 2. *SELEN*^{4} initializes the global topography, assuming to a first approximation that it corresponds to present-day topography during the whole time interval since the inception of melting, setting $T_{p,n} = T_{p,N}$. A first guess of the OF $O_{p,n}$ is obtained using this approximation of topography and the chosen input ice model. Initial values of the CSH coefficients $\mathcal{S}_{j,n}$ are computed assuming a globally uniform sea-level change, matching the ocean-averaged value evaluated by the initialized OF, *i.e.,* setting $\mathcal{S}_{j,n}^{(0)} = \mathcal{S}_{j,n}^{ave}$.

- Phases 3 and 4. The program executes two nested do-loops (iterations). The external iteration is performed n_{ext} times over the topography, which is progressively updated taking advantage of the PT equation (see Eq. S10) once the internal iterations are accomplished. In the external iteration, the response functions $\mathcal{R}_{j,n}^a$ and $\mathcal{R}_{j,n}^c$ are evaluated, as well as arrays $\mathcal{K}_{j,n}^a$ and $\mathcal{K}_{j,n}^c$, which do not depend upon the value of $\mathcal{Z}_{j,n}$. The solution of the SLE in terms of variable $\mathcal{Z} = O\mathcal{S}$ is performed in the internal iteration, based on an iterative scheme as well and performed n_{int} times, assuming as starting value $\mathcal{Z}_{j,n} = \mathcal{Z}_{j,n}^{ave}$. Here, the $\mathcal{Z}_{j,n}$-dependent response functions $\mathcal{R}_{j,n}^b$ and $\mathcal{R}_{j,n}^{rot}$ are progressively updated, as well as $\mathcal{K}_{j,n}^b$ and the rotational contribution $\mathcal{K}_{j,n}^{rot}$.

- Phase 5. The CSH components of the response functions $\mathcal{U}_{j,n}$, $\mathcal{G}_{j,n}$ and $\mathcal{N}_{j,n}$ (including their surface and rotational components) are evaluated, using the outcomes of the last external iteration executed. In this phase, *SELEN*^{4} writes several outputs on external files; however some outputs are also created (or updated) during the previous phases.

- Phase 6. *SELEN*^{4} executes some post-processing steps, in which the CSH coefficients previously copied on the output files are read and synthesized to obtain several geophysical quantities of interest (RSL variations at specific sites, paleo-topography grids, geodetic variations at specific locations, the excursion of the Earth's axis of rotation, variations of the Stokes coefficients of the Earth's gravity field, geodetic fingerprints, *et cetera*). In SM19, an intermediate-resolution *test run* of *SELEN*^{4} (*i.e.,* $R = 44$, $l_{max} = 128$ and $n_{ext} = n_{int} = 3$) is performed to illustrate the outputs that are available at end of the post-processing phase.

Workflow of *SELEN*^{4}. Below, we outline the workflow of the Fortran 90 program that we have progressively developed to solve the SLE, based on the theory illustrated in this supplement.

Declarations

The program begins

■ Phase 1: Data input.

Read: $(\gamma_p,\ \mathcal{Y}_{j,p},\ T_{p,N},\ I_{p,n})$,
Read: $\left(\beta_{l,n}^{ug},\ \gamma_n^{ug}\right)$.

■ Phase 2: Initialisation.

Set: $T_{p,n} = T_{p,N}$,
Write: $T_{p,n}$,
$O_{p,n} \Longleftarrow (T_{p,n}, I_{p,n})$,
Write: $O_{p,n}$,
$\mathcal{S}_n^{equ} \Longleftarrow (I_{p,n}, O_{p,n})$,
$\mathcal{S}_n^{ofu} \Longleftarrow (T_{p,0}, O_{p,n})$,
$\mathcal{S}_n^{ave} \Longleftarrow \left(\mathcal{S}_n^{equ}, \mathcal{S}_n^{ofu}\right)$,
$\mathcal{S}_{j,n}^{ave} \Longleftarrow (\mathcal{S}_n^{ave})$,
Set: $\mathcal{S}_{j,n}^{(0)} = \mathcal{S}_{j,n}^{ave}$.

■ Phase 3: External iteration *(over the topography)*

DO i_ext = 1, n_ext

$Q_p \Longleftarrow (T_{p,0}, I_{p,0})$,
$O_{j,n} \Longleftarrow \left(O_{p,n}, \mathcal{Y}_{j,p}^*\right)$,
$\mathcal{Z}_{j,n}^{ave} \Longleftarrow (\mathcal{S}_n^{ave}, O_{j,n})$,

[Computing $\mathcal{K}_{j,n}^a$]

$\mathcal{W}_{j,n} \Longleftarrow \left(I_{p,n}, O_{p,n}, \mathcal{Y}_{j,p}^*\right)$,
$\mathcal{L}_{21,n}^a \Longleftarrow (\mathcal{W}_{21,n})$,
$\mathcal{R}_{j,n}^a \Longleftarrow \left(\mathcal{W}_{j,n}, \beta_{l,n}^s\right)$,
$< \mathcal{R}^a >_n^o \Longleftarrow \left(\mathcal{R}_{j,n}^a, O_{j,n}^*\right)$,
$\mathcal{R}_{j,n}^{'a} \Longleftarrow \left(\mathcal{R}_{j,n}^a, < \mathcal{R}^a >_n^o\right)$,
$\chi_{p,n}^a \Longleftarrow \left(\mathcal{R}_{j,n}^{'a}, \mathcal{Y}_{j,p}\right)$,
$\mathcal{K}_{j,n}^a \Longleftarrow \left(\chi_{p,n}^a, \mathcal{Y}_{j,p}^*\right)$,

[Computing $\mathcal{K}_{j,n}^c$]

$\mathcal{X}_{j,n} \Longleftarrow \left(Q_p, O_{p,n}, \mathcal{Y}_{j,p}^*\right)$,
$\mathcal{L}_{21,n}^c \Longleftarrow (\mathcal{X}_{21,n})$,

$\mathcal{R}^{c}_{j,n} \Longleftarrow (\mathcal{X}_{j,n}, \beta^{s}_{l,n})$,
$< \mathcal{R}^{c} >^{o}_{n} \Longleftarrow (\mathcal{R}^{c}_{j,n}, O^{*}_{j,n})$,
$\mathcal{R}^{'c}_{j,n} \Longleftarrow (\mathcal{R}^{c}_{j,n}, < \mathcal{R}^{c} >^{o}_{n})$,
$\chi^{c}_{p,n} \Longleftarrow (\mathcal{R}^{'c}_{j,n}, \mathcal{Y}_{j,p})$,
$\mathcal{K}^{c}_{j,n} \Longleftarrow (\chi^{c}_{p,n}, \mathcal{Y}^{*}_{j,p})$,

Set: $\mathcal{Z}^{(0)}_{j,n} = \mathcal{Z}^{ave}_{j,n}$.

■ **Phase 4: Internal iteration** ***(to solve the SLE)***

DO i_int = 1, n_int

[Computing $\mathcal{K}^{b}_{j,n}$]

$\mathcal{L}^{b}_{21,n} \Longleftarrow (\mathcal{Z}^{i\_int-1}_{21,n})$,
$\mathcal{R}^{b}_{j,n} \Longleftarrow (\mathcal{Z}^{i\_int-1}_{j,n}, \beta^{s}_{l,n})$,
$< \mathcal{R}^{b} >^{o}_{n} \Longleftarrow (\mathcal{R}^{b}_{j,n}, O^{*}_{j,n})$,
$\mathcal{R}^{'b}_{j,n} \Longleftarrow (\mathcal{R}^{b}_{j,n}, < \mathcal{R}^{b} >^{o}_{n})$,
$\chi^{b}_{p,n} \Longleftarrow (\mathcal{R}^{'b}_{j,n}, \mathcal{Y}_{j,p})$,
$\mathcal{K}^{b}_{j,n} \Longleftarrow (\chi^{b}_{p,n}, \mathcal{Y}^{*}_{j,p})$,

[Computing $\mathcal{K}^{rot}_{j,n}$]

$\mathcal{L}_{21,n} \Longleftarrow (\mathcal{L}^{a}_{21,n}, \mathcal{L}^{b}_{21,n}, \mathcal{L}^{c}_{21,n})$,
$\mathcal{G}^{rot}_{21,n} \Longleftarrow (\mathcal{L}_{21,n}, \gamma^{g}_{n})$,
$\mathcal{U}^{rot}_{21,n} \Longleftarrow (\mathcal{L}_{21,n}, \gamma^{u}_{n})$,
$\mathcal{R}^{rot}_{j,n} \Longleftarrow (\mathcal{G}^{rot}_{j,n}, \mathcal{U}^{rot}_{j,n})$,
$< \mathcal{R}^{rot} >^{o}_{n} \Longleftarrow (\mathcal{R}^{rot}_{j,n}, O^{*}_{j,n})$,
$\mathcal{R}^{'rot}_{j,n} \Longleftarrow (\mathcal{R}^{rot}_{j,n}, < \mathcal{R}^{rot} >^{o}_{n})$,
$\chi^{rot}_{p,n} \Longleftarrow (\mathcal{R}^{'rot}_{j,n}, \mathcal{Y}_{j,p})$,
$\mathcal{K}^{rot}_{j,n} \Longleftarrow (\chi^{rot}_{p,n}, \mathcal{Y}^{*}_{j,p})$,

$\Psi^{rig}_{n} \Longleftarrow (\mathcal{L}^{*}_{21,n})$,
$c_{n} \Longleftarrow (\mathcal{S}^{ave}_{n}, < \mathcal{R}^{abc} >^{o}_{n}, < \mathcal{R}^{rot} >^{o}_{n})$,
$\mathcal{Z}^{(i\_int)}_{j,n} \Longleftarrow (\mathcal{Z}^{ave}_{j,n}, \mathcal{K}^{abc}_{j,n}, \mathcal{K}^{rot}_{j,n})$.

ENDDO

$\mathcal{S}^{(i\_ext)}_{j,n} \Longleftarrow (\mathcal{S}^{ave}_{j,n}, \mathcal{R}^{'abc}_{j,n}, \mathcal{R}^{'rot}_{j,n})$,
$\mathcal{S}_{p,n} \Longleftarrow (\mathcal{S}^{(i\_ext)}_{j,n}, \mathcal{Y}_{j,p})$,
$T_{p,n} \Longleftarrow (T_{p,N}, \mathcal{S}_{p,n}, \mathcal{S}_{p,N})$,
Write: $T_{p,n}$
$O_{p,n} \Longleftarrow (T_{p,n}, I_{p,n})$,
Write: $O_{p,n}$
$\mathcal{S}^{equ}_{n} \Longleftarrow (I_{p,n}, O_{p,n})$,
$\mathcal{S}^{ofu}_{n} \Longleftarrow (T_{p,0}, O_{p,n})$,
$\mathcal{S}^{ave}_{n} \Longleftarrow (\mathcal{S}^{equ}_{n}, \mathcal{S}^{ofu}_{n})$,
$\mathcal{S}^{ave}_{j,n} \Longleftarrow (\mathcal{S}^{ave}_{n})$.

ENDDO

Write: $S_{j,n}$

■ **Phase 5: Response functions**

$\mathcal{U}^{a}_{j,n} \Longleftarrow (\mathcal{W}_{j,n}, \beta^{u}_{l,n})$,
$\mathcal{U}^{b}_{j,n} \Longleftarrow (\mathcal{Z}^{i\_int\_max}_{j,n}, \beta^{u}_{l,n})$,
$\mathcal{U}^{c}_{j,n} \Longleftarrow (\mathcal{X}_{j,n}, \beta^{u}_{l,n})$,
$\mathcal{U}^{sur}_{j,n} \Longleftarrow (\mathcal{U}^{a}_{j,n}, \mathcal{U}^{b}_{j,n}, \mathcal{U}^{c}_{j,n})$,
$\mathcal{U}_{j,n} \Longleftarrow (\mathcal{U}^{sur}_{j,n}, \mathcal{U}^{rot}_{j,n})$,
Write: $\mathcal{U}_{j,n}$
$\mathcal{G}^{a}_{j,n} \Longleftarrow (\mathcal{W}_{j,n}, \beta^{g}_{l,n})$,
$\mathcal{G}^{b}_{j,n} \Longleftarrow (\mathcal{Z}^{i\_int\_max}_{j,n}, \beta^{g}_{l,n})$,
$\mathcal{G}^{c}_{j,n} \Longleftarrow (\mathcal{X}_{j,n}, \beta^{g}_{l,n})$,
$\mathcal{G}^{sur}_{j,n} \Longleftarrow (\mathcal{G}^{a}_{j,n}, \mathcal{G}^{b}_{j,n}, \mathcal{G}^{c}_{j,n})$,
$\mathcal{G}_{j,n} \Longleftarrow (\mathcal{G}^{sur}_{j,n}, \mathcal{G}^{rot}_{j,n})$,
Write: $\mathcal{G}_{j,n}$
$\mathcal{N}_{j,n} \Longleftarrow (\mathcal{G}_{j,n}, c_n)$.
Write: $\mathcal{N}_{j,n}$
Write: ψ^{rig}_{n}
Write: $\mathcal{S}^{ave}_{n}$

■ **Phase 6: Post-processing**

End of Program

Convergence to the solution. In Figure S7 we address the problem of the rate of convergence to a stable solution of the iterative process which we have set up to solve the SLE (see §S8.7). In ***SELEN***^{4}, we have not assumed a pre-defined stopping criterion, like done by *e.g.,*Milne and Mitrovica (1998) and Kendall et al. (2005). Indeed, the user is requested to configure *a priori* the number n_{ext} of external iterations and the number n_{int} of internal iterations. To help the user to establish a number of iterations that ensure a reasonable accuracy of the solution obtained, in Figure S7 we visualize the convergence pattern of two ***SELEN***^{4} outputs as a function of the number of iterations, keeping fixed the spatial resolution to *R44/L128*. The first is γ, *i.e.,* the average rate[12] of present-day sea-level change at the tide gauges sites considered by Douglas (1997) in his study of global sea-level rise (left frame, see also Table 5 in SM19). The second is $< \dot{\mathcal{S}} >^{e}$, which represents the whole-Earth-surface average of the fingerprint $\dot{\mathcal{S}}$ (right frame, see also Fig. 4 of SM19).

The asymmetry of the convergence pattern obtained with varying n_{ext} and n_{int} is apparent. We recall that the external iteration determines the topography and consequently the ocean function (OF) while the internal iteration solves the SLE for a given topography. Thus, the two iteration processes have a different nature and similar patterns of convergence should not be expected *a priori*. When n_{int} is varied, for a fixed value of n_{ext}, a substantial convergence (indicated by the *plateau* in Figure S7), is monotonically achieved already for $n_{int} = 3$. This holds for both γ and $< \dot{\mathcal{S}} >^{e}$. Our finding is fully consistent with Milne and Mitrovica (1998), who noted that ... *three to five iterations are required for convergence* for a pre-determined convergence parameter $\varepsilon = 10^{-4}$ (see their Eq. 48). However, Figure S7 clearly shows that when n_{ext} is varied keeping n_{int} fixed, the convergence is not monotonic, and a value $n_{ext} = 5$ would certainly appear more appropriate in this case. So, the reconstruction of paleo-topography (and of the OF) is more burdensome than the solution of the SLE, for a given topography and ice distribution. This finding disagrees with Milne and Mitrovica (1998), who found that ... *one or two (external) iterations are normally adequate*. The cause of the different pattern of convergence probably depends on how the algorithms have been designed, and on the starting values (the *zero order* guess) adopted to initialize the iteration. Anyway, according to our experience and based on the results obtained for the test run in the body of the paper, we agree with Milne and Mitrovica (1998) that the choice $n_{int} = n_{ext} = 3$ provides reliable results for the whole output set of ***SELEN***^{4}. The user can push the algorithm to higher values in the case the data set under study requires a high-precision evaluation of the GIA predictions.

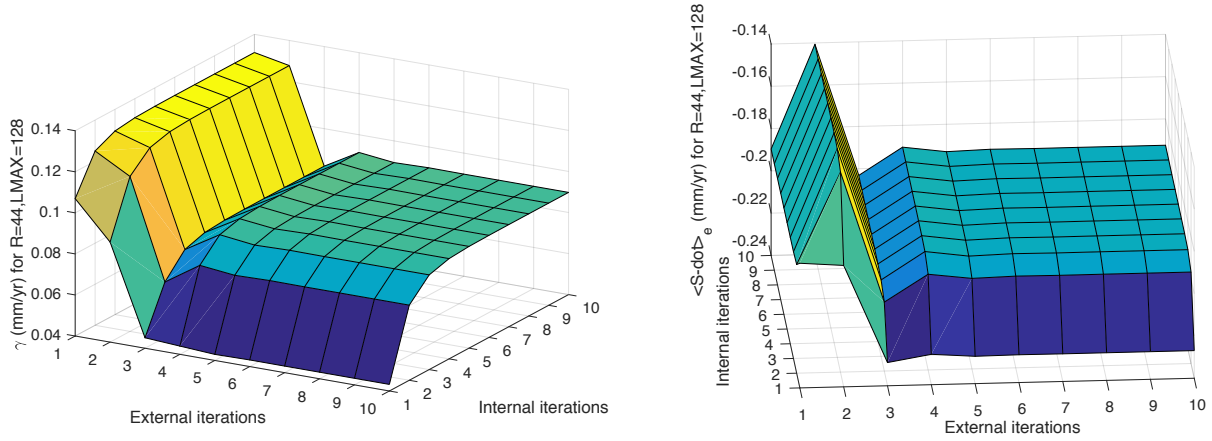

Figure S7. Convergence plots for γ (left) and for $<\dot{\mathcal{S}}>$ (right) using configuration *R44/L128*, as a function of the number of internal and of external iterations in the SLE.

Execution times. On a given computer system, the time needed by SELEN[4] to obtain a numerical solution of the SLE scales with the following parameters: *i)* the number of external and internal iterations (n_{ext} and n_{int}, respectively); *ii)* the number of pixels in the Tegmark grid, $P = 40R(R-1)+12$; *iii)* the number of harmonic terms of degree $0 \le m \le l \le l_{max}$, given $j_{max} = (l_{max}+1)(l_{max}+2)/2$. To help the user in estimating the run time of SELEN for a given choice of these parameters, we configured a test run in the *R44/L128/I33* setup, and performed four sets of runs in which we varied one of the four parameters (R, l_{max}, n_{ext} and n_{int}) while keeping the remaining three fixed to their nominal value. Figure S8 shows the measured execution times as a function of the corresponding parameter for each suite of runs. Increasing the number of iterations (either external or internal) results in a linear increase of execution time. Increasing l_{max} results in a nearly quadratic increase of execution time, that corresponds to a linear proportionality with the number of harmonic terms (indeed, $j_{max} \sim l_{max}^2$). Conversely, run time turns out to scale with resolution R as $\sim R^{2.7}$, which corresponds to a $\sim P^{1.4}$ scaling with the nummber of grid pixels, since $P \sim R^2$. The lack of a linear proportionality between run time and the number of grid nodes may be attributed to memory overhead and/or disk I/O, and its investigation is beyond the scope of the present work.

Code parallelism. On modern multi-core systems, SELEN takes advantage of shared-memory parallelism in order to speed up the most computationally intensive portions of the code. As first pointed out by Amdahl (1967), if inter-thread communication overhead is negligible the execution time t_{exe} of a parallel code can be written as

$$t_{exe} = t_0 \left(f_s + \frac{f_p}{n} \right) \tag{S453}$$

where n is the number of threads, f_s and f_p are the serial and parallel fractions of the code ($f_s + f_p = 1$) and t_0 is the execution time for $n = 1$. Eq. (S453) can be rewritten as

$$n\, t_{exe} = t_0 \left(f_p + n f_s \right) \tag{S454}$$

[12]This symbol should not be confused with $\gamma = (\theta, \lambda)$ used extensively in this document to indicate the spherical coordinates of an arbitrary point of the surface of the sphere.

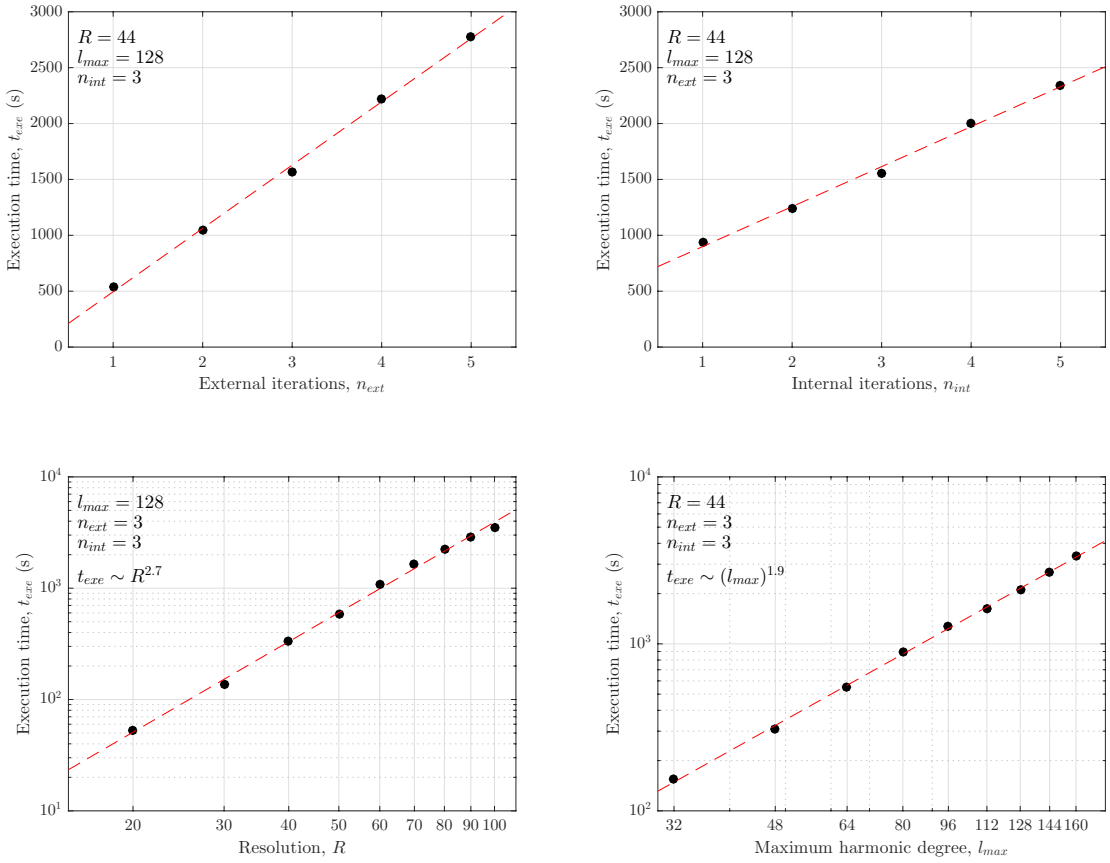

Figure S8. SELEN^4 execution times as a function of resolution R, maximum harmonic degree l_{max} and number of iterations n_{ext} and n_{int}. Each set of runs is based on a *R44/L128/I33* configuration, in which the investigated parameter is varied while keeping the remaining ones fixed to their nominal values. Execution times have been measured on a quad-processor Intel Xeon E7 "Broadwell" system running CentOS Linux 7.3, using 16 out of 56 cores.

showing that, if the communication overhead is negligible, a linear relation exists between $n\,t_{exe}$ and n. Eq. (S454) can be used to determine through a linear regression the parallel fraction f_p, by running a code for different values of n and measuring the corresponding execution times. Figure S9 shows measured values of t_{exe} and $n\,t_{exe}$ as a function of n for a SELEN run in the *R30/L64/I33* configuration. Scaling of $n\,t_{exe}$ with n is linear up to $n \sim 30$, after which significant oscillations arise due to the increasing impact of communication overhead and bandwith saturation. A dashed red line shows the best-fitting linear relation obtained through least squares, from which we can estimate $t_0 \sim 1072$ s and $f_p \sim 0.98$, indicating that a remarkably high level of parallelism is attained by SELEN.

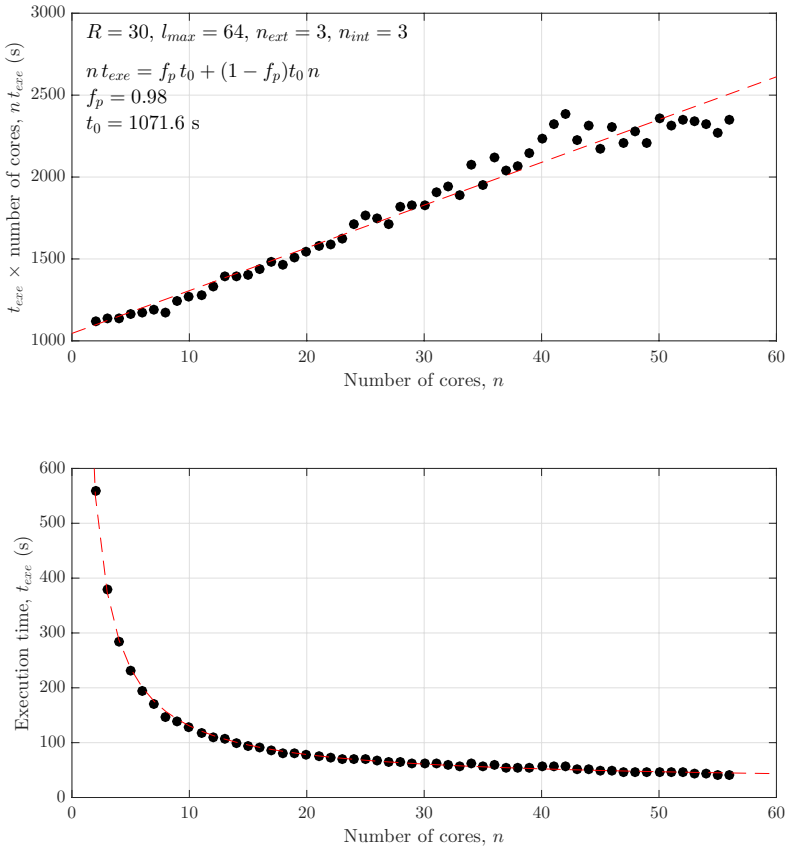

Figure S9. Execution time t_{exe} for a SELEN run in *R30/L64/I33* configuration as a function of the number of compute cores n, measured on a quad-processor Intel Xeon E7 "Broadwell" system running CentOS Linux 7.3. A red dashed curve shows the best-fitting relation between t_{exe} and n obtained with Eq. (S454).

S8.8 Relative sea-level variations

Geological and archaeological evidence of sea-level variations from various regions of the globe constitute an essential constraint to GIA models (*e.g.,* Tushingham and Peltier, 1991; Lambeck and Chappell, 2001). In particular, *relative sea level* (RSL) variations since the Last Glacial Maximum represent the amount of sea-level rise (or fall) relative to present datum (*e.g.,* Farrell and Clark, 1976).

More specifically, RSL stems from the difference

$$RSL(\gamma, t) = B - B_N, \tag{S455}$$

where γ indicates the coordinates of the RSL site (θ, λ), t is the epoch at which RSL is determined, $B = B(\gamma, t)$ is *sea level* at that epoch, and $B_N = B(\gamma, t_N)$ is present sea level at the site. Hence, by the same definition of RSL, we have $RSL(\gamma, t_N) = 0$.

We note, however, that the solution of the SLE (see *e.g.,* Eq. S200) yields $\mathcal{S}$ (*i.e., sea-level change*), not $RSL(\gamma,t)$. According to the discussion in §S2.2, sea-level change $\mathcal{S}$ is defined as

$$\mathcal{S}(\gamma,t) = B - B_0, \tag{S456}$$

where $B_0 = B(\gamma,t_0)$ *is not* present sea level, but sea level at a remote (and arbitrary) reference epoch that we have previously denoted by $t = t_0$. Nonetheless, the relationship between RSL and $\mathcal{S}$ can be easily established observing that

$$\begin{aligned} RSL(\gamma,t) &= (B - B_0) - (B_N - B_0) \\ &= \mathcal{S} - \mathcal{S}_N\,, \end{aligned} \tag{S457}$$

where we have used Eq. (S456). This shows that the history of RSL can be immediately obtained once the solution of the SLE has been determined at site γ and at all time steps, by taking the difference (S457).

Combining Eq. (S457) with the PT equation (S10), or simply recalling that the topography is defined as $T = -B$ (see Eq. S2), we note that at a time t RSL can be interpreted as the difference between the value of present-day topography and the value of topography at that time, with

$$RSL(\gamma,t) = T_N - T. \tag{S458}$$

This last equation shows that reconstructing the evolution of the variations of the Earth's topography is indeed equivalent to reconstruct the history of RSL variations (Peltier, 1994); the present relief T_N constitutes the basic constraint of the process of reconstruction. The locus

$$\gamma = \gamma_s(t) \tag{S459}$$

for which

$$RSL(\gamma_s(t),t) = 0 \tag{S460}$$

determines the location (*i.e.,* longitude and latitude) of the shoreline at time t, apart from correction to compensate for the erosion or sedimentation processes (see Lambeck, 2004, page 685).

In *SELEN*^{4}, the user can schedule the computation of $RSL(\gamma,t)$ at specific locations of interest. In the default configuration of the program, the sites are those belonging to the RSL database of Tushingham and Peltier (1993) (TP), which has had (and still maintains) a central importance in GIA studies (*e.g.,* Tushingham and Peltier, 1991, 1992; Melini and Spada, 2019). Of course, other input dataset can be supplied, provided that they are properly formatted (or the source code is suitably adapted). In the post-processing phase, the program first computes $\mathcal{S}_{i,n}$ by spherical harmonic synthesis of the $\mathcal{S}_{j,n}$ coefficients, where $\gamma_i = (\theta_i, \lambda_i)$ are the spherical coordinates of the i-th site of the TP database. Then, according to Eq. (S457), at time t_k Before Present (BP), RSL is evaluated by

$$RSL_{i,k} = \mathcal{S}_{i,N-k} - \mathcal{S}_{i,N}, \tag{S461}$$

where index k varies in the range $(0,1,2,\ldots N)$.

S8.9 Geodetic effects of GIA

GIA produces a number of geodetically observable effects (see *e.g.,* King et al., 2010). At the current stage of development, the geodetic predictions of *SELEN*^{4} include so-called *GIA fingerprints*, the rate of relative sea-level variation at tide gauges, vertical movements at GPS stations, the current rates of change of the Stokes coefficients of the Earth's gravity field, and polar motion.

GIA fingerprints. The *GIA fingerprints* are functions that describe the spatial variability of any quantity involved into the process of isostatic readjustment. The variability manifests the effects of deformation, gravitational attraction, and rotation

within the system composed by the solid Earth, the oceans and the ice sheets. As far as we know, in GIA studies the concept of *fingerprint function* has been first explicitly introduced by Plag and Jüettner (2001) in the context of the inversion of global tide gauge data for modern load changes. However, the concept is not limited to present-day signatures, since it also encompasses the effects of GIA on past variations of sea level or of other physical quantities (Clark et al., 1978; Mitrovica and Milne, 2002).

Currently, the term *GIA fingerprints* is normally (but not uniquely) adopted to indicate the present-day effects of GIA, being either caused by past or contemporary ice sources, expressed as *rates of change*. Hence, in the following, we shall refer to the basic set of GIA fingerprints to as $\dot{\mathcal{S}}, \dot{\mathcal{U}}, \dot{\mathcal{N}}$, and $\dot{\mathcal{G}}$, where the dot indicates the time detivative evaluated at present time. Some physical and geometrical properties of the GIA fingerprints have been presented by *e.g.,* Tamisiea (2011) and Spada (2017); a short discussion can be found in SM19.

In *SELEN*^{4}, the GIA fingerprints constitute one of the standard outputs of the post-processing phase. Examples of fingerprints obtained for a specific test run can be found in SM19. Specifically, the program produces arrays of $\dot{\mathcal{S}}_p, \dot{\mathcal{U}}_p, \dot{\mathcal{N}}_p$ and $\dot{\mathcal{G}}_p$, where the over-dot indicates the time-derivative evaluated at present time $t = t_N$, and subscript p indicates that the fingerprints are computed at $\gamma_p = (\theta_p, \lambda_p)$, *i.e.,* on the pixels of the Tegmark grid adopted in the numerical solution of the SLE.

In practice, using the output of the SLE solver, the fingerprints are evaluated according to

$$\dot{\mathcal{F}}_p = \frac{1}{2\Delta t} \sum_j \left(\mathcal{X}_{j,N+1} - \mathcal{X}_{j,N-1} \right) \mathcal{Y}_{j,p}, \tag{S462}$$

where $\sum_j$ indicates a sum over lm to maximum degree l_{max} and here $\dot{\mathcal{F}}_p$ stands for $\dot{\mathcal{S}}_p$, $\dot{\mathcal{U}}_p$, $\dot{\mathcal{N}}_p$, or $\dot{\mathcal{G}}_p$, Δt is the natural step of the 1-D time grid described in §S8.1, $\mathcal{F}_{j,n}$ represents any of the harmonic coefficients $\mathcal{S}_{j,n}, \mathcal{U}_{j,n}, \mathcal{N}_{j,n}$ and $\mathcal{G}_{j,n}$, with j_{max} we denote the maximum harmonic degree, and we have performed a numerical differentiation in time by computing a symmetric difference quotient.

Spatial averages of GIA fingerprints. Spatial averages of the fingerprints, either computed over the (present-day) oceans or across the whole Earth's surface, are also provided as a default *SELEN*^{4} output. According to Eq. (S217), the ocean-averages are evaluated by computing:

$$< \dot{\mathcal{F}} >^o = \frac{\sum_p \dot{\mathcal{F}}_p O_p}{\sum_p O_p}, \tag{S463}$$

where $\dot{\mathcal{F}}_p$ is given by Eq. (S462) and $O_p \equiv O_{p,N}$ is the discretized OF at present time. Based on (S219) the whole-Earth-surface averages are evaluated by means of

$$< \dot{\mathcal{F}} >^e = \frac{1}{P} \sum_p \dot{\mathcal{F}}_p, \tag{S464}$$

where we recall that P is the number of pixels over the grid.

Since we are always adopting mass conserving surface loads (*i.e.,* a *plausible* surface load, see §S2.4), to a very high degree of precision, in our numerical experiments for the geoid height fingerprint we obtain

$$< \dot{\mathcal{G}} >^e = \frac{1}{P} \sum_p \dot{\mathcal{G}}_p = 0, \tag{S465}$$

and similarly for the vertical displacement fingerprint

$$< \dot{\mathcal{U}} >^e = \frac{1}{P} \sum_p \dot{\mathcal{U}}_p = 0. \tag{S466}$$

GIA and altimetric sea-level rise. According to Eq. (S463), the ocean-average of the $\dot{\mathcal{N}}$ fingerprint reads

$$<\dot{\mathcal{N}}>^o = \frac{\sum_p \dot{\mathcal{N}}_p O_p}{\sum_p O_p}. \tag{S467}$$

Often, this quantity is adopted to correct absolute sea-level rise obtained from altimetry for the effects of GIA (Tamisiea, 2011; Spada and Galassi, 2015; Spada, 2017; Melini and Spada, 2019). The value of $<\dot{\mathcal{N}}>^o$ depends quite weakly from the GIA model adopted; according to the literature quoted above, a useful rule of thumb is

$$<\dot{\mathcal{N}}>^o \approx -0.30 \text{ mm yr}^{-1}. \tag{S468}$$

GIA at tide gauges. Tide gauges (TGs) observe sea-level relative to the solid Earth (*e.g.,* Spada and Galassi, 2012; Wöppelmann and Marcos, 2016). In order to decontaminate the long-term rates of relative sea-level change from GIA to enlighten the effects of present climate change, an appropriate GIA correction is to be performed. To obtain such correction, we directly map the fingerprint for relative sea-level on the geographical coordinates $\gamma_{tg} = (\theta_{tg}, \lambda_{tg})$ of the TG, computing

$$\dot{\mathcal{S}}_{tg} = \frac{1}{2\Delta t} \sum_j \left(\mathcal{S}_{j,N+1} - \mathcal{S}_{j,N-1}\right) \mathcal{Y}_{j,tg}, \tag{S469}$$

where $\mathcal{Y}_{j,tg}$ are the CSHs evaluated at the TG locations. For the sake of completeness, in the post-processing phase of *SELEN*^{4}, the values of $\dot{\mathcal{U}}_{tg}$, $\dot{\mathcal{N}}_{tg}$ and $\dot{\mathcal{G}}_{tg}$ at TGs are also evaluated (of course, by virtue of the SLE, condition $\dot{\mathcal{N}}_{tg} = \dot{\mathcal{S}}_{tg} + \dot{\mathcal{U}}_{tg}$ is met).

GIA at GPS stations (vertical component). In order to evaluate the GIA-induced rate of vertical displacement at GPS stations (see *e.g.,* Serpelloni et al., 2013, for a specific case study), we follow exactly the same approach adopted for the TGs above, but we employ the $\dot{\mathcal{U}}$ fingerprint, with

$$\dot{\mathcal{U}}_{gps} = \frac{1}{2\Delta t} \sum_j \left(\mathcal{U}_{j,N+1} - \mathcal{U}_{j,N-1}\right) \mathcal{Y}_{j,gps}, \tag{S470}$$

where subscript gps indicates that the corresponding quantity is computed at the GPS station coordinates $\gamma_{gps} = (\theta_{gps}, \lambda_{gps})$.

GIA at GPS stations (horizontal component). The topic shall be covered in the NEXT EDITION of *SELEN*^{4}.

Stokes coefficients. In gravity field studies, the Earth's exterior potential (or geopotential) at a point of geocentric radius r, geographic colatitude θ and longitude λ is conventionally represented using a spherical harmonics expansion like

$$V(r,\theta,\lambda,t) = \frac{G m_e}{r} \left(1 + \sum_{l=2}^{l_{max}} \left(\frac{a}{r}\right)^l \sum_{m=0}^{l} \left(\overline{c}_{lm}(t) \cos m\lambda + \overline{s}_{lm}(t) \sin m\lambda\right) \overline{P}_{lm}(\cos\theta)\right), \tag{S471}$$

where G is the universal gravitational constant, m_e is the mass of the Earth, a is its mean radius, $\overline{P}_{lm}(\cos\theta)$ are the fully normalised associated Legendre polynomials (FNALPs) of harmonic degree l and order m, and the non-dimensional real-valued quantities $\overline{c}_{lm}$ and $\overline{s}_{lm}$ are referred to as Stokes coefficients of the geopotential (Heiskanen and Moritz, 1967). Due to mass movement and exchanges between the components of the Earth system, V is in general time-dependent and this is reflected in the time dependence of the Stokes coefficients (see *e.g.,* Bettadpur, 2018).

We observe that in writing Eq. (S471) the origin of the reference frame has been chosen to be the center of mass (CM) of the whole Earth, including the solid and the fluid portions; thus there are no terms of harmonic degree $l = 1$ in the spherical harmonics expansion of V (Heiskanen and Moritz, 1967). The Stokes coefficients of degree $l = 2$ are determined by the time variations of the inertia tensor of the Earth (see *e.g.,* Heiskanen and Moritz, 1967). By a proper choice cartesian reference

frame, with the z-axis aligned with the *axis of figure* of the Earth (*i.e.,* the axis of maximum inertia), the terms of degree and order 2 and 1 vanish, all first degree harmonics and the degree $l = 2$ and order $m = 1$ terms are indeed referred to as *forbidden harmonics* by Hofmann-Wellenhof and Moritz (2006).

GIA perturbs the geopotential and, in consequence of that, it causes a time-variation of the Stokes coefficients. In SM19, the geopotential variation Φ induced by GIA at the Earth's surface ($r = a$) has been quantified in terms of the geoid response function $\mathcal{G}$, with

$$\mathcal{G}(\gamma, t) = \frac{\Phi}{g}, \tag{S472}$$

where $\gamma = (\theta, \lambda)$ and g is the (constant) reference gravity acceleration. It is useful to recall that

$$\mathcal{G} = \mathcal{G}^{sur} + \mathcal{G}^{rot}, \tag{S473}$$

where $\mathcal{G}^{sur}$ and $\mathcal{G}^{rot}$ are associated with changes in the load at the Earth's surface (see Eq. S82) and changes of the rotational potential (Eq. S172), respectively. Furthermore, we note that both terms contain a *direct effect* and an *indirect effect*, stemming from the '$\delta(t)$' and the '$k(t)$' terms in Eqs. (S83) and (S173), respectively. Henceforth, we assume that both direct and indirect contributions are included in $\mathcal{G}$, hence in the Stokes coefficients variations through Φ. Note, however, that an instrument like GRACE does not see the direct centrifugal effect on gravity potential, since it is not tied to the rotating Earth. About this point, it is interesting to read a personal communication of J Wahr to WR Peltier in 2011, reported in the supplementary Text S3 of Peltier et al. (2012). Hence, a comparison between the GRACE-derived rates of gravity change of harmonic degree 2 and order 1 and the GIA prediction Φ may be misleading (Chambers et al., 2010; Peltier et al., 2012; Chambers et al., 2012).

In close analogy with Eq. (S471), we now write

$$\Phi(\gamma, t) = \frac{G m_e}{a} \sum_{l=2}^{l_{max}} \sum_{m=0}^{l} \left(\overline{\delta c}_{lm}(t) \cos m\lambda + \overline{\delta s}_{lm}(t) \sin m\lambda \right) \overline{P}_{lm}(\cos\theta), \tag{S474}$$

where $\overline{\delta c}_{lm}(t)$ and $\overline{\delta s}_{lm}(t)$ are the Stokes coefficients that describe variations of the geopotential induced by GIA. Recalling that $g = \frac{G m_e}{a^2}$, from Eq. (S472) it follows that the surface response function $\mathcal{G}$ can be also expressed in series of spherical harmonics

$$\mathcal{G}(\gamma, t) = a \sum_{l=2}^{l_{max}} \sum_{m=0}^{l} \left(\overline{\delta c}_{lm}(t) \cos m\lambda + \overline{\delta s}_{lm}(t) \sin m\lambda \right) \overline{P}_{lm}(\cos\theta), \tag{S475}$$

where no terms of degree $l = 0$ appear since *i)* we are only considering mass-conserving loads for which $\mathcal{G}^{sur}_{00} = 0$ (see Eq. S129) and *ii)* $\mathcal{G}^{rot}$ is a pure degree $l = 2$ order $m = 1$ quantity (see §S6.2). Furthermore, harmonic degree $l = 1$ terms are also missing from (S475), since we are conventionally using a reference frame with origin in the CM, so that there are no such terms in the surface GF for the geoid (see §S4.1).

The present-day ($t = t_p$), GIA-induced rates of change of the Stokes coefficients in Eq. (S475) are related with the harmonic coefficients in the CSH expansion of the $\dot{\mathcal{G}}$ fingerprint. In fact, taking the time-derivative and recalling Eq. (S438), we obtain

$$\dot{\overline{\delta c}}_{lm} + i\,\dot{\overline{\delta s}}_{lm} = a^{-1} \sqrt{2 - \delta_{0m}}\, \dot{\mathcal{G}}^{*}_{lm}(t_p), \quad l \geq 2, m = 0, \ldots l, \tag{S476}$$

where the asterisk denotes complex conjugation (these expressions are consistent with those used by Melini and Spada, 2019). We note that since the sea surface variation is defined as $\mathcal{N} = \mathcal{G} + c$ (see Eq. 22 of SM19), where c is the "FC76 constant", in the range of harmonic degrees $l \geq 2$, we have $\dot{\mathcal{G}}_{lm}(t) = \dot{\mathcal{N}}_{lm}(t)$, since c is a harmonic degree 0 quantity. We observe that in the context of the Gravity Recovery and Climate Experiment (GRACE) the spherical harmonics normalization convention does *not* include the *Condon-Shortley phase factor* $(-1)^m$ (see Bettadpur, 2018, page 6). Hence, the right hand side of Eq. (S476) should be multiplied by this factor in order to conform to GRACE conventions for spherical harmonics.

The quantity

$$S^2(l) = \sum_{m=0}^{l} \left(\left(\overline{\dot{\delta c}}_{lm} \right)^2 + \left(\overline{\dot{\delta s}}_{lm} \right)^2 \right) \tag{S477}$$

represents the *power spectrum* of the Stokes coefficients at a given harmonic degree l where the present day rates of change of the Stokes coefficients are given by Eq. (S476). It provides information on how the "energy" of the GIA-induced variations of the geopotential depends on wavelength of each harmonic component, which according to Jean's rule is

$$\lambda \sim \frac{2\pi a}{2l+1} \tag{S478}$$

(see *e.g.,* Spada and Galassi, 2015).

Performing a numerical differentiation in time by a symmetric difference quotient, in *SELEN*^{4} the rates of change of the Stokes coefficients are computed, at present time, according to

$$\overline{\dot{\delta c}}_j = +a^{-1}(-1)^m \sqrt{2-\delta_{0m}}\, \mathrm{Re}\left(\mathcal{N}_{j,N+1} - \mathcal{N}_{j,N-1}\right)/(2\Delta t) \tag{S479}$$

$$\overline{\dot{\delta s}}_j = -a^{-1}(-1)^m \sqrt{2-\delta_{0m}}\, \mathrm{Im}\left(\mathcal{N}_{j,N+1} - \mathcal{N}_{j,N-1}\right)/(2\Delta t), \tag{S480}$$

where $j = lm$, Δt is the time step and the GRACE convention on the FNALPs is used.

Polar motion. The fundamental solution of the Liouville equations for polar motion is given by Eq. (S167). In the numerical implementation of *SELEN*^{4}, this solution is discretized according to the general scheme outlined in §S7. Accordingly, for the history of polar motion we have

$$\mathbf{m}_n \equiv \mathbf{m}(t=t_n) = \sum_{k=0}^{n-1} \psi_k^{rig} \left(A'^e + A'^s\,(n-k)\Delta t + \sum_{i=1}^{M'} \frac{A'^i}{a_i} \left(\mathrm{e}^{a_i(n-k)\Delta t} - 1 \right) \right), \tag{S481}$$

where we recall that $\mathbf{m}$ is a complex variable $\mathbf{m}_n = m_{1n} + i\, m_{2n}$ and Δt is the increment of the time grid. In (S481) $\mathbf{m}_n$ is expressed in the natural units of *radians*, so that it must be rescaled by the factor $f = \frac{180^\circ}{\pi}$ to be given in the more common units of *degrees* on the Earth's surface.

For the rate of polar motion, we discretise the derivative of the fundamental solution of Liouville equations, given by (S168), obtaining

$$\dot{\mathbf{m}}_n \equiv \dot{\mathbf{m}}(t=t_n) = \sum_{k=0}^{n-1} \psi_k^{rig} \left(A'^s + \sum_{i=1}^{M'} A'^i \mathrm{e}^{a_i(n-k)\Delta t} \right), \tag{S482}$$

which in *SELEN*^{4} has the standard units of kyrs^{-1}. So, to transform it into the commonly used unit of deg Myr^{-1} (degrees per million years), it must be rescaled by factor $g = f \times 10^3$.

To characterise the history of polar motion, other quantities are worth to be defined. These are the *displacement of the pole of rotation* over the Earth's surface (in degrees)

$$p_n = f\sqrt{m_{1n}^2 + m_{2n}^2}, \tag{S483}$$

the *rate of polar displacement* (in deg Myr^{-1})

$$\dot{p}_n = g\,\frac{m_{1n}\dot{m}_{1n} + m_{2n}\dot{m}_{2n}}{\sqrt{m_{1n}^2 + m_{2n}^2}}, \tag{S484}$$

and the *direction of polar motion* on the xy plane (in degrees)

$$\phi_n = f\,\mathrm{atan2}\left(m_{2n}, m_{1n}\right). \tag{S485}$$

Field‡	Discretised field(*s*)	Definitions, equivalences, and notes ...
$\mathcal{Y}_{lm}(\gamma)$	$\mathcal{Y}_{j,p}$	CSH of degree and order $j = lm$ and its c.c.
$I(\gamma,t)$	$I_{p,n}$	Obtained by pixelizing the input ice model (*e.g., ICE-X*)
$T(\gamma,t)$	$T_{p,n}$	$= T_{p,N} - (\mathcal{S}_{p,n} - \mathcal{S}_{p,N})$, with $T_{p,N}$ from *e.g., ETOPO1*
$O(\gamma,t)$	$O_{p,n}, O_{j,n}$	For $O_{p,n}$, see Eq. (S210); $O_{j,n} = (1/P)\sum_p O_{p,n}\mathcal{Y}^*_{j,p}$
$C(\gamma,t)$	$C_{p,n}, C_{j,n}$	$C_{p,n} = 1 - O_{p,n}$; $C_{j,n} = \delta_{l0}\delta_{m0} - O_{j,n}$
$< F >^o (t)$	$< F >^o_n$	$\left(\sum_p F_{p,n} O_{p,n}\right) / \left(\sum_p O_{p,n}\right)$
$< F >^e (t)$	$< F >^e_n$	$(1/P)\sum_p F_{p,n}$
$A^o(t)$	A^o_n	$= A^c \sum_p O_{p,n} = 4\pi a^2 O_{00,n}$
$\mu(t)$	μ_n	$= \rho^i A^c \sum_p (I_{p,n} C_{p,n} - I_{p,0} C_{p,0})$
$\mathcal{S}^{equ}(t)$	$\mathcal{S}^{equ}_n, \mathcal{S}^{equ}_{j,n}$	$S^{equ}_n = -\frac{\rho^i}{\rho^w}\left(\frac{\sum_p (I_{p,n}C_{p,n} - I_{p,0}C_{p,0})}{\sum_p O_{p,n}}\right)$; $\mathcal{S}^{equ}_{j,n} = S^{equ}_n \delta_{l0}\delta_{m0}$
$\mathcal{S}^{ofu}(t)$	$\mathcal{S}^{ofu}_n, \mathcal{S}^{ofu}_{j,n}$	$\mathcal{S}^{ofu}_n = \left(\sum_p T_{p,0}(O_{p,n} - O_{p,0})\right) / \left(\sum_p O_{p,n}\right)$; $\mathcal{S}^{ofu}_{j,n} = S^{ofu}_n \delta_{l0}\delta_{m0}$
$\mathcal{S}^{ave}(t)$	$\mathcal{S}^{ave}_n, \mathcal{S}^{ave}_{j,n}$	$\mathcal{S}^{ave}_n = \mathcal{S}^{equ}_n + \mathcal{S}^{ofu}_n$; $\mathcal{S}^{ave}_{j,n} = S^{ave}_n \delta_{l0}\delta_{m0}$
$c(t)$	c_n	$= \mathcal{S}^{ave}_n - < \mathcal{R}^a >^o_n - < \mathcal{R}^b >^o_n - < \mathcal{R}^c >^o_n - < \mathcal{R}^{rot} >^o_n$
$\mathcal{Z}^{ave}(\gamma,t)$	$\mathcal{Z}^{ave}_{j,n}$	$= O_{j,n}(S^{equ}_n + S^{ofu}_n) = O_{j,n} S^{ave}_n$
$\mathcal{W}(\gamma,t)$	$\mathcal{W}_{j,n}$	$= (1/P)\sum_p (I_{p,n} - I_{p,0})(1 - O_{p,n})\mathcal{Y}^*_{j,p}$
$\mathcal{X}(\gamma,t)$	$\mathcal{X}_{j,n}$	$= (1/P)\sum_p Q_p (O_{p,n} - O_{p,0})\mathcal{Y}^*_{j,p}(\gamma)$
$\mathcal{L}^{abc}(\gamma,t)$	$\mathcal{L}^{abc}_{j,n}$	$\mathcal{L}^a_{j,n} = \rho^i \mathcal{W}_{j,n}$, $\mathcal{L}^b_{j,n} = \rho^w \mathcal{Z}_{j,n}$, $\mathcal{L}^c_{j,n} = \rho^r \mathcal{X}_{j,n}$
$\beta^{sgu}_l(t)$	$\beta^{sgu}_{l,n}$	$= \beta^{sgu}_l(n\Delta t)$
$(\mathcal{R},\mathcal{G},\mathcal{U})^{abc}(\gamma,t)$	$(\mathcal{R},\mathcal{G},\mathcal{U})^{abc}_{j,n}$	See Eqs. (S249-S251), (S257-S259), and (S262-S264), respectively.
$< \mathcal{R}^{abc} >^o (t)$	$< \mathcal{R}^{abc} >^o_n$	$= \left(\sum_j \mathcal{R}^{abc}_{j,n} O^*_{j,n}\right) / \left(O_{00,n}\right)$
$\mathcal{R}'^{abc}$	$\mathcal{R}'^{abc}_{j,n}$	$= \mathcal{R}^{abc}_{j,n} - < \mathcal{R}^{abc} >^o_n \delta_{l0}\delta_{m0}$
$\mathcal{K}^{abc}(\gamma,t)$	$\mathcal{K}^{abc}_{j,n}$	$= \sum_{(p:\, O_{p,n}=1)} \chi^{abc}_{p,n} \mathcal{Y}^*_{j,p}$, with $\chi^{abc}_{p,n} \equiv (1/P)\sum_j \mathcal{R}'^{abc}_{j,n} \mathcal{Y}_{j,p}$
$\gamma^{sgu}(t)$	γ^{sgu}_n	$= \gamma^{sug}(n\Delta t)$
$(\mathcal{R},\mathcal{G},\mathcal{U})^{rot}(\gamma,t)$	$(\mathcal{R},\mathcal{G},\mathcal{U})^{rot}_{j,n}$	$= \delta_{l2}\delta_{m\pm1}\left(c^{\psi}_{21} c^{\lambda}_{21}/g\right)\sum_{k=0}^{n-1} \Delta\mathcal{L}_{j,k}\gamma^{sug}_{n-k}$
$< \mathcal{R}^{rot} >^o (t)$	$< \mathcal{R}^{rot} >^o_n$	$= \left(\sum_j \mathcal{R}^{rot}_{j,n} O^*_{j,n}\right) / \left(O_{00,n}\right)$
$\mathcal{R}'^{rot}(\gamma,t)$	$\mathcal{R}'^{rot}_{j,n}$	$= \mathcal{R}^{rot}_{j,n} - < \mathcal{R}^{rot} >^o_n \delta_{l0}\delta_{m0}$
$\mathcal{K}^{rot}(\gamma,t)$	$\mathcal{K}^{rot}_{j,n}$	$= \sum_{(p:\, O_{p,n}=1)} \chi^{rot}_{p,n} \mathcal{Y}^*_{j,p}$, with $\chi^{rot}_{p,n} \equiv (1/P)\sum_j \mathcal{R}'^{rot}_{j,n} \mathcal{Y}_{j,p}$
$\Psi^{rig}(t)$	Ψ^{rig}_n	$= c^{\psi}_{21} \mathcal{L}^*_{21,n}$
$\mathcal{S}(\gamma,t)$	$\mathcal{S}_{p,n}, \mathcal{S}_{j,n}$	$\mathcal{S}_{j,n} = \mathcal{S}^{ave}_{j,n} + \mathcal{R}'^{a}_{j,n} + \mathcal{R}'^{b}_{j,n}(\mathcal{Z}) + \mathcal{R}'^{c}_{j,n} + \mathcal{R}'^{rot}_{j,n}(\mathcal{Z})$
$\mathcal{Z}(\gamma,t)$	$\mathcal{Z}_{j,n}$	$= \mathcal{Z}^{ave}_{j,n} + \mathcal{K}^a_{j,n} + \mathcal{K}^b_{j,n}(\mathcal{Z}) + \mathcal{K}^c_{j,n} + \mathcal{K}^{rot}_{j,n}(\mathcal{Z})$

Table S3. Scalar fields involved in the SLE (left) and discretised forms (middle), with notes (right). See §S7 for details of the discretisation.

degree, l	order, m	$P_l(x)$	$P_{lm}(\cos\theta)$
0	0	1	1
1	0	x	$\cos\theta$
1	1		$-\sin\theta$
2	0	$\frac{1}{2}(3x^2-1)$	$\frac{1}{2}\left(3\cos^2\theta-1\right)$
2	1		$-3\sin\theta\cos\theta$
2	2		$3\sin^2\theta$

Table S4. Low-degree Legendre polynomials $P_l(x)$ with $x=\cos\theta$, and (un-normalised) ALPs $P_{lm}(\cos\theta)$ of harmonic degree $0\leq l\leq 2$ and order $0\leq m\leq l$.

degree, l	order, m	$\mathcal{Y}_{lm}(\gamma)$	$\mathcal{Y}_{lm}(\gamma)$
0	0	1	1
1	0	$\sqrt{3}P_{10}(\cos\theta)$	$\sqrt{3}\cos\theta$
1	1	$\sqrt{\frac{3}{2}}P_{11}(\cos\theta)\mathrm{e}^{i\lambda}$	$-\sqrt{\frac{3}{2}}\sin\theta\mathrm{e}^{i\lambda}$
2	0	$\sqrt{5}P_{20}(\cos\theta)$	$\frac{\sqrt{5}}{2}\left(3\cos^2\theta-1\right)$
2	1	$\sqrt{\frac{5}{6}}P_{21}(\cos\theta)\mathrm{e}^{i\lambda}$	$-3\sqrt{\frac{5}{6}}\sin\theta\cos\theta\mathrm{e}^{i\lambda}$
2	2	$\sqrt{\frac{5}{24}}P_{22}(\cos\theta)\mathrm{e}^{2i\lambda}$	$3\sqrt{\frac{5}{24}}\sin^2\theta e^{2i\lambda}$

Table S5. Low-degree, 4π-normalised complex spherical harmonics (CSHs) of degree $l\leq 2$ and order $0\leq m\leq l$, for argument $\gamma=(\theta,\lambda)$. In the third column, the CSHs are expressed in terms of $P_{lm}(x)$ while in the fourth column they are written explicitely in terms of trigonometric functions. Note that, for negative orders, $\mathcal{Y}_{l-m}(\gamma)=(-1)^m\mathcal{Y}^*_{lm}(\gamma)$.

R	P	δ (deg)	r_{cell} (km)	L_M
14	7,292	1.34	149.22	147
18	12,252	1.04	115.12	191
24	22,092	0.77	85.73	257
32	39,692	0.58	63.96	345
44	75,692	0.42	46.31	476
60	141,612	0.30	33.86	651
80	252,812	0.23	25.34	870
100	396,012	0.18	20.25	1089
200	1,592,012	0.09	10.10	2185
500	9,980,012	0.04	4.03	5471
2,000	159,920,012	~ 0.01	~ 1	21,903

Table S6. Statistics of the Tegmark grid. R is the grid resolution, P is the corresponding number of pixels, δ is the radius of the equivalent (*i.e.,* with the same area) disk on the sphere, r_{cell} is the *approximate* radius of the equivalent disk on a plane, and L_M is the maximum harmonic degree admissible for the chosen R value. Note that a characteristic cell size of ~ 1 km is attained for $R = 2,000$.

S8.10 Complementary tables

Acronym	Meaning
ALP	Associated Legendre Polynomial
CF	Continent Function
CSH	Complex Spherical Harmonic
FC76	Farrell and Clark (1976)
GIA	Glacial Isostatic Adjustment
GF	Green's Function
LLN	Loading Love Number
LT	Laplace Transform
OF	Ocean Function
PC	Piecewise Constant
PGR	Post Glacial Rebound
PMTF	Polar Motion Transfer Function
PT	(true) paleo-topography
RSL	Relative Sea Level
SELEN^4	a Sea LEvel EquatioN solver, version 4
SGF	Surface Green's Function
SRF	Surface Response Function
RRF	Rotational Response Function
RGF	Rotation Green's Function
TLN	Tidal Love Number

Table S7. Acronyms used in this manuscript.

Symbol	Definition	Comments, notes, links, dimensions, units, ...
a_i	Rotational roots	$(i = 1, \dots M')$, see §S5.3 and Eq. (S149), natural units are kyrs^{-1}
$\mathcal{A}, \mathcal{A}'$	PMTF and its modified form†	See Eqs. (S149) and (S163), both dimensionless
A^o	Area of the oceans	See Eq. (S50) and §S7.2, units are m^2
A^c	Area of the Tegmark cells	Eq. (S220), units are m^2
A^e, A'^e	elastic component of the PMTF	Eqs. (S348) and (S164), dimensionless
A^s, A'^s	secular component of the PMTF	Eqs. (S348) and (S164), units are kyrs^{-1}
A_i, A'_i, A''_i	Rotational residues	$(i = 1, \dots M')$, Eqs. (S348) and (S164), §S8.2, units are kyrs^{-1}
$B, \mathcal{S}$	Sea level and sea-level change†	See Eq. (S2), (S7); units are m
$c(t)$	The "*c constant*" of FC76	See Eq. (S52), units are m
C	The "Continent Function"	Eq. (S3), also denoted by CF, dimensionless
γ	Stands for the couple (θ, λ)	$\theta =$ colatitude, $\lambda =$ longitude, units are radians or degrees
Γ, Υ	Surface and rotation GFs	§S4.1 and §S6.1, units are [T^{-1}LM^{-1}] and [TL^{-1}], respectively
dA	Element of area	Defined as $dA = a^2 \sin\theta d\theta d\lambda$ = $a^2 d\gamma$, units are m^2
$\delta(t)$	Dirac delta	See footnote on page 20, dimensions are [T^{-1}]
$(h_l, \ell_l, k_l)^L(t)$	Time-domain LLNs^a	$(l = 1, \dots l_{max})$, see Eqs. (S56-S58), units are kyrs^{-1}
$(h_l, \ell_l, k_l)^L(s)$	Laplace-domain LLNs^a	Eq. (S59), dimensionless
$(h_l, \ell_l, k_l)^{Le}$	Elastic LLNs^a	Eqs. (S56-S58), dimensionless
$(h_l, \ell_l, k_l)^{Lf}$	Fluid LLNs^a	Eqs. (S64), dimensionless
$(h_{li}, \ell_{li}, k_{li})^L$	Visco-elastic LLNs^a	$(i = 1, \dots M)$, see Eqs. (S56-S58), units are kyrs^{-1}
H	Heaviside (unit step) function	See §S8.1 and Eq. (S290)
I, $\mathcal{I}$	Ice thickness†	See §S2 and Eq. (S26)
J_{ij}	Inertia tensor variation	See §S5.4, units are kg m^2
k^s	Secular 'k' Love number	See Eq. (S140), dimensionless
l, m	Harmonic degree and order	$0 \leq l \leq l_{max}$, $\lvert m \rvert \leq l$
l_{max}	Maximum harmonic degree	*e.g.,* $l_{max} = 128, 256, 512 \dots$
L, $\mathcal{L}$	Surface load†	See §S2.3, Eqs. (S12) and (S24), units are kg m^{-2}
m_i	Cartesian polar motion components	$(i = 1, 2, 3)$, see §S5.1 and Eq. (S134), dimensionless
M, $\mathcal{M}$	Surface mass and its time variation†	See §S2.3, units are kg
M, M'	No. of Isostatic and Rotational Modes	See §S3.2 and §S5.3, respectively; dimensionless
μ	Variation of the grounded ice mass	See Eq. (S45), units are kg
$\mathcal{N}$	Sea surface variation	Units are m
O, $\mathcal{O}$	The "Ocean Function"†	Eqs. (S1) and (S27), also denoted by OF, dimensionless
P, R	Tegmark pixels and grid resolution	See the whole §S8.6, Eq. (S439) and Table S6; dimensionless
P_l, P_{lm}	Legendre polynomial and ALP	See §S8.5 for definition and properties
Q	An auxiliary variable	See Eq. (S36), units are m
$\mathcal{R}$, $\mathcal{G}$, $\mathcal{U}$	Response functions	See §S4 for the SRFs and §S6, for the RRFs, units are m
$\rho^i\mathcal{W}, \rho^w\mathcal{Z}, \rho^r\mathcal{X}$	Components of $\mathcal{L}$	see Eqs. (S30-S32) and (S33-S35), same units as $\mathcal{L}$
s	Complex Laplace variable	Dimensions are [T^{-1}], units are kyrs^{-1}
s_i	Isostatic roots	$(i = 1, \dots M)$, see §S3.2 and §S3.3, Eq. (S62), units are kyrs^{-1}
t, t_n, t_k	Time	[T], the natural unit is kyr
T	Topography	Eq. (S2), units are m
U^c, Λ	Centrifugal potential and its variation	See Eq. (S384) and whole §S8.4, dimensions are [L^{2}T^{-2}]
$\mathcal{Y}_j$	4-π normalised CSHs, with $j = lm$	See §S8.5 for definition and properties
Ψ	Excitation function	see whole §S5, dimensionless
ω_i, Ω	Angular velocity	$(i = 1, 2, 3)$, see whole §S5, dimensions are [T^{-1}]

Table S8. Glossary of the some recurrent symbols, with some brief comments. *Notes:* ^{a}similar expressions hold for the TLNs (see §S3.3), †the calligraphic symbols denote time variations of the corresponding variables.

Symbol	Constant or parameter	Value	SI Units
a	Earth's radius	6.371×10^6	m
A	Polar inertia	8.0131×10^{37}	kg m^2
C	Equatorial inertia	8.0394×10^{37}	kg m^2
g	Surface gravity	9.81	m s^{-2}
G	Universal gravitational constant	6.67×10^{-11}	N m^2 kg^{-2}
ρ^e	Earth's average density	5514	kg m^{-3}
ρ^i	Ice density	931	kg m^{-3}
ρ^w	Water density	1000	kg m^{-3}
ρ^r	Reference density	900	kg m^{-3}
ω^e	Earth's angular velocity	7.292115×10^{-5}	s^{-1}

Table S9. Physical constants and parameters used in this supplement and in SM19, with the corresponding numerical values and SI units.

Acknowledgements. GS is funded by a FFABR (Finanziamento delle Attività Base di Ricerca) grant of MIUR (Ministero dell'Istruzione, dell'Università e della Ricerca) and by a research grant of DISPEA (Dipartimento di Scienze Pure e Applicate) of the Urbino University "Carlo Bo". We thank D. Riposati from the INGV Laboratorio Grafica e Immagini for drawing the SELEN logo. We thank M. Tegmark for having made available his pixelization routines, which have had an essential role in the development of SELEN (see *https://space.mit.edu/ home/ tegmark/ isosahedron.html*). We also thank M. Wieczorek for distributing the SHTOOLS (the Spherical Harmonics Tools) to the community (*https://shtools.oca.eu/shtools*). Some of the figures have been drawn using the Generic Mapping Tools (GMT) of Wessel and Smith (1998). We are indebted to all the colleagues who participated to the various stages of the Glacial Isostatic Adjustment and Sea Level Equation benchmark activities, namely: V. R. Barletta, P. Gasperini, T.S. James, M.A. King, S.B. Kachuck, V. Klemann, B. Lund, Z. Martinec, R.E.M. Riva, K. Simon, Y. Sun, L.L.A. Vermeersen, W. van der Wal and D.Wolf (see Spada et al., 2011; Martinec et al., 2018). A special acknowledgement goes to F. Colleoni for help in the code implementation and to F. Mainardi for advice on the theory of linear visco-elasticity. We are also indebted to M. Bevis and E. Ivins for encouragement and advice. R. Mascetti has patiently revised the manuscript during various stages of its development, also providing invaluable inspiration.

Code and data availability. SELEN^4 is available from Zenodo at the link *https://zenodo.org/record/3520451* (DOI: 0.5281/zenodo.3520451) and from the Computational Infrastructure for Geodynamics (CIG) at *github.com/geodynamics/selen*. The ice history data for ICE-6G (VM5a) have been downloaded from *http://www.atmosp.physics.utoronto.ca/ ∼peltier/ data.php* (last accessed 20 Apr 2019). The Model ETOPO1 has been obtained from *https://www.ngdc.noaa.gov/ mgg/ global/* (last accessed 26 Feb 2019).

Author contributions. G.S. and D.M. have both contributed to the design and implementation of the research, to the analysis of the results and to the writing of the manuscript. The supplement has been written by G.S. with the support of D.M. The code has been progressively developed by G.S. and D.M., who has edited the User Guide and the on-line version of the code.

Competing interests. The authors declare no competing interests.

References

Amante, C. and Eakins, B.: ETOPO1 Arc-Minute Global Relief Model: Procedures, Data Source and Analysis, Tech. rep., 2009.

Amdahl, G. M.: Validity of the single processor approach to achieving large scale computing capabilities, in: Proceedings of the April 18-20, 1967, spring joint computer conference, pp. 483–485, ACM, 1967.

Atkinson, K. and Han, W.: Spherical harmonics and approximations on the unit sphere: an introduction, vol. 2044, Springer Science & Business Media, 2012.

Balmino, G., Lambeck, K., and Kaula, W. M.: A spherical harmonic analysis of the Earth's topography, Journal of Geophysical Research, 78, 478–481, 1973.

Bettadpur, S.: Level-2 gravity field product user handbook, The GRACE Project (Jet Propulsion Laboratory, Pasadena, CA, 2003), ftp://podaac.jpl.nasa.gov/allData/grace/docs/L2-UserHandbook_v4.0.pdf, 2018.

Caron, L., Métivier, L., Greff-Lefftz, M., Fleitout, L., and Rouby, H.: Inverting Glacial Isostatic Adjustment signal using Bayesian framework and two linearly relaxing rheologies, Geophysical Journal International, 209, 1126–1147, 2017.

Chambers, D., Wahr, J., Tamisiea, M., and Nerem, R.: Ocean mass from GRACE and glacial isostatic adjustment, J. Geophys. Res., 115, B11 415, https://doi.org/10.1029/2010JB007530, 2010.

Chambers, D. P., Wahr, J., Tamisiea, M. E., and Nerem, R. S.: Reply to comment by WR Peltier et al. on Ocean mass from GRACE and glacial isostatic adjustment, Journal of Geophysical Research: Solid Earth (1978–2012), 117, 2012.

Clark, J. A., Farrell, W. E., and Peltier, W. R.: Global changes in postglacial sea level: a numerical calculation, Quaternary Research, 9, 265–287, 1978.

Douglas, B.: Global sea leve rise: a redetermination, Surveys in Geophysics, 18, 279–292, 1997.

Dziewonski, A. M. and Anderson, D. L.: Preliminary reference Earth model, Physics of the Earth and Planetary Interiors, 25, 297–356, 1981.

Eakins, B. and Sharman, G.: Hypsographic curve of Earth's surface from ETOPO1, NOAA National Geophysical Data Center, Boulder, CO, 2012.

Farrell, W.: Deformation of the Earth by surface loads, Reviews of Geophysics, 10, 761–797, 1972.

Farrell, W. and Clark, J.: On postglacial sea-level, Geophys. J. Roy. Astr. S., 46, 647–667, 1976.

Ferrers, N. M.: An elementary treatise on spherical harmonics and subjects connected with them, Macmillan and Company, 1877.

Greff-Lefftz, M.: Secular variation of the geocenter, J. Geophys. Res., 25, 25,685–25,692, 2000.

Greff-Lefftz, M. and Legros, H.: Some remarks about the degree one deformations of the Earth, Geophys. J. Int., 131, 699–723, 1997.

Han, D. and Wahr, J.: Post-glacial rebound analysis for a rotating Earth, in: Slow Deformations and Transmission of Stress in the Earth, edited by Cohen, S. and Vanicek, P., pp. 1–6, AGU Mono. Series 49, 1989.

Heiskanen, W. A. and Moritz, H.: Physical geodesy, Bulletin Géodésique (1946-1975), 86, 491–492, 1967.

Hofmann-Wellenhof, B. and Moritz, H.: Physical geodesy, Springer Science & Business Media, 2006.

Jerri, A.: Introduction to integral equations with applications, John Wiley & Sons, 1999.

Kendall, R. A., Mitrovica, J. X., and Milne, G. A.: On post-glacial sea level–II. Numerical formulation and comparative results on spherically symmetric models, Geophysical Journal International, 161, 679–706, 2005.

King, M. A., Altamimi, Z., Boehm, J., Bos, M., Dach, R., Elosegui, P., Fund, F., Hernández-Pajares, M., Lavallee, D., Cerveira, P. J. M., et al.: Improved constraints on models of glacial isostatic adjustment: a review of the contribution of ground-based geodetic observations, Surveys in Geophysics, 31, 465–507, 2010.

Lambeck, K.: The Earth's variable rotation: geophysical causes and consequences, Cambridge University Press, 1980.

Lambeck, K.: Sea-level change through the last glacial cycle: geophysical, glaciological and palaeogeographic consequences, Comptes Rendus Geoscience, 336, 677–689, 2004.

Lambeck, K. and Chappell, J.: Sea level change through the last glacial cycle, Science, 292, 679–686, 2001.

Landau, L. D., Lifsic, E. M., Pitaevskii, L., and Kosevich, A.: Course of Theoretical Physics: Volume 7, Theory of Elasticity, Pergamon Press, 1986.

Longman, I.: A Green's function for determining the deformation of the Earth under surface mass loads: 1. Theory, Journal of Geophysical Research, 67, 845–850, 1962.

Longman, I.: A Green's function for determining the deformation of the Earth under surface mass loads. 2. Computations and numerical results, Journal of Geophysical Research, 68, 485–496, 1963.

Longman, I. and Sharir, M.: Laplace transform inversion of rational functions, Geophysical Journal International, 25, 299–305, 1971.

Love, A. E. H.: Some Problems of Geodynamics: Being an Essay to which the Adams Prize in the University of Cambridge was Adjudged in 1911, CUP Archive, 1911.

MacRobert, T. M.: Spherical harmonics: an elementary treatise on harmonic functions with applications, 1947.

Martinec, Z., Klemann, V., van der Wal, W., Riva, R., Spada, G., Sun, Y., Melini, D., Kachuck, S., Barletta, V., and Simon, K.: A benchmark study of numerical implementations of the sea level equation in GIA modelling, Geophysical Journal International, 215, 389–414, 2018.

Melini, D. and Spada, G.: Some remarks on Glacial Isostatic Adjustment modelling uncertainties, Geophysical Journal International, 218, 401–413, https://doi.org/10.1093/gji/ggz158, 2019.

Milne, G. A. and Mitrovica, J. X.: Postglacial sea-level change on a rotating Earth, Geophysical Journal International, 133, 1–19, 1998.

Mitrovica, J. and Milne, G.: On the origin of late Holocene sea-level highstands within equatorial ocean basins, Quaternary Science Reviews, 21, 2179–2190, 2002.

Mitrovica, J. X. and Milne, G. A.: On post-glacial sea level: I. General theory, Geophysical Journal International, 154, 253–267, 2003.

Mitrovica, J. X. and Peltier, W.: On postglacial geoid subsidence over the equatorial oceans, Journal of Geophysical Research: Solid Earth, 96, 20 053–20 071, 1991.

Mitrovica, J. X. and Wahr, J.: Ice Age Earth Rotation, Annual Review of Earth and Planetary Sciences, 39, 577–616, 2011.

Mitrovica, J. X., Wahr, J., Matsuyama, I., and Paulson, A.: The rotational stability of an ice-age earth, Geophysical Journal International, 161, 491–506, 2005.

Molodensky, S.: Relation between Love numbers and load factors, Izv. Phys. Solid Earth, 13, 147–9, 1977.

Munk, W. H. and MacDonald, G. J.: The Rotation of the Earth: A Geophysical Discussion, Cambridge Univ. Press, New York, 1960.

Nakiboglu, S.: Hydrostatic theory of the Earth and its mechanical implications, Physics of the Earth and Planetary Interiors, 28, 302–311, 1982.

Peltier, W., Drummond, R., and Roy, K.: Comment on Ocean mass from GRACE and glacial isostatic adjustment by DP Chambers et al., Journal of Geophysical Research: Solid Earth (1978–2012), 117, 2012.

Peltier, W. R.: The impulse response of a Maxwell Earth, Review of Geophysics and Space Physics, 12, 649–669, 1974.

Peltier, W. R.: Ice age paleotopography, Science, 265, 195–201, 1994.

Plag, H.-P. and Jüettner, H.-U.: Inversion of global tide gauge data for present-day ice load changes (scientific paper), Memoirs of National Institute of Polar Research. Special issue, 54, 301–317, 2001.

Press, W. H.: Numerical recipes 3rd edition: The art of scientific computing, Cambridge University Press, 2007.

Prey, A.: Darstellung der Höhen-und Tiefenverhältnisse der Erde: Durch eine Entwicklung nach Kugelfunktionen bis zur 16. Ordnung..., Weidmann, 1922.

Ricard, Y., Sabadini, R., and Spada, G.: Isostatic deformations and polar wander induced by redistribution of mass within the Earth, Journal of Geophysical Research: Solid Earth, 97, 14 223–14 236, 1992.

Ricard, Y., Spada, G., and Sabadini, R.: Polar wandering of a dynamic Earth, Geophysical Journal International, 113, 284–298, 1993.

Routh, E. J.: The Advanced Part of a Treatise on the Dynamics of a System of Rigid Bodies., 1905.

Sabadini, R., Yuen, D., and Gasperini, P.: The effects of transient rheology on the interpretation of lower mantle viscosity, Geophysical Research Letters, 12, 361–364, 1985.

Saito, M.: Some problems of static deformation of the Earth, Journal of Physics of the Earth, 22, 123–140, 1974.

Saito, M.: Relationship between tidal and load Love numbers, Journal of Physics of the Earth, 26, 13–16, 1978.

Serpelloni, E., Faccenna, C., Spada, G., Dong, D., and Williams, S. D.: Vertical GPS ground motion rates in the Euro-Mediterranean region: New evidence of velocity gradients at different spatial scales along the Nubia-Eurasia plate boundary, Journal of Geophysical Research: Solid Earth, 118, 6003–6024, 2013.

Shida, T.: On the elasticity of the Earth and the Earth's crust, Kyoto Imperial University, 1912.

Spada, G.: Glacial Isostatic Adjustment and Contemporary Sea Level Rise: An Overview, Surveys in Geophysics, 38, 1–33, 2017.

Spada, G. and Galassi, G.: New estimates of secular sea level rise from tide gauge data and GIA modelling, Geophys. J. Int., 191, 1067–1094, 2012.

Spada, G. and Galassi, G.: Spectral analysis of sea-level during the altimetry era, and evidence for GIA and glacial melting fingerprints, Global and Planetary Change, 143, 34–49, 2015.

Spada, G. and Galassi, G.: Extent and dynamic evolution of the lost land *aquaterra* since the Last Glacial Maximum, Comptes Rendus Geoscience, 349, 151–158, 2017.

Spada, G. and Melini, D.: `SELEN`: a program for solving the "Sea Level Equation" - Manual version 1.2, December 2015, Computational Infrastructure for Geodynamics (CIG), available from: http://www.geodynamics.org/, 2015.

Spada, G. and Stocchi, P.: The Sea Level Equation, Theory and Numerical Examples, Aracne, Roma, 2006.

Spada, G. and Stocchi, P.: SELEN: a Fortran 90 program for solving the "Sea Level Equation", Comput. and Geosci., 33, 538–562, 2007.

Spada, G., Ricard, Y., and Sabadini, R.: Excitation of true polar wander by subduction, Nature, 360, 452–454, 1992a.

Spada, G., Sabadini, R., Yuen, D. A., and Ricard, Y.: Effects on post-glacial rebound from the hard rheology in the transition zone, Geophysical Journal International, 109, 683–700, 1992b.

Spada, G., Barletta, V. R., Klemann, V., Riva, R., Martinec, Z., Gasperini, P., Lund, B., Wolf, D., Vermeersen, L., and King, M.: A benchmark study for glacial isostatic adjustment codes, Geophysical Journal International, 185, 106–132, 2011.

Spada, G., Melini, D., Galassi, G., and Colleoni, F.: Modeling sea level changes and geodetic variations by glacial isostasy: the improved SELEN code, ArXiv e-prints, 2012.

Sternberg, W. J., Smith, T. L., and Smith, T. L.: The theory of potential and spherical harmonics, 3, University of Toronto Press Toronto, 1946.

Suess, E.: Face of the Earth, Clarendon Press, Oxford, 1906.

Tamisiea, M. E.: Ongoing glacial isostatic contributions to observations of sea level change, Geophysical Journal International, 186, 1036–1044, 2011.

Tegmark, M.: An icosahedron-based method for pixelizing the celestial sphere, The Astrophysical Journal, 470, L81, 1996.

Tegmark, M., de Oliveira-Costa, A., and Hamilton, A. J.: High resolution foreground cleaned CMB map from WMAP, Physical Review D, 68, 123 523, 2003.

Tschoegl, N. W.: The phenomenological theory of linear viscoelastic behavior: an introduction, Springer Science & Business Media, 2012.

Tushingham, A. and Peltier, W.: ICE-3G – A new global model of late Pleistocene deglaciation based upon geophysical predictions of post-glacial relative sea level change, Journal of Geophysical Research, 96, 4497–4523, 1991.

Tushingham, A. and Peltier, W.: Validation of the ICE-3G model of Würm-Wisconsin deglaciation using a global data base of relative sea level histories, Journal of Geophysical Research, 97, 3285–3304, 1992.

Tushingham, A. and Peltier, W.: Relative Sea Level Database. IGPB PAGES/World Data Center-A for Paleoclimatology Data Contribution Series, Tech. Rep. 93-106, 1993.

Vermeersen, L. and Sabadini, R.: A new class of stratified viscoelastic models by analytical techniques, Geophysical Journal International, 129, 531–570, 1997.

Vermeersen, L. A., Sabadini, R., and Spada, G.: Analytical visco-elastic relaxation models, Geophysical Research Letters, 23, 697–700, 1996a.

Vermeersen, L. L. A., Sabadini, R., and Spada, G.: Compressible rotational deformation, Geophysical Journal International, 126, 735–761, 1996b.

Wessel, P. and Smith, W. H. F.: New, improved version of Generic Mapping Tools released, Eos T. Am. Geophys. Un., 79, 579, 1998.

Whitehouse, P.: Glacial isostatic adjustment and sea-level change, State of the art report. Svensk Kärnbränslehantering AB, Swedish Nuclear Fuel and Waste Management Co., Stockholm, p. 105, 2009.

Whitehouse, P. L.: Glacial isostatic adjustment modelling: historical perspectives, recent advances, and future directions, Earth Surface Dynamics, 6, 401–429, https://doi.org/10.5194/esurf-6-401-2018, 2018.

Wieczorek, M. A. and Meschede, M.: Shtools: Tools for working with spherical harmonics, Geochemistry, Geophysics, Geosystems, 19, 2574–2592, 2018.

Wöppelmann, G. and Marcos, M.: Vertical land motion as a key to understanding sea level change and variability, Reviews of Geophysics, 54, 64–92, 2016.

Wu, P. and Ni, Z.: Some analytical solutions for the viscoelastic gravitational relaxation of a two-layer non-self-gravitating incompressible spherical earth, Geophys. J. Int., 126, 413–436, 1996.

Wu, P. and Peltier, W.: Viscous gravitational relaxation, Geophysical Journal International, 70, 435–485, 1982.

Wu, P. and Peltier, W.: Pleistocene deglaciation and the Earth's rotation: a new analysis, Geophysical Journal International, 76, 753–791, 1984.

Yuen, D. A., Sabadini, R. C. A., Gasperini, P., and Boschi, E.: On transient rheology and glacial isostasy, Journal of Geophysical Research, 91, 11,420–11,438, 1986.